



From Institute for Signal Processing

Director:
Prof. Dr. -Ing. Alfred Mertins

A Multimodal, Wearable Health Monitor using a Dual-core Smartphone Processor

Dissertation

for Fulfilment of requirements for
Doctoral Degree of the University of Luebeck
- from the Dept. of Informatics/Technology



Submitted by Kunal Mankodiya

Born in Ahmedabad, India

Luebeck, October 2010.

Names of the examiners:

1. Prof. Dr. rer. nat. Ulrich G. Hofmann
2. Prof. Dr. med. Hartmut Gehring
3. Prof. Dr.-Ing. Andreas Schrader

Date of oral examination: 17.Dec.2010

Dissertation submitted on 27.Oct.2010, Luebeck.



Kunal Mankodiya

Research Assistant

Institute for Signal Processing

University of Luebeck

Ratzeburger Allee 160,

23562 Luebeck, Germany

Dedicated to
Lin & Wenjing

ACKNOWLEDGEMENT

Sincerest and deepest thanks are extended to my advisor, Prof. Dr. rer nat. Ulrich G. Hofmann, who has supported, advised, mentored and inspired me to achieve success in the doctoral research. He brought me an opportunity of the state-of-the-art smartphone processor programming for medical applications. He also poured in me the research methodologies and scientific writing skills.

I also offer special thanks to my clinical supervisor, Prof. Dr. med. Hartmut Gehring who provided me the medical expertise. I would like to express my thanks to Prof. H. Gehring and our institute director, Prof. Dr.-Ing. Alfred Mertins for their financial assistance for several international conferences, which not only broadened my vision but also brought me the opportunity to talk to world renown scientists and technologists.

I would like to convey many thanks to my colleagues Simon Vogt, Matthias Klostermann, and Alexander Opp for their incessant support during the doctoral research challenges. I convey my thanks to Abdallah Mohabbedani and Yassir Ali Hassan for their cooperation in the PhD projects. I am thankful to Bhavin Chamadiya and Olaf Christ, who assisted me during my research. I would like to express my appreciation to all Neuro-engineering group and ISIP members for their concern and cordiality. I also thank Dr. Matthias Klinger for his guidance and support concerning human anatomy during cerebral oximetry measurements. Many thanks go to BeagleBoard googlegroup for its support in solving the embedded related challenges. I thank TED online motivating talks on science and technology, which throughout poured energy and creativity in me.

I offer my most profound thanks to my family, in particular my beloved wife Lin and my little daughter Wenjing, who have endured, sacrificed and encouraged me during my studies. Lin constantly observed my research progress and proofread my scientific papers and dissertation. Finally, I thank my parents for their unwavering love and support.

ABSTRACT

Increasing rate of chronic conditions has not only resulted in lower quality of life for many but also increased the personal and societal burden. The growing interest in personal health supervision could help to prevent detect, avoid and comply therapy with these chronic conditions if implemented in daily life activities. Since multi-parametric health monitoring is not a job for a single sensor, there needs to be a system that could integrate patient's on-body as well as personal environmental sensors. Portability, ease of use, high computing performance, multimodal capabilities and low cost are the prerequisites for such a multi-parametric and smart monitoring.

The purpose of this dissertation is to reach the target of designing a multi-modal, wearable health monitor. To cope with an estimated computing need of several hundred MIPS in such multimodal monitoring, embedded smartphone processors were taken into investigation. The thorough market survey found TI's dual-core smartphone processor OMAP3530 with a superscalar ARM Cortex-A8 and the DSP c64x+, to be the most suitable for such multimodal health monitoring application.

The development on the OMAP3530 speeded up with the OMAP3530-based BeagleBoard and our virtual appliance containing all necessary development tools. Two feasibility tests on the OMAP3035 were conducted, in which the BeagleBoard successfully collected, processed and displayed the data of commercial medical devices on a single platform. In this test, the OMAP3530 also generated distinctive alarm sounds for each monitoring parameter.

Considering the objective of the multimodal monitoring, the OMAP3530 was linked to a high-resolution multichannel ADC for receiving multichannel digital data. Consecutively, multimodal sensors for electrocardiogram (ECG), saturation of peripheral oxygen (SpO₂) and regional oxygen saturation (rSO₂) were chosen out of many parameters due to their high significance in clinical and diagnostic applications. Moreover, some type of humidity and temperature sensors were also selected to achieve the personal environment monitoring.

Objective of wearable monitoring is to bring the sensor on the body and enable continuous health monitoring without hindering the individual's life activity. Therefore, the mentioned sensors and their analog front-ends needed to be wearable and miniaturized. Three miniaturized sensor modules; an "Active Belt" for continuous ECG, a oximeter module for cerebral and pulse oximetry, and a personal environment module for humidity and temperature was designed and tested. They separately function in conjunction with the BeagleBoard and build the wearable real-time monitoring applications.

Finally, after accomplishing design and development of individual modules, the multimodal, wearable health monitoring (MHM) system was formed by integrating them on a single platform. The MHM deploys the minimally obtrusive sensor array on the daily-life wearable objects and facilitates an individual with continuous health monitoring. The MHM system successfully collected, processed and produced onsite visual biofeedback of the multimodal health parameters from an individual in laboratory-run experiments.

Thus, the MHM system practically realized the concept of utilizing a smartphone processor in portable and wearable multimodal medical monitoring, which in the future will be as ubiquitous as current cellphones.

CONTENTS

Abstract	vi
Contents	viii
1. Introduction	1
1.1 Multi-modal Sensors for Wearable Health Monitoring.....	4
1.2 Objective of this research work	6
1.3 References	8
2. Embedded & Smartphone Processors	10
2.1 An Embedded Processor	10
2.2 ARM Processors	14
2.3 Dual-core Application Processors.....	19
2.4 OMAP3530 - Dual-core Application/Smartphone Processor	23
2.5 BeagleBoard – OMAP3530 Development Board.....	27
2.6 References	30
3. Programming the OMAP3530	33
3.1 First Hands-on the BeagleBoard.....	33
3.2 Running Ångström on the BeagleBoard	34
3.3 Development Environment on a PC	35
3.4 Data Handling on the Beagleboard	40
3.5 Feasibility Test I – Heart Rate Monitoring.....	41
3.6 Feasibility Test II – Patient Monitor Integration	43
3.7 References	50

4. Novel Hardware Interfacing with the OMAP3530	51
4.1 Generalized Biosignal Acquisition System	51
4.2 ADS1258 – 16-Channel ADC	54
4.3 Serial Peripheral Interface (SPI) on the ADS1258	56
4.4 ADS1258 Communication Protocol.....	58
4.5 Expansion Header on the BeagleBoard	61
4.6 Communication between the ADS1258 and the OMAP3530	65
4.7 Feasibility Test – Portable Personal Environment Module	68
4.8 References	74
5. Wearable ECG Belt for Continuous Monitoring	75
5.1 Introduction.....	75
5.2 Background Theory.....	78
5.3 Active Belt Components	89
5.4 Active Belt Firmware	95
5.5 Experiments & Results.....	96
5.6 Conclusions & Outlook.....	103
5.7 References	105
6. A Miniaturized Cerebral Oximeter.....	108
6.1 A Demand for the Miniaturized Oximetry System	108
6.2 Background Theory.....	110
6.3 System Components.....	119
6.4 System Firmware	124
6.5 Experiments & Results.....	126
6.6 Conclusions	131
6.7 References	133
7. Multimodal, Wearable Health Monitoring through Daily-life Objects	135
7.1 Demand of a Multi-parametric Wearable Monitor	135

7.2	System Components.....	140
7.3	System Firmware	145
7.4	Experiments & Results.....	147
7.5	Conclusions	151
7.6	References	152
8.	Conclusions & Outlook.....	154
8.1	Problem Encountered & Related Solutions.....	156
	Publications associated with the Research Work.....	160
	List of Figures	162
	List of Tables.....	166
	List of Equations.....	167
	Abbreviations.....	168
	Appendix.....	171

1. INTRODUCTION

Extended periods of chronic conditions like cardiovascular diseases, diabetes, stroke, asthma, cancer or chronic bronchitis result in low quality of life and depression for millions of people worldwide and an associated high financial burden to society, although global life expectancy of individual has been increased [1]. One way to alleviate this personal and societal burden would be to support those individuals by continuous personal monitoring as part of a strategy to *detect* causes of acute phases, *prevent* them and *comply* to therapy prescribed [2, 24]. However, such health maintenance highly increases the costs of state-of-the-art treatments not only for people with chronic diseases but also for a growing number of old patients. Providing affordable and high-level care is one of the biggest issues in public health care systems today [3]. At the same time, the older generation has never before had such huge amounts of personal income at its disposal, willing to track their personal well being and health beyond governmental support [19, 20, 22]. Also, a growing number of life-style oriented individuals is beginning to use medical monitoring devices for recreational use in sports and daily life.

All aspects of the current societal situation funnel into one big and exciting technological conclusion: a clear demand for mobile, yet powerful monitoring systems exists, serving both the patient in need by maintaining qualified but remote supervision (“Telemedicine”), as well as the life-style and fitness oriented, financially independent person [24]. These particularly require the acquisition, fusion and analysis of a large number of physiological parameters by a light-weight, portable and power-saving device that is able to give qualified and autonomous warnings or suggestions to improve the level of fitness of its bearer. Therefore, European Commission’s ICT Work Programme 2011 section 6.5 on “Health and Aging well” will focus exclusively on multi-parametric data in the context of Personal

Health Systems [14]. The programme will also deliver roadmaps for research to wise use of mobile eHealth (mHealth) solutions for lifestyle and disease management [15, 16, 21]. In other words, personalized health monitoring systems might in the future become as ubiquitous as current cell phones are today. There are already several such personalized health monitors available or in the pipeline:

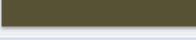
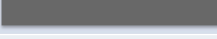
- Heart rate monitor (WearLink, Polar, Finland) consists of a chest belt and monitors beat-to-beat interval of wearer's heart during sports and daily activity [9].
- Glucose monitor (Mendor, Finland) is a cellphone-sized all-in-one blood glucometer [10].
- The Zio™ Patch (iRhythm Technologies, USA) is a long-term cardiac rhythm monitor that provides continuous monitoring for up to 7-14 days [3].
- A PiiX™ (Corventis, USA) adheres to the skin and automatically detects, records and transmits physiological information [4].
- SMHEART LINK™ (iTMP Technologies, Inc., USA) communicates with a variety of fitness sensors to enable integration with iPhone apps [5].
- Fitbit (Fitbit, USA) tracks with accelerometers person's calories burned, steps taken, distance travelled and sleep quality [6].
- Zeo (Zeo Inc., USA) produces a device designed to detect different stages of person's sleep to analyze and improve its pattern [7].
- iShoe™ (iShoe, USA) detects the individual's balance and also prevents from falling [8].

Each personal health monitoring device listed above indeed shows an useful application, which is aiming at specific disease or life-style purpose. However, many of the diseases can't be diagnosed or detected based on a single health parameter. Table 1-1 reveals the analysis of US-based studies showing the major diseases and their monitoring requirements. It infers from Table 1-1 that with respect to above mentioned basic principles (*detect, prevent and comply*) meaningful monitoring

must not only collect body sensor data from an individual, but instead has to integrate multi-sensors collecting individual's health and surrounding environment information.

Let's take an example of an individual with asthma disease (Table 1-1). In order to detect the asthma attack for taking preventive actions, a number of body parameters such as respiratory rate, FEV1 (forced expiratory volume in 1 sec), oximetry are normally required to be monitored. On top of that, the surrounding environment parameters such as air quality and pollen count, which highly affect asthmatic patient, are equally important to monitor in preventing asthma attack. In the same manner, multi-sensor monitoring system can be implemented such as to minimize the impact of the other chronic and life-threatening diseases.

Table 1-1: A list of major diseases with the monitoring requirements (US-based study) [13].

Disease	No. affected	Monitoring required
Cardiovascular	 16.7M	ECG, HR, BP, weight, activity, caloric in/out
Asthma	 23M	RR, FEV1, oximetry, air quality, pollen count
Breast cancer	 3M	Ultrasound
COPD	 10M	RR, FEV1, oximetry, air quality
Depression	 21M	Med compliance, activity, communication
Diabetes	 24M	Glucose, hemoglobin A1C
Alzheimer's	 5M	Vital signs, locations, activity, balance
Hypertension	 74M	Continuous BP, med compliance
Obesity	 80M	Smart scales, glucose, caloric in/out, activity
Sleeping disorder	 40M	Sleep phases, quality, apnea, vital signs

In other words, health monitoring has to be truly multimodal and smart to find its way to the persons in need. Moreover, a multimodal health monitoring needs to be as pervasive as possible. The notion of pervasive health monitoring presents us with a paradigm shift from the traditional event-driven model (i.e. go to doctor

when sick) to one where we are continuously monitoring a person's "well-being" through the use of bio-sensors, smart-environments, smart-homes and information networks. This allows more proactive health maintenance, as well as allowing the health care provider to make more informed decisions with a greater wealth of accurate data [12].

1.1 MULTI-MODAL SENSORS FOR WEARABLE HEALTH MONITORING

Fig. 1-1 gives an overview of several potentially relevant health parameters that should be monitored in a continuous and user-friendly portable manner. The sensors are categorized according to their locations around the body. On-body sensors generally have a direct contact with the body, while peripheral sensors collect the information on the surrounding environment influencing one's health. The number of the sensors in a single system is highly dependent on the area of its application.

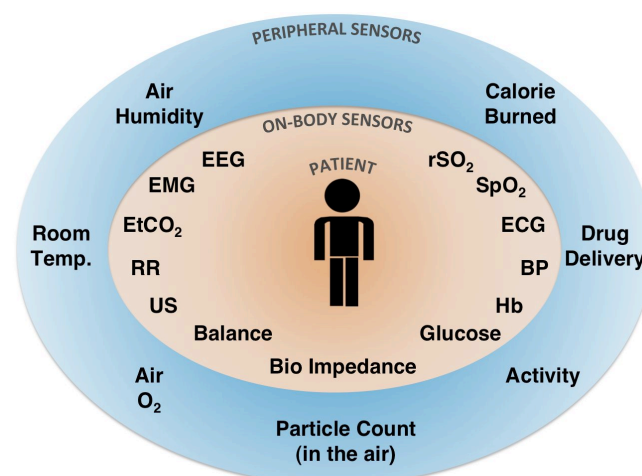


Fig. 1-1: A multi-modal health monitoring scenario showing on-body and peripheral sensors.

Table 1-2: Potential sensors for continuous health monitoring and their data throughputs.

Sensors	Max. Freq. Component (Hz)	No. of Channels	Sampling Rate (samples / sec *channel)	bits / sample	Data Throughput (bits/sec)
ECG (limbs)	100	3	200	12	7.2k
EEG	100	16	400	12	76.8k
EMG	1k	2	2k	12	48k
Breathing Rate	2	1	10	8	80
SpO ₂	250	1	1k	12	12k
EtCO ₂	2	1	10	8	80
BP	1 Hz	1	10	8	80
Glucose (hourly)	-	1	1	8	0.13
Hb (hourly)	-	1	1	8	0.13
Body Temp.	-	1	10	8	80
Balance	-	6	2k	8	96k
Bio Impedance	50k	1	100k	8	800k
Air-O ₂ level	-	1	10	8	80
Air-Humidity	-	1	10	8	80
Air-Specific Particle Count (SO _x , NO _x , CO, volcanic ash, pollen, etc.)	-	5 or more	10	8	400
Atmospheric Temp.	-	1	10	8	80
Total					≈ 1M

Table 1-2 shows an approximation on the data volume these sensors might produce, which then needs to be analysed on-site, displayed and potentially - transmitted for further use. Even though the data throughput in the range of 1 Mbit/sec is not too impressive and could certainly be handled by a simple microcontroller e.g., PIC18F8720 (Microchip Technology Inc., USA), on-site real-time analysis and diagnostic feedback actions for huge amount of data require high computing power [16]. Since even a simple Fourier transform is of computational order $n \cdot \log(n)$, the estimated computational load is approx. 6 MIPS to transform a continuous data stream of 1 Mbit/sec. This estimate is clearly a lower boundary, as it doesn't account for more complex analysis or classification procedures and overhead. To be on the safe side, a computing need of several hundred MIPS on a mobile platform is postulated.

The solution to meet the high computing requirement with a low power consumption is found in current smartphones. Current smartphones possess powerful embedded processor capable of real-time task handling and computing. Most of the smartphone embedded processors are dual-core with each core dedicated to specific task. One of

such dual-core smartphone processor is OMAP3530 from Texas Instruments Inc., USA, which is based on TI's OMAP3 architecture found in several smartphones e.g., Nokia N900, Moto Droid, Palm Pre etc [17]. The OMAP3530 is comprised of the most advanced ARM Cortex A-8 and the DSP c64x+ [18].

The superscalar Cortex-A8 (ARM, UK) on the OMAP3530 promises up to 2000 MIPS with a low power consumption [11] and motivated us to investigate this architecture for the portable medical monitoring. Furthermore, additional computing support for the real-time medical signal processing can be achieved by the DSP core on the OMAP3530. Therefore, the OMAP3530 because of its dual-core functionality was considered a suitable platform in meeting the requirements of the multi-parametric health monitors. Duality in such processors increases the speed by parallel processing and tremendously reduces the size of the system.

1.2 OBJECTIVE OF THIS RESEARCH WORK

As shown in Fig. 1-2, the main goal of this research is to design and develop a multi-modal wearable health monitor, which must integrate the multiple sensory modules with high performance dual-core smartphone processor. The target device needs to furnish a common platform to collect, process and display the multi-sensory data in real-time manner [11].

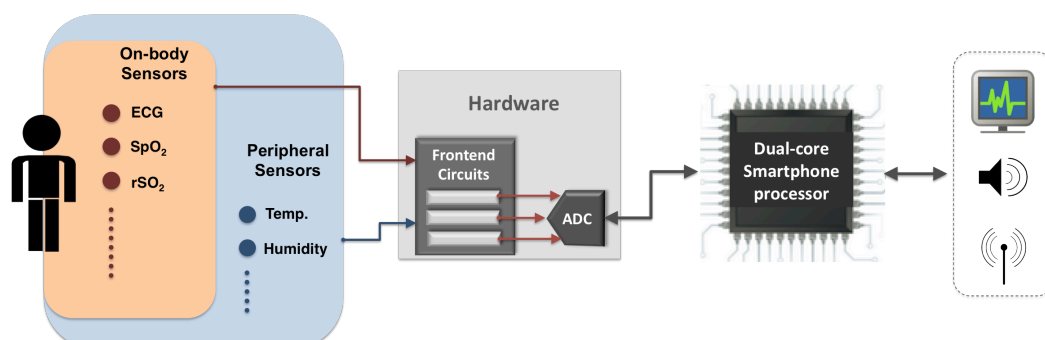


Fig. 1-2: A system block diagram of the multi-modal wearable health monitor (MHM).

This research work addresses the problem of a huge amount of the data to be handled in continuous health monitoring and also suggests a solution by using dual-core smartphone processors. Although smartphone processors furnish high-performance with low-power consumption, their usability is not yet fully-explored into medical technology and applications. This work is an endeavour to bring the dual-core processor into medical technological development and produce a powerful portable medical monitor. Cross-communication between the dual-core processor and novel analog front-ends is a challenge, which has been solved in this work.

Bringing multi-modality with the wearable health monitoring in a true sense requires a collection of sensors (as listed in Table 1-2) and the corresponding analog hardware on the body in a wearable manner. To develop all the sensors along with the corresponding hardware is overwhelming and hence out of this context. However, three significant parameters electrocardiogram (ECG), saturation of peripheral oxygen (SpO_2) and regional oxygen saturation (rSO_2), which provide a significant information of the individual's cardiovascular system, respiratory system and brain, were selected for on-body sensor monitoring. On the other hand, humidity and temperature sensor are selected for monitoring the individual's body environment. Miniaturized novel hardware was designed for each sensor in order to locate it in proximity to the sensor location on the body. This research also demonstrates the application of the MHM into the out-of-the-hospital and home environments.

The research goal was subdivided into the following major objectives:

- To survey the available smartphone processors in the market and select a suitable dual-core smartphone processor. (Section 2)
- To construct a development environment, which allows the development of the embedded software applications for the smartphone processor platform. (Section 3)
- To test the processor's feasibility for the medical monitoring applications. (Section 3)
- To realize novel communication between the processor and hardware e.g., ADC. (Section 4)

- To design and develop novel multi-modal analog front-end hardware which collects and conditions signal representative for the health and body-environment. (Section 4, 5 and 6)
- To integrate the novel analog front-ends with smartphone processor to form a prototypic multi-modal, wearable health monitoring system to be used during daily life activity. (Section 8)

1.3 REFERENCES

- [1] “Insuring American’s Health: Principles and Recommendations.” Committee on insuring health, Institute of Medicine, Washington, DC, 2004.
- [2] iRhythm Technologies, Inc. <http://www.irhythmtech.com/zio-solution/zio-patch/>. Web. 22 Apr. 2010.
- [3] Corventis. <http://www.corventis.com/EU/medprof.asp>. Web. 22 Apr. 2010.
- [4] iTMP Technologies, Inc. <http://store.smheartlink.com/> Web. 22 Apr. 2010.
- [5] Fitbit, <http://www.fitbit.com/product>. Web. 22 Apr. 2010
- [6] Zeo Inc. <http://whatiszeo3.myzeo.com/hp/3/whatiszeo.php>. Web. 22 Apr.
- [7] iShoe. <http://www.i-shoe.net/products.html>. Web. 22 Apr. 2010.
- [8] WearLink. <http://http://www.polar.fi/>. Web 22 Apr. 2010.
- [9] All-in-one glucose meter. <http://www.mendor.com> Web 15 Sept. 2010.
- [10] ARM Cortex-A8 Datasheet: ARM. The Cortex A8 Microprocessor. Mar. 2008.
- [11] A GOOD AGE: Aging and technology. <http://ledger.southofboston.com/articles/2004/03/29/life/life02.txt>.
- [12] Braecklein, M., J. Dehm, et al. (2007). VDE Anwendungsempfehlungen für TeleMonitoring H. Korb. Frankfurt, VDE.
- [13] Eric Topol, “The wireless future of medicine”, TEDMED, TEDtalks Vid-

eo. Oct. 2009.

- [14] Work Programme 2011 document, Theme 3, ICT, European Commission C. Filename: c-wp-201101_en
- [15] Vital Wave Consulting (February 2009). mHealth for Development: The Opportunity of Mobile Technology for Healthcare in the Developing World. United Nations Foundation, Vodafone Foundation. p. 9.
- [16] PIC18F8720 datasheet, www.microchip.com
- [17] Mankodiya, K., Vogt, S., et al. (2010). Near Patient Sensor Integration with Smart Phone Processors. In Biomedizinische Technik 2010, Rostock, Germany.
- [18] OMAP3530 datasheet: Texas Instruments. OMAP3530/25 Application Processors. Feb. 2008. Literature Number : SPRS507F.
- [19] <http://www.un.org/ageing/popageing.html>
- [20] López-de-ipiña, Diego, Xabier Laiseca, Ander Barbier, and Unai Aguilera. “Infra-structural Support for Ambient Assisted Living.” 3rd Symposium of Ubiquitous Computing and Ambient Intelligence 2008, Advances in Soft Computing, pp 66-75.
- [21] Hanak, David, Gabor Szijarto, and Barnabas Takacs. “A mobile approach to ambient assisted living.” 3rd Symposium of Ubiquitous Computing and Ambient Intelligence 2008, Advances in Soft Computing, pp 66-75.
- [22] Fuchsberger, Mag Verena. “Ambient Assisted Living: Elderly People ’ s Needs and How to Face Them.” In SAME’08, 21-24. Vancouver, Canada, 2008.
- [23] Leff B, Burton L, Mader SL, et al. Hospital at home: feasibility and outcomes of a program to provide hospital-level care at home for acutely ill older patients. Ann Intern Med 2005;143:798-808.
- [24] Steven H. Landers. Why Health Care is Going Home, Prospective of the New England Journal of Medicine, 2010.

2. EMBEDDED & SMARTPHONE PROCESSORS

As discussed in the previous section, the state-of-the art smartphone processors with the dual-core architecture fulfil the requirement of the high-computing performance and low-power consumption to realize the multi-modal health monitoring. The following furnishes with the complete market survey of the embedded processors used in current smartphones. The focus of the market survey was to find a suitable smartphone processor, which can provide the portability, high computing performance, multimodal analysis, low-cost and ease of application development required for this research work.

2.1 AN EMBEDDED PROCESSOR

An Embedded System

An embedded system is a special-purpose computing device designed to perform dedicated functions. Today, they are widely used to serve various purposes such as:

- consumer electronics (mp3 player, cellphones, digital cameras, etc.),
- house hold appliances (microwaves, washing machine, televisions, etc.),
- mission critical systems (satellite, flight control, etc.)
- network equipment (firewall, router, etc.)

An embedded system consists of its hardware and software. The hardware includes a microprocessor or microcontroller with additional attached external memory, I/O, and other components such as sensors, keypad, LEDs, LCDs, and any kind of actuators (see Fig. 2-1). The embedded software is the driving force of an embedded system. The embedded software is usually called firmware because this type software is loaded to ROM, EPROM, or Flash memory [1].

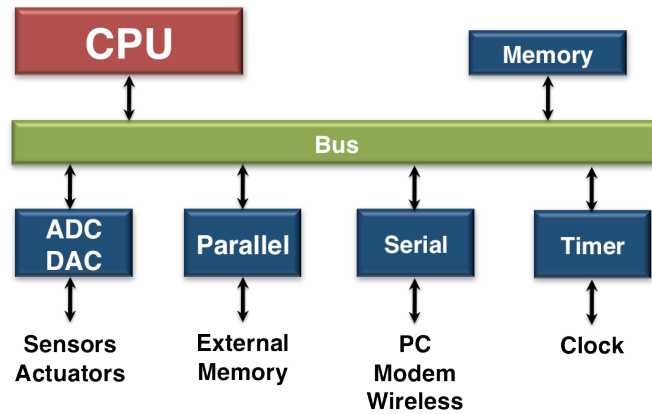


Fig. 2-1: A generalized block diagram of an embedded system.

The embedded systems is basically divided into two categories: 1) a simple embedded system (e.g., intel's 8086) is used for some simple tasking purpose such as, digital calculators, digital diary, etc. 2) a complex embedded system (e.g., ARM Cortex-A8) is now-a-days found in many complex functional devices which varies from modern smartphones to the satellite vehicle. Embedded systems are not always standalone devices, instead parts within a larger device.

Following are the key factors that differentiate an embedded system from a desktop computer [26]:

- Embedded systems are usually cost sensitive.
- Most embedded systems have real-time constraints.
- There are multitudes of CPU architectures (such as ARM®, MIPS®, PowerPC™, etc.) that are used in embedded systems. Embedded systems employ application-specific processors.
- Embedded systems have (and require) very few resources in terms of RAM, ROM, or other I/O devices as compared to a desktop computer.
- Power management is an important aspect in most embedded systems.

An Embedded Processor or SoC

In recent years, there have been great advancements in the speed, power, and complexity of integrated circuits, such as application specific integrated circuit (ASIC)

chips, random access memory (RAM) chips and microprocessor chips [2]. These advancements have led the development of system-on-a-chip (SoC), also known as embedded processor, which is an integrated circuit that includes most of the above (Fig. 2-1) mentioned components such as a processor, a bus, and other elements (clocks, memory, serial interfaces, etc.) on a single monolithic substrate. The primary advantages of the SoC devices are lower costs, greatly decreased size and reduced power consumption. The additional benefits of the embedded processor over the conventional embedded system are:

- Software and firmware are cheaper and flexible.
- Short interconnections and less capacitance (compare to off-chip processor)
- Platform independency
- Immune to obsolescence

Sometimes, the system complexity increases in such a way that it becomes difficult to integrate the system in a single chip. In such cases, a system-in-package (SiP) is an option to incorporate multiple components into a single package, although SiP increases the manufacturing cost [3]. One more cost effective option is package-on-package (PoP) stacking during board assembly [3]. The PoP technique allows vertically installing the packages on top of one another and also enables higher density, for example in the smartphone / PDA market.

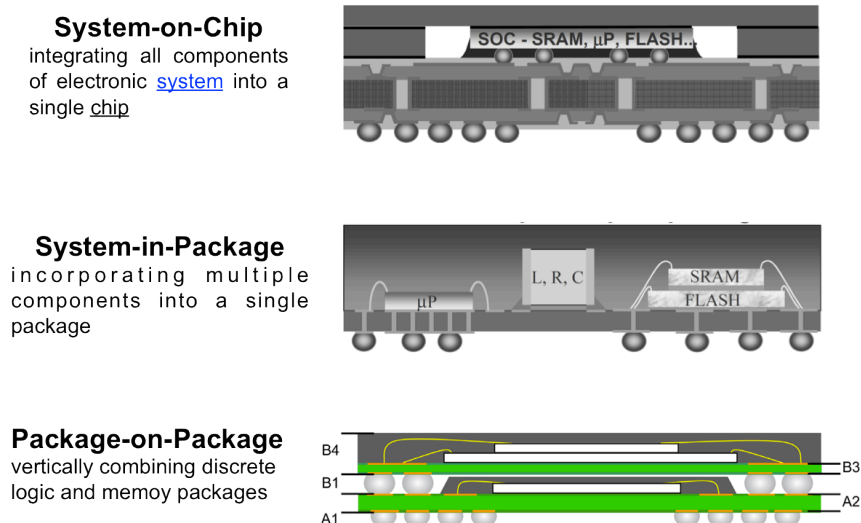


Fig. 2-2: Different packaging techniques of the embedded systems.

Embedded Processor Architectures

There is a huge variety of the embedded processor architectures in the market. Their extraordinary diversity and fast pace of development make it difficult to compare them at a certain time. The graph in Fig. 2-3 depicts some of the popular architectures of the embedded processors. The shown architectures ranges from a small embedded processors to the micro-computers including the laptop-like performances. In last few years, ARM displaced x86 as the most frequently deployed embedded architecture. Some 30 percent of projects were based on ARM, while 28 percent used x86. However, use of both ARM and x86 grew, year-over-year, at the expense of every other architecture except PowerPC. The relative simplicity of ARM processors compare to its competitor x86 made them suitable for low power applications [27]. As of 2007, about 98% of the more than one billion mobile phones sold each year use at least one ARM processor [4]. As of 2009, ARM processors account for approximately 90% of all embedded 32-bit RISC processors [5].

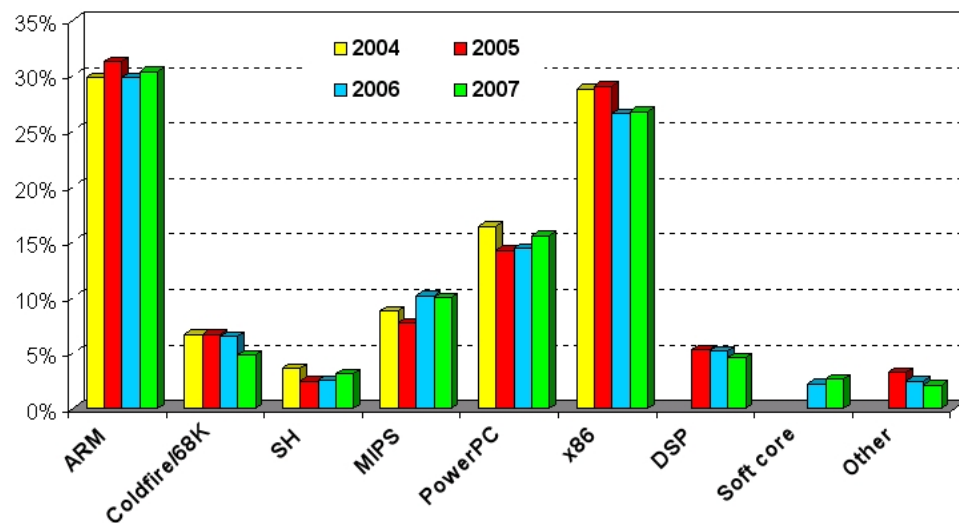


Fig. 2-3: The embedded processors and their role in the market [7].

The ARM, known as the Advanced RISC Machine is a 32-bit RISC instruction set architecture (ISA) developed by the company ARM Holdings. The ARM architecture has the following benefits over other architectures and hence has topped in the current smartphone market [6]:

- ARM-based processors are designed for all-in-one concept for mobile devices and low power consumption.
- ARM supports major embedded / mobile OSs, e.g., Linux, Windows CE, QNX, VxWorks, etc. [8]
- ARM processors add more functions and increase performance. This saves additional circuits on board that can reduce system size.
- For more complex software environment, ARM increases performance for new OS and software environment (e.g., Java hardware acceleration)

2.2 ARM PROCESSORS

The business model behind ARM Holdings is based on licensing the ARM architecture to companies that want to manufacture ARM-based CPU's or system-on-a-chip products [28]. The ARM Holding itself never built their chip, but rather architecture. The two main types of licenses are the Implementation license and the Architecture license. ARM architecture offers a wide range of processors that deliver high performance, industry leading power efficiency and reduced system cost. Fig. 2-4 shows the evolution of the ARM-base processors, which are subdivided into the following categories [8]:

1. Classic Processors

These processors are based on 32-bit ARM and 16-bit Thumb ISA, and are used for general-purpose applications.

2. Embedded Cortex Processors

Cortex-M series are used for deterministic microcontroller applications. Cortex-R series is used for real-time applications. These processors often execute a Real-Time Operating System (RTOS) alongside user-developed application code.

3. Application Cortex Processors

These processors come in single- or multi-core, that deliver performance of up to 2GHz+ typical frequency in advanced process nodes, enabling the next generation of mobile internet devices. Application Processors are defined by the processor's ability to execute complex operating systems, and to enable complex graphic user interfaces. This class of processors integrate an Memory Management Unit (MMU) to manage the memory requirements of these complex OSs, and enable the download and execution of third party software. [8]

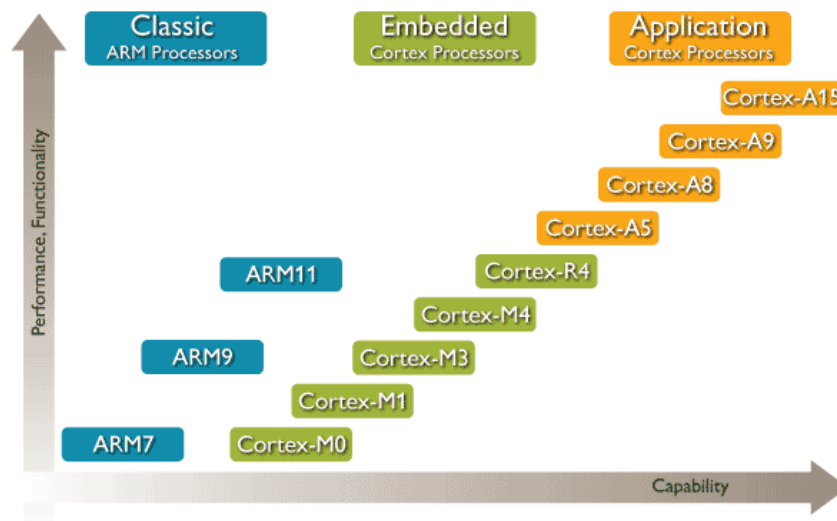


Fig. 2-4: An overview of a range of the ARM processors [8].

Role of ARM-based Processors in latest Smartphones

A smartphone is a mobile phone that offers more advanced computing ability and connectivity than a contemporary basic feature phone [29]. Over the last few months, the smartphone industry has seen an unprecedented focus on processing hardware. Smartphones are essentially pocket-sized computers that have a few extra radios and operate in extremely confined conditions vis-à-vis power consumption, heat output, etc. Most of the smartphones contain two processors, which fulfil two different pur-

poses. Baseband processor is responsible for cellular wireless communication and an application processor is responsible for general processing (CPU) and confines other in-built functions.

Table 2-1: A comparative overview of major smartphone processors [9].

Mobile Chipset	Applications processors	Instruction set	DMIPS	Max. clock speed	Phone examples
Qualcomm MSM72xx	ARM1136-JS	ARMv6	660 MIPS @667MHz	523 MHz	HTC Touch Series
Marvell XScale PXA320	Marvell XScale	ARMv5	800MIPS @624MHz	800 MHz	Samsung Omina
Samsung S3C6xxx	ARM1136JF-S	ARMv6	660 MIPS @667MHz	800 MHz	iPhone Samsung Omnia
Samsung S3C100	ARM Cortex A8	ARMv7	1200 MIPS @600MHz	833 MHz	iPhone 3GS
Samsung S3C110	ARM Cortex A8 (45nm)	ARMv7	2000 MIPS @1GHz	1000 MHz	Samsung Wave
TI OMAP3	ARM Cortex A8	ARMv7	1000 MIPS @500MHz	500 MHz	PalmPre Moto Droid Nokia N900
Qualcomm QSD8250	Qualcomm Scorpion	ARMv7	2100 MIPS @1GHz	1000 MHz	HTC HD2, Toshiba TG01, Acer F1
Intel Atom N270	Intel Atom	x86	3300MIPS @1.6GHz	2GHz	Netbooks

Table 2-1 infers that the current smartphones are overwhelmingly run on ARM architecture. ARM architecture is found in low/high-end mobiles from the giant companies like Nokia, Samsung, Motorola, Apple, etc. The reason behind the adoption of ARM in the smartphones is the varieties of the instruction sets. ARM's most recent instruction set is version v7, which is integrated in Cortex A8 architecture found in today's high-end smartphones.

ARM Cortex A8

The ARM[®] Cortex[™]-A8 microprocessor is the first applications microprocessor in ARM's new Cortex family. The Cortex-A8 processor offers a different range of performance depending on the implementation, delivering over to 2000 Dhrystone MIPS (DMIPS) of performance for demanding consumer applications and consuming less than 300mW for low-power mobile devices [10].

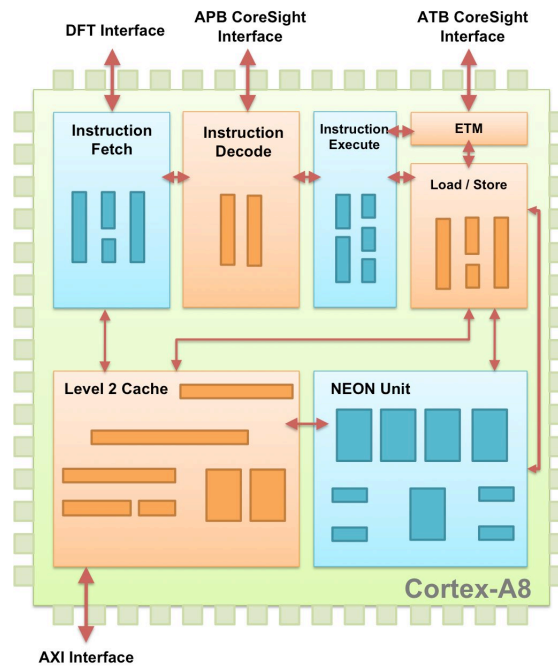


Fig. 2-5: A system-level diagram of ARM Cortex-A8.

Thumb-2 technology of the Cortex-A8 combines the original ARM instruction set of fixed length 32-bit with 16-bit [10]. The ARM Cortex-A8 processor's pipeline architecture is based on dual, symmetric, in-order issue, 13-stage pipelines with advanced dynamic branch prediction and static scheduling achieving 2.0 DMIPS/MHz [11]. As shown in Fig. 2-5, the Cortex-A8 processor uses a combination of synthesized, structured, and custom circuits. The design was divided into seven functional units and then subdivided into blocks, and the appropriate implementation technique chosen for each.

Instruction fetch

The instruction fetch unit predicts the instruction stream, fetches instructions from the L1 instruction cache and places the instructions into a buffer. It also includes the L1 instruction cache. [24]

Instruction decode

The instruction decode unit decodes and sequences all ARM and Thumb-2 instructions. The instruction decode unit handles the sequencing of exceptions, debug events, reset initialization, memory built-in self test, wait-for-interrupt and other unusual events. [24]

Instruction execute

The instruction execute unit consists of an address generator for load-and-store instructions, and the multiple pipeline. Execute pipelines also perform register write back [24].

Load/store

The load/store unit encompasses the entire L1 data side memory system and integer load/store pipeline [24].

L2 cache

The L2 cache unit includes the L2 cache and the Buffer Interface Unit (BIU). It services L1 cache misses from both the instruction fetch unit and the load/store unit [24].

ETM (Embedded Trace Macrocell)

An Embedded Trace Macrocell (ETM) is a real-time trace module providing instruction and data tracing of a processor. The ETM unit is a non-intrusive trace macrocell that filters and compresses an instruction and data trace for use in system debugging and system profiling [24].

NEON

The NEON unit includes the full 10-stage NEON pipeline that decodes and executes the NEON media instruction set [24]. NEON unit operates as a data processing en-

gine attached to the end of the main processor pipeline and is able to process demanding applications such as VGA H.264 30fps video decode with a clock frequency as low as 400MHz. Both the main pipeline and the NEON engine are supported directly by integrated high-performance Level 1 and Level 2 caches that work together to minimize access latency, minimize external bus traffic, and support high bandwidth data streaming to NEON media engine [11].

2.3 DUAL-CORE APPLICATION PROCESSORS

In order to meet current digital processing not only for smartphone but also for other digital devices such as wireless/portable medical devices, navigators, digital cameras, handy-cams, netbooks, etc. designer needs an application processor that delivers excellent real-time signal processing, fast CPU processing and abundant memory bandwidth. Even though the ARM Cortex series is able to fulfil some of these requirements, it lags behind in providing real-time signal processing in parallel with the other general-purpose tasks. Such limitation of the current general-purpose processor architecture empowered evolution of a new generation of embedded processors known as dual-core or multi-core processors incorporating two or more independent cores. The selection of the integrated cores is completely dependent on the area of application.

In the field of embedded applications, Texas Instruments Inc. introduced a technology known as OMAP (open media application platform) technology, in which some of the embedded processor contains a dual-core architecture consisting of both a general-purpose host ARM processor and one or more DSP. The DSP, which is optimized for intensive signal processing in real time with extremely low power consumption, becomes the primary processor for both the modem and the applications component. The GPP plays a secondary role, taking care of system management, command, control, and certain user interface activities. The OMAP architecture provides a means to coordinate dual processors and to seamlessly take advantage of the unique capabilities of each. Fig. 2-6 shows the advancements in the OMAP technology and its processor:

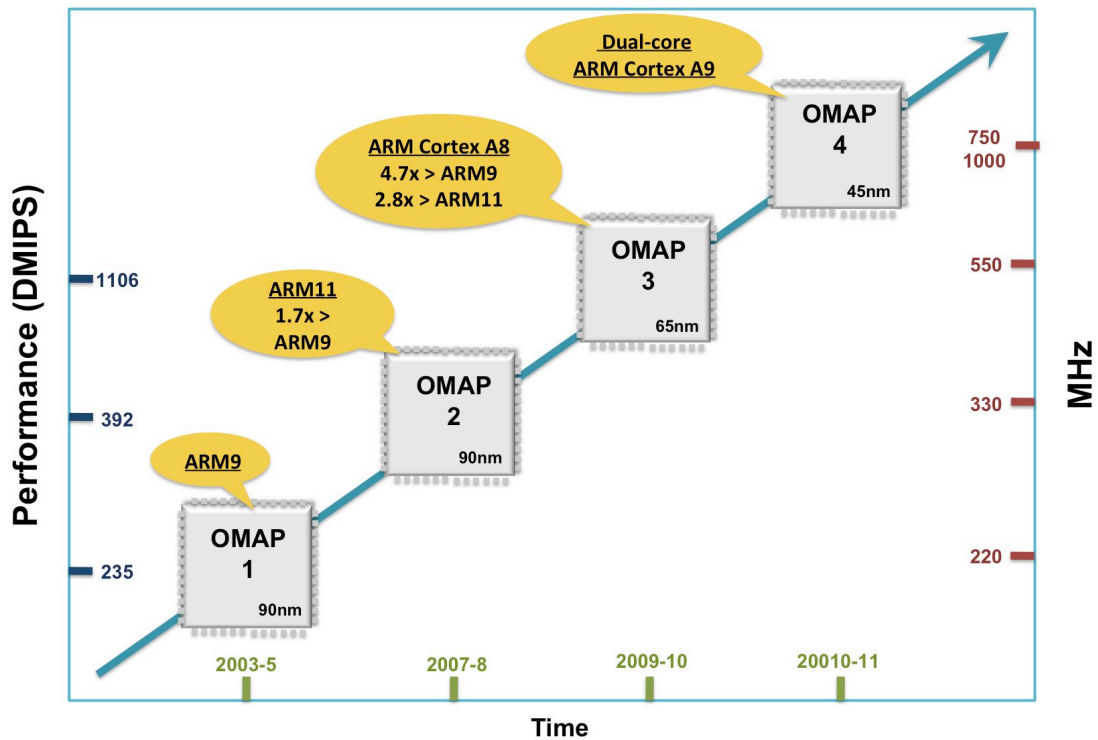


Fig. 2-6: The advancements in the OMAP dual-core application processors.

- Some of the OMAP1 family processors are dual-core and contain ARM926 core along with C55x DSP core.
- The OMAP2 family processors are made of ARM11 and C64x cores.
- The OMAP3 family processors consist of ARM Cortex-A8 and C64x DSP cores. They are broken into 3 distinct groups based on their market and application area: the OMAP34x, OMAP35x and the OMAP36x.
- As announced recently, the OMAP4 contains dual-core ARM Cortex-A9 with C64x core.

Advantages of ARM/DSP Architecture

DSP processors are microprocessors designed to perform digital signal processing—the mathematical manipulation of digitally represented signals. Digital signal processing is one of the core technologies in rapidly growing application areas such as wireless communications, audio and video processing and medical signal processing. Today's DSP processors are sophisticated devices with impressive capabilities [12].

Most DSP processors use a fixed-point numeric data type instead of the floating-point format, they tend to be cheaper and less power consuming and the floating-point formats require more complex hardware to implement [13].

As shown in Fig. 2-7, all DSP processors from TI supports high-performance, repetitive, numerically-intensive and signal-processing-specific tasks [12]. On the other hand, ARM processors evolve to deliver high-performance in general purpose handling.

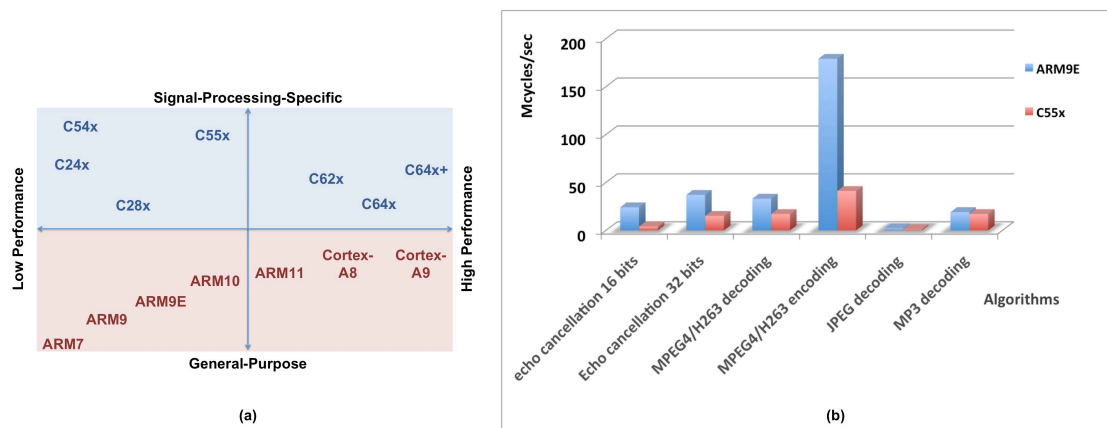


Fig. 2-7: (a) A generalized performance analysis of DSP and ARM processors [25] and (b) performance comparison between ARM9E and DSP C55x based on execution of several signal/image processing algorithms [14].

TI conducted a comparative benchmarking study, based on published data, which shows that a typical signal processing task executed on the ARM9E averagely requires three times as many cycles as the same task requires on a C55x™ DSP (see Fig. 2-7) [14]. In terms of power consumption, tests show that a given signal-processing task executed on such a RISC engine consumes more than twice the power required to execute the same task on a C55x DSP architecture [14]. Battery life, critical for mobile applications, therefore, is much greater when such tasks are executed on a DSP. The OMAP architecture's use of two processors provides this kind of power consumption benefits. At the same time, it allows the DSP to gain support from the ARM processor.

For instance, a single C55x DSP can process, in real-time, a full ECG diagnostic ap-

plication, using only 40% of the available computational capability [14]. Therefore, 60% of the capacity can be employed to run other applications concurrently. At the same time, in the OMAP dual-core architecture, the ARM processor stands ready to handle any other task such as receiving a data, controlling the hardware, etc. Thus OMAP architecture is more energy efficient as well as a powerful performer.

OMAP Processors in Medical Monitoring and Diagnostics

Current trends in medical monitoring focuses on moving the patient monitoring and treatment outside of the hospital in order to reduce hospital stay and the healthcare cost [16]. Moreover, remote patient monitoring and telemedicine in emerging economies and aging societies in Europe demand portable and wireless medical system augmenting current cellular phone system.

The dual-core OMAP application processors directly address the challenges in delivering powerful medical devices. There has been a big leap in development of OMAP-based medical devices in last few years. The following are some of the academically developed medical applications where OMAP technology is in their core design:

- Automatic QT interval measurement based on OMAP 730 processor [15]
- Connected Health - a pervasive health monitoring system based on mobiles with OMAP processors [16]
- Wireless ECG monitoring system based on OMAP5912 [17]
- OMAP1510-based real-time driver's drowsiness detection and warning [18]
- Portable electrophysiologic monitoring using OMAP-family processor [19]

In the era of OMAP2 developments, OMAP5912 processor and its development board OSK5912 used by many academic groups are ceased to exist due to lack of support and propriety development software. Moreover, OMAP5912 processors are no more in production. But on the other hand, OMAP3, which is a forerunner of OMAP2, picked the pace not only in industry but also in biomedical academic environments. The OMAP3 processors are offering the following advantages over the

OMAP2 architecture:

- OMAP3 processors are the application processors based in the ARM Cortex-A8 and are a scalable processing platform that provides the general purpose, signal and graphics processing [20].
- The ARM Cortex-A8 on OMAP3 chip provides a 4.7x and 2.8x performance improvement over ARM9 and ARM11 respectively to achieve high performance [20].
- Reduction in size and power consumption of the OMAP3 processors allows battery-operated and energy efficient end-products [20].
- Development on the OMAP3 processors has exponentially risen, since the TI announced the open-source support for these processors [20].
- The OMAP3 architecture support almost all the embedded operating systems e.g., WindowsCE, Embedded-Linux, QNX, Maemo, Android, etc [20].

The OMAP3 architecture currently supports two product families: OMAP35x and OMAP34x. The OMAP34x is intended for high-volume wireless OEMS and ODMs, while the OMAP35x family processors are designed to meet the requirement of high performance with low power consumption. The FIRST OMAP35x was developed with only ARM Cortex-A8 and later added C64x+ DSP, video accelerator and SGX graphics in its most recent processor OMAP3530 (see Appendix). Taking the advantages of the OMAP3 platform into considerations, the OMAP3530 processor was chosen for our multimodal signal processing. The OMAP3530 processor's ability to speed up the performance in peripheral task handling and signal processing were the vital features to be used in this application.

2.4 OMAP3530 - DUAL-CORE APPLICATION/SMARTPHONE PROCESSOR

OMAP3530 is a high-performance, applications processor based on OMAP™ 3 architecture provided by Texas Instruments in 2008, which is designed to provide lap-

top like performance with excellent real-time computing capability [11].

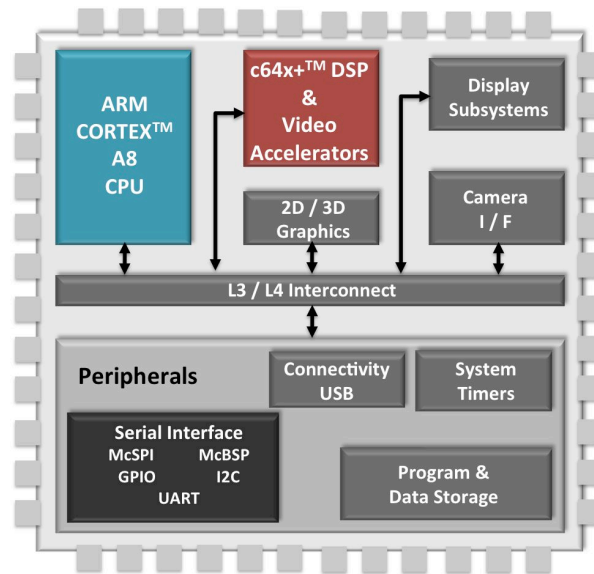


Fig. 2-8: An overview of OMAP3530 subsystems.

General subsystems of OMAP3530 shown in Fig. 2-8 are summarized as:

MPU - ARM Cortex-A8

As discussed earlier, the Cortex-A8 core fulfils the role of a general-purpose processor running various Embedded Linux distributions like Ångström, Debian ARM, Ubuntu ARM or even Google's Android. With the ability to scale in speed from 600MHz to greater than 1GHz, the Cortex-A8 processor can meet the requirements for power optimized mobile devices with a power budget of less than 300mW and for performance optimized consumer applications requiring up to 1200 Dhrystone MIPS [21].

IVA2.2 Subsystem with a TSMC320C64x+ DSP

This is the DSP Core, which provides dedicated signal processing and computing [21]. This core is very advanced very-long-instruction-word processor targeted for hand-held devices, gaming consoles, video and image processing and communication devices.

2D/3D Graphics

POWERVR SGX™ subsystem provides **2D / 3D graphics** for advanced display using a graphics accelerator (only on OMAP3530) [21].

Display Subsystem

Display subsystem with a wide variety of features for multiple concurrent image manipulation, and a programmable interface supporting a wide variety of displays. The display subsystem also supports NTSC/PAL video out.

L3 and L4 interconnects

The interconnects provide high-bandwidth data transfers for multiple initiators to the internal and external memory controllers and to on-chip peripherals e.g, timers, memory, etc [21].

Serial interfaces

The interfaces furnish communication between OMAP3530 and external peripherals, They are multifunctional pins and can be accessed through programmable selection [21]. The multiplexing of the serial interfaces are discussed in Section 4.

The OMAP3530 also offers:

- A comprehensive power and clock-management scheme that enables high-performance, low-power operation, and ultralow-power standby features. The device also supports SmartReflex™ adaptative voltage control. This power management technique for automatic control of the operating voltage of a module reduces the active power consumption.
- Memory stacking feature using the package-on-package (PoP) implementation

Developments on the OMAP3530 processor

Embedded development boards/kits are generally produced to facilitate the necessary hardware components with the embedded processor on the same PCB. These boards allow the developers to prototype the peripheral hardware and program the embed-

ded processor. In the same way, one requires a basic set of peripherals to communicate with the OMAP3530 processor. Therefore, there is a growing number of evaluation boards available in the market since the launch of the OMAP3530 chip in 2008 (listed in appendix). As shown in Table 2-2, we had four choices for the OMAP3530 board to begin the developments and embedded programming at the time of project initialization.

Table 2-2: A list of OMAP3530 development boards available at the launch of the OMAP3530 processor [22]

Board	Company	Peripherals	Support / Community	Price (\$)
OMAP35x EVM	TI with Mistral Solution	Nearly all	Commercial and TI developers community	1495.00
BeagleBoard	Beagleboard.org	Nearly all	Commercial, open source and google groups	149.00
EMP3530	Empower	For video processing	Commercial & open source	900.00
Overo	Gumtrix	Expansion board	Commercial, open source and Gumtrix mailing list	219.00

We considered the following factors in choosing the board best suited for our applications and requirements:

- Performance
- Development efforts
- Development risk
- Roadmap risk
- Cost
- Size
- Power consumption

The OMAP3530 processor can be ordered as part of an official full-scale evaluation module (OMAP3530EVM, Texas Instruments) that provides most peripherals such as a numeric keypad and a TFT display for completeness. The EMP3530 and Overo are customized and facilitate only limited number of peripherals. For our purposes

more suitable is a different interesting approach to development boards and follows the idea of keeping the board as simple as possible and supplying only the most needed peripheral hardware mounted on the board itself. Such a system has been developed for the OMAP3530 by an open source community under the name BeagleBoard (BeagleBoard.org, USA).

Unlike commercial development boards, the BeagleBoard has an open source and freely supported operating system coming with a growing repository of working applications. The large and advantageous development community of BeagleBoard developers can often solve a problem faster than the technical support of TI can do, although most community efforts are currently still aimed towards the Embedded Linux ARM part of the system [30]. On top of the low price and large and fast support, the BeagleBoard has another advantage: Its physical dimensions are just around 10x10 cm, making it more suitable for portable and mobile applications.

2.5 BEAGLEBOARD – OMAP3530 DEVELOPMENT BOARD

The USB-powered BeagleBoard is a low-cost, fan-less single board computer based on a TI OMAP3530 dual core processor that is said to reach laptop-like performance and integrates a 600MHz ARM Cortex-A8 core with a high-end 430MHz DSP-TMS320C64x core [23]. Fig. 2-9 shows the BeagleBoard with its component names and the peripheral connections. The important features and connections of the BeagleBoard are discussed below [23]:

- OMAP3530, mounted in the center of the BeagleBoard is surrounded by the needed peripherals.
- The BeagleBoard can be powered from the power jack or USB on-the-go (OTG) port.
- The serial-port is provided to boot and program the BeagleBoard on the PC.

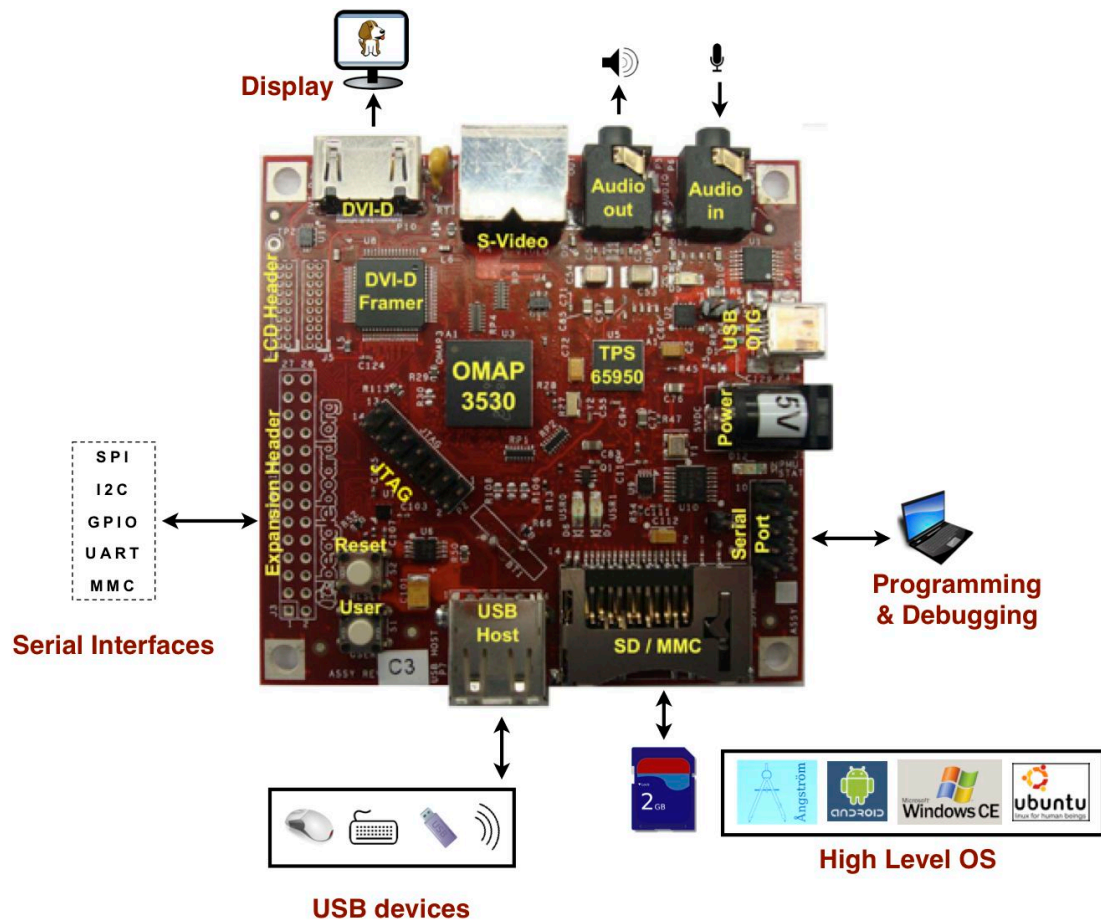


Fig. 2-9: The BeagleBoard rev. C3 and its peripheral connections.

- The SDcard containing the portable high-level operating systems e.g., embedded Linux, WindowsCE, Ubuntu etc. can be plugged in the card slot.
- The USB host provides an access to the user interaction peripherals e.g., mouse, keyboard, WLAN adaptor, USB sticks, etc.
- The expansion header, which is an array of the serial pins from OMAP3530, provides the serial linking to the outer hardware. The multiplexing the serial interfaces are discussed in section 4.
- The LCD Header can be used for enabling touch screen display.
- The DVI-D port can be linked to the conventional display monitors and provides the visualization of the desktop environment.
- The Audio-in and -out jacks give access to the audio devices such as speakers and microphones.

- The JTEG is provided for the programming and debugging purpose.
- The push-switches USER and RESET can be used for changing user and re-booting the BeagleBoard respectively.

Some of the important specifications of the BeagleBoard:

Size: 7.62cm X 7.62cm

PCB Layers: 6

Power consumption: 1.75W

Voltage requirement: 5V DC

On board clock: 48MHz

Thus, the BeagleBoard provides the platform to the OMAP3530 with required peripheral. It also facilitates programming the OMAP3530. The BeagleBoard development environment, which has been created in order to program the OMAP3530 for our application, is discussed in the next chap.

2.6 REFERENCES

- [1] K. Qian, D. Haring and L. Cao. *Embedded Software Development with C*, New York: Springer, 2009. Print.
- [2] <http://www.electronics-manufacturers.com/products/electrical-electronic-components/integrated-circuit-ic/system-on-chip-soc/> Web 20. Sept. 2010.
- [3] Wikipedia article, SoC. Web 20. Sept. 2010.
- [4] http://news.cnet.com/ARMed-for-the-living-room/2100-1006_3-6056729.html. Web. 20 Sept. 2010.
- [5] http://en.wikipedia.org/wiki/ARM_architecture. Web 20. Sept. 2010.
- [6] document, Vortex86SX and ARM-Based SoC Comparison, Web 17 Dec. 2007.
- [7] <http://www.linuxfordevices.com/c/a/Linux-For-Devices-Articles/Snapshot-of-the-embedded-Linux-market-May-2006/> Web. 21 Sept. 2010.
- [8] <http://www.arm.com/products/processors/index.php>. Web. 21 Sept. 2010.
- [9] <http://www.techautos.com/2010/03/14/smartphone-processor-guide/>. Web. 21 Sept. 2010
- [10] White paper, ARM Ltd, www.arm.com. File name: tiger_whitepaper_fina
- [11] Document, Texas Instruments Inc. www.ti.com. File name: spry112a
- [12] Whitepaper. "Choosing a DSP Processor". Berkeley Design Technology, Inc. 2000.
- [13] K. Kariya, "Evolution of DSPs," *Credit Report*, Indian Institute of Technology, 2002, pp. 1-13.
- [14] Whitepaper. "OMAP™: Enabling Multimedia Applications in Third Generation (3G) Wireless Terminals". Texas Instruments Inc., Dec. 2000. File name: SWPA001.
- [15] E. Lim, X. Chen, C. Ho, Z. Tin, and M. Sankaranarayanan, "Smart phone-based automatic QT interval measurement," *2007 Computers in Cardiology*, 2007, pp. 645-648.

- [16] William Walker, A. L. Praveen Aroul, Dinesh Bhatia, "Mobile Health Monitoring System", IEEE Engineering in Medicine and Biology Conference, Minneapolis, September 2009.
- [17] J. Liang and Y. Wu, "Wireless ECG Monitoring System Based on OMAP," *2009 International Conference on Computational Science and Engineering*, 2009, pp. 1002-1006.
- [18] C. Lin, Y. Chen, T. Huang, T. Chiu, L. Ko, S. Liang, H. Hsieh, S. Hsu, and J. Duann, "Development of Wireless Brain Computer Interface With Embedded Multitask Scheduling and its Application on Real-Time Driver's Drowsiness Detection and Warning," *IEEE TRANSACTIONS ON BIOMEDICAL ENGINEERING*, vol. 55, 2008, pp. 1582-1591.
- [19] K. Mankodiya, S. Vogt, A. Kundu, M. Klostermann, J. Pohl, A. Ayoub, H. Gehring, and U. Hofmann, "Portable electrophysiologic monitoring based on the omap-family processor from a beginners' prospective," *16th International Conference on Digital Signal Processing*, 2009.
- [20] OMAP35xx bulletin. www.ti.com. File name: sprt457b
- [21] OMAP3530 datasheet: Texas Instruments. OMAP3530/25 Application Processors. Feb. 2008. Literature Number : SPRS507F.
- [22] http://processors.wiki.ti.com/index.php/OMAP3_Boards. Web. 05 Oct. 2010.
- [23] <http://www.beagleboard.org>, BeagleBoards Software Reference Manual, Rev. B.5. 2008.
- [24] Datasheet-ARM Cortex-A8, ARM Ltd, www.arm.com, File name: DDI0344
- [25] Presentation. "Use a microprocessor, a DSP or both?". Berkeley Design Technology, Inc. 2008.
- [26] P. Raghavan, Amol Lad, Sriram Neelakandan. Embedded linux design and development. New York, Auerbach publications, 2006
- [27] Mark Hackmann, ARM Cores Climb into 3G territory. <http://www.extremetech.com/article2/0,3973,633095,00.asp?kc=ETTH102099TX1K0100486>
- [28] Markus Levy. The history of the ARM architecture: From inception to IPO.

ARM IQ, 4(1), 2005.

- [29] Andrew Nusca (20 August 2009). "Smartphone vs. feature phone arms race heats up; which did you buy?"
- [30] Mankodiya, K., Vogt, S., et al. (2009). Portable electrophysiologic monitoring based on the omap-family processor from a beginners' prospective. In 16th International Conference on Digital Signal Processing, Santorini, Greece.

3. PROGRAMMING THE OMAP3530

The BeagleBoard is the development board, which is comprised of the dual-core smartphone processor, OMAP3530 and the necessary hardware components. The BeagleBoard provides the platform for developers to program and debug the OMAP3530. Moreover, it eases the rapid prototyping of the external controllable hardware. In this work, virtual appliance containing the BeagleBoard development environment was created in order to design and compile the BeagleBoard executable algorithms. This section describes the development environment as well as how to create and compile BeagleBoard executable programs. At the end, two embedded programs with the BeagleBoard are demonstrated in order to validate the functioning of the development environment for medical applications.

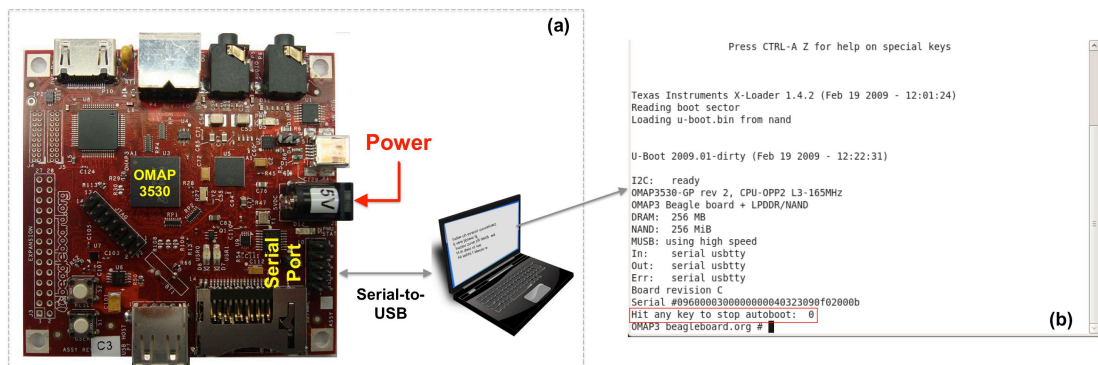


Fig. 3-1: Out-of-box testing of the BeagleBoard.

(a) The BeagleBoard connected to a PC via serial-to-USB link. (b) The BeagleBoard booting screen on the PC.

3.1 FIRST HANDS-ON THE BEAGLEBOARD

The BeagleBoard comes without any peripheral devices required to build a complete

system. A 5V DC adaptor can be used to power it. Secondly, in order to see the BeagleBoard booting, a serial-to-USB adaptor is required to link to the PC [1]. On a PC, by configuring serial communication parameters, the BeagleBoard booting can be visualized as shown in Fig. 3-1.

3.2 RUNNING ÅNGSTRÖM ON THE BEAGLEBOARD

The OMAP3530 on the BeagleBoard is a dual-core processor, in which the ARM Cortex-A8 plays as the role of a general-purpose processor (GPP). The ARM Cortex-A8 has an ability to run various high-level operating systems such as WindowsCE, Embedded-Linux, Google's Android, QNX, Nokia's Maemo, Ångström, etc. The Ångström (angstrom-distribution.org, USA) was chosen for the BeagleBoard in this work, because it is a stable, user-friendly Linux distributions for embedded devices [2]. The following lists the features of the Ångström:

- Ångström is a distribution with a highly portable and reconfigurable core, using the OpenEmbedded build system.
- It is intended to run on all devices with a 2.6.x kernel OpenEmbedded supports, with special attention to embedded devices (PDAs, handhelds, phones, routers, etc.).
- Ångström is a modern Linux-based distribution, and thus offers all features similar to a "desktop" distribution.

Ångström is bootstrapped using an "image", which is essentially a set of core packages already merged into archive or file-system image. This image is installed using device-specific means, and provides basic Ångström functionality. Like other embedded platforms, the Ångström image is also made available for the BeagleBoard.

Porting the Ångström on the BeagleBoard requires to follow a special procedure, which allows to prepare dual-partition on an SDcard [4]. Bootloader and linux-kernel are tranfered on each partition. The loaded SDcard is then inserted into the BeagleBoard connected to all its necessary peripheral devices shown in Fig. 3-2. By powering the BeagleBoard, the booting screen can be visualized on the screen. Consecu-

tively, the login screen pops up and allows access to the Ångström desktop environment which consists of conventional desktop environment with different computer applications such as word processing, graphics editing, gaming, music player, video player, etc. Internet can also be accessed via USB WLAN adaptor.

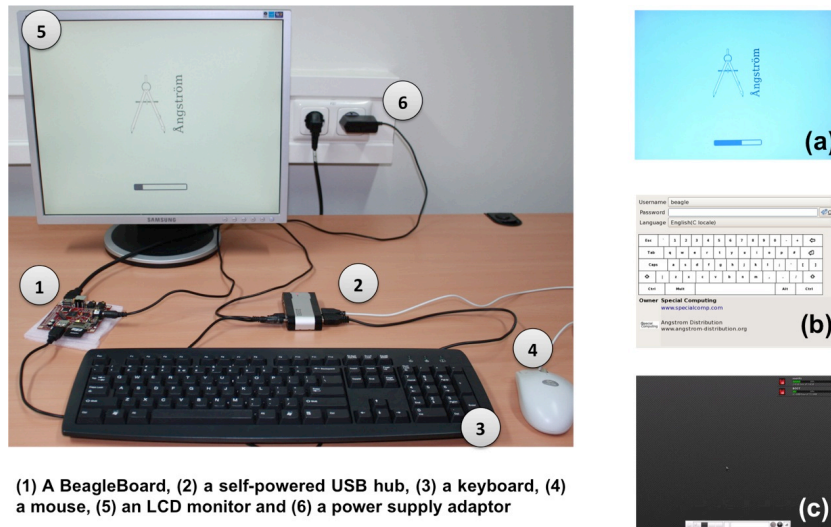


Fig. 3-2: An image of the BeagleBoard with peripheral devices. (a), (b) and (c) an Ångström booting screenshots on the BeagleBoard

3.3 DEVELOPMENT ENVIRONMENT ON A PC

With any embedded system, every developer faces the opportunity as well as the challenge to generate applications, which can be executable on the specific architecture or platform. The OMAP3530 on the BeagleBoard confines two architectures, the ARM Cortex A8 Core and the TSMC320C64x+ DSP Core. Developing applications for such dual architecture demands a suitable development environment, which can fulfil the following requirements (see Fig. 3-3):

- Ease in the process of generating applications for each architecture.
- Two different sets of tool-chains and cross-compilers for each architecture.
- Flexibility of choosing any host operating system.
- Easy transfer of the embedded executable files from the host PC to the embedded board.

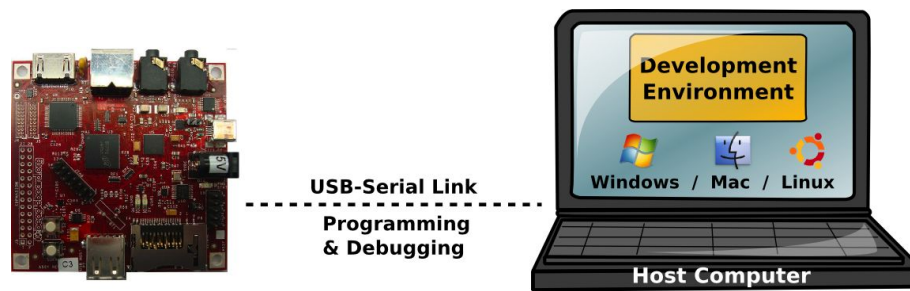


Fig. 3-3: The concept of BeagleBoard development environment.

TI's Code Composer Studio (CCS): Specialized on TI's line of DSP hardware, it provides a complete suite for code editing, generation and debugging (e.g. JTAG), needed to get started immediately. For industrial use it comes with a hefty price tag, but an academic research license is available. TI's free C6x Code Generation tool chain accompanied by the DSP/BIOS 5.X.X sources poses a fairly basic alternative to the full-fledged CCS. However it is only possible to generate plain binaries for the DSP with them. A non-proprietary way to compensate the lack of an IDE, a debugging facility and a transfer of generated DSP-binaries to the DSP-core is needed.

An alternative to the IDE part of CCS may be found in several different open source IDEs like Code::Blocks [6] or Eclipse [7], though the level of integration varies from a mere text-editor up to plugins for the transfer of binaries to the board. If there is no such plugin available, the transfer may be done with a USB stick, USB hard-drive or an SD card.

For data visualization and especially debug output we utilize the ARM Cortex itself: CodeSourcery, developer of a commercial GNU compiler collection [5] offers with Sourcery G++Lite a free open source C/C++ tool chain for ARM processors, making it relatively easy to write applications for the Linux distribution running on the OMAP35x. The missing link between the ARM- and the DSP-core is supplied by TI's DSP/BIOS-link API in a master-slave constellation. Thus, the DSP/BIOS-link API is controlling the DSP from the ARM side, starting it, stopping it and feeding it with the DSP binaries.

BeagleBoard Virtual Appliance

A significant part of the presented work involved writing C/C++ programs for dual platform of the OMAP3530 processor. This requires the setup of the whole tool-chain, from CodeSourcery ARM Compiler, DSP/BIOS-Link API and the DSP Compiler, to the Integrated Development Environment. We chose to follow a different approach than CCS, which makes the setup portable and flexible. An image of an Ubuntu installation along with all the tools needed for the embedded development was created. The image is not meant to run directly on the computer, but in a sand-box.

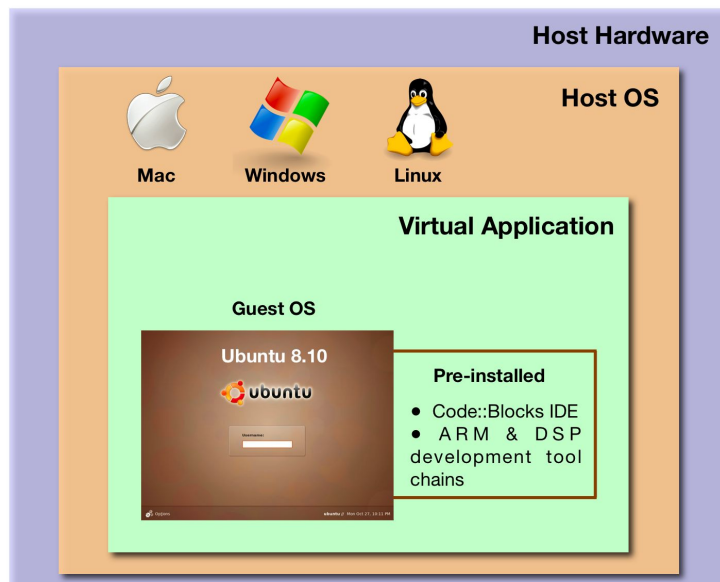


Fig. 3-4: An illustration of a virtual appliance.

The guest operating system Ubuntu 8.10 with some pre-installed programs operates in a virtual machine, which runs within any of the host operating systems such as mac, linux, windows etc.

The sandbox is called a “virtual machine” and is provided by the application VirtualBox (virtualbox.org, USA). The image on the virtual machine is called the BeagleBoard student virtual appliance, since it was intended to use for embedded development in academia and education. As shown in Fig. 3-4, the virtual machine can be run with popular host operating systems such as Mac OSX, MS Windows or Linux.

The virtual appliance contains the following tools/applications fully-installed:

- **Minicom** is an unix-based terminal emulation program which provides an access to BeagleBoard for booting, programming and debugging
- **Code::Blocks** is a C/C++ programming IDE [6]
- **GNU compiler collection** is a set of compilers and cross-compilers for ARM-based embedded systems [5].
- **CodeSourcery toolchain** is a set of tools required for ARM GNU/Linux EABI processors.
- **TI CodeGeneration toolchain** is a set of tools required for TI DSPs.
- **DSP/BIOS Link** is the foundation software for the inter-processor communication between ARM-DSP. It provides a generic API that abstracts the characteristics of the physical link connecting ARM and DSP from the applications [3].

Generating a BeagleBoard Executable Applications

The typical development cycle of an application for the BeagleBoard can be broken down in the following steps:

- Create a concept for the application.
- Implement/prove the concept in the virtual appliance.
- Cross-compile the application and test it on the BeagleBoard.

The advantages of implementing the application in the virtual appliance before going to the BeagleBoard are:

- Changes are easy to test and no transfer to the board is required.
- Compiling on a computer usually is a lot faster than compiling on the board.
- Different libraries for certain tasks may be tested without porting them to the board first.
- Both the virtual appliance and the board use a Linux Distribution and the Compiler Toolchain for both Systems is quite similar.

Implementation of “Hello World!” Program for the BeagleBoard

It has become a tradition to start the programming practice with the famous program “Hello World!”. In the same manner, a “Hello World!” example program is here shown to describe the BeagleBoard application development cycle.

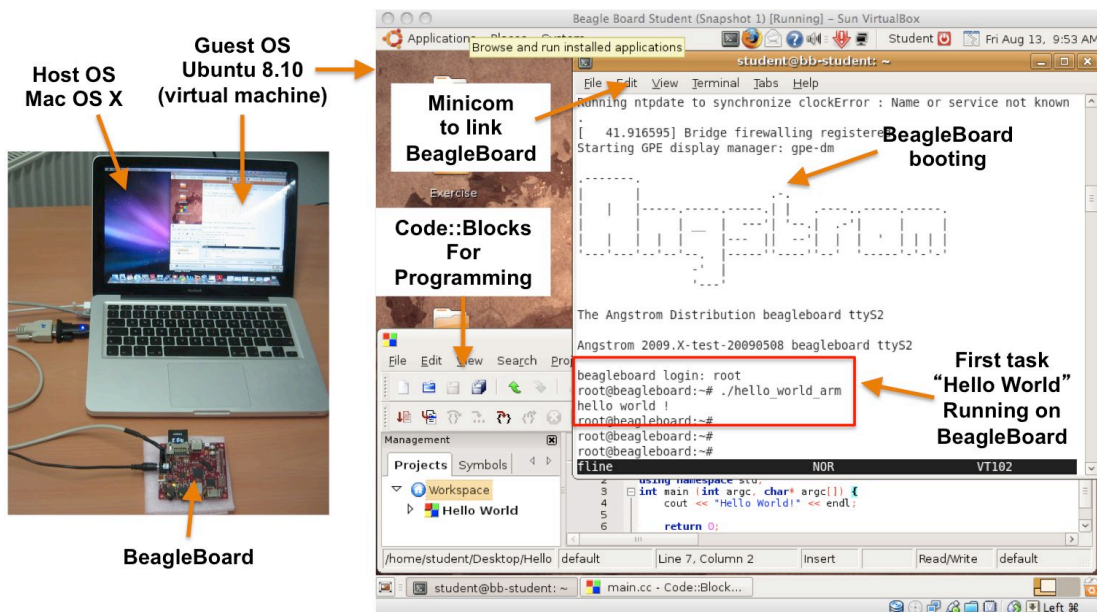


Fig. 3-5: A setup of the “Hello World!” program running on the ARM-core of the OMAP3530.

The program is developed in two simple steps (see Fig. 3-5):

1. On the virtual appliance
 - Write a simple C++ code for the famous “Hello World!” program using Code::Blocks
 - Compile it with “g++” compiler on the virtual appliance.
 - Run it to check the functionality.
2. On the BeagleBoard
 - Cross-compile the same “Hello World!” program with “arm-none-linux-gnueabi-g++” compiler on the virtual appliance.
 - By following the previous step, the BeagleBoard executable “Hello World!” application will be generated on the virtual appliance.
 - Finally, the executable file needs to be transferred to the BeagleBoard and checked for its functionality.

3.4 DATA HANDLING ON THE BEAGLEBOARD

The major part of the presented work involves real-time computing, visualization, alarming and transmission of data coming to the BeagleBoard from various hardware sensor modules. The BeagleBoard needed powerful libraries on top of C/C++ program which can effectively deliver the mentioned data handling. In this context, we chose the Simple DirectMedia Layer (SDL) libraries, which is a cross-platform multimedia library designed to provide low level access to audio, keyboard, mouse, joystick, 3D hardware via OpenGL, and 2D video frame-buffer. It also offers many advantages for embedded application development:

- It is free and written in C and C++.
- It provides a simple API to query the capabilities of the sound card.
- It facilitates the raw pixel based on the signal value, which is a foundation for different types of graphic generation including 2D plotting.
- It also supports OpenGL to perform 2D and 3D graphics.
- It includes a low level networking API for setting up and controls both TCP/IP and UDP/IP sockets.
- It provides input from the keyboard, mouse, and joystick, using an event based model
- The mailing list archives represent an enormous resource full of information about how to use SDL to solve programming problems.

In the presented work, the SDL libraries, `libSDL`, `libSDL-image`, `libSDL-ttf` and `libSDL-audio` are installed with 1.2-dev versions and used to display the real-time data plots and to generate alarms. The usage and the performance of the SDL libraries are shown in consecutive sections.

After the programming setup with the virtual environment for the BeagleBoard was ready, it was necessary to check its feasibility, especially for medical embedded applications. The following presents the performance of the BeagleBoard for two medical applications.

3.5 FEASIBILITY TEST I – HEART RATE MONITORING

Continuous monitoring of an athlete's heart rate (HR) using a wearable chest belt has been well-adopted in last few years. As shown in Fig. 3-6, a chest belt (Polar WearLink, Polar, Finland) attached on the thorax is currently in practice to detect HR and send it wirelessly to a close receiver device. A heart-rate monitor interface (HRMI, Sparkfun Electronics, USA) is one of such receivers, which receives the HR data and passes it on to the processor or computer via serial protocol. The goal of this experiment was to design an interface between the HRMI and the BeagleBoard for continuously monitoring wearer's heart rate along with the real-time plotting of the resulting HR values.

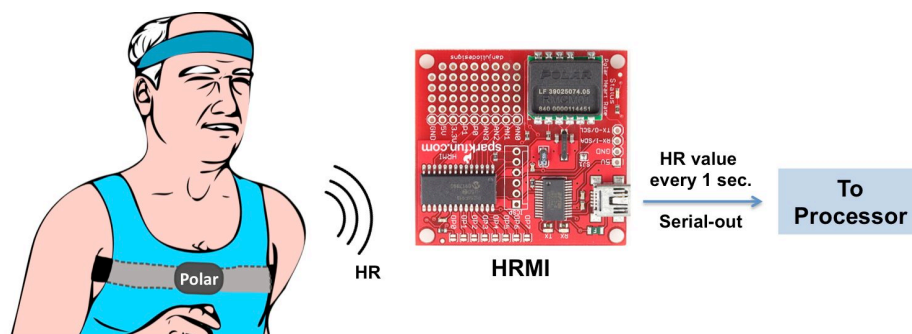


Fig. 3-6: An illustration of the heart rate monitoring using polar chest belt which transmits HR value to the HRMI

HRMI – BeagleBoard Interface

The Heart Rate Monitor Interface is a peripheral device that converts the ECG signal from Polar Electro Heart Rate Monitor (HRM) transmitters into easy-to-use heart rate data. The HRMI also provides analog inputs and a digital input/output utility port to ease integration into custom applications. General features of the HRMI are:

- multiple interfaces : USB, logic level serial and I2C
- 32-entry heart rate data history buffer
- four 8-bit ADC

- Programmable power-on default operation

In this experiment, the USB (serial) communication protocol was used to connect to the BeagleBoard due to its ease of use and programming. A USB Mini-B connector allows quick connection to the BeagleBoard. The USB interface provides both power and a data connection to the HRMI. The USB interface uses a FTDI FT232RL interface IC that exposes the HRMI as a serial device to the BeagleBoard.

On the BeagleBoard side, a program “HRV_plot” was designed by following the same development cycle mentioned earlier in this section. In the beginning, the program sets the serial communication parameters which leads to the HR data receipt at every 1 sec. As shown in Fig. 3-7, the received HR data is being plotted on the BeagleBoard desktop environment using the SDL libraries.

The HR plotting windows shows 10 min of data then it updates with new coming data. The right panel of the display shows the current HR value, the emotional status of a wearer (as detected from its HR value), the current time and the recording time. The emotional status, which is categorized in three levels; calm, normal and stressed, is extracted from the latest HR value by limiting with set of boundaries. The outlook of this work is to establish a sophisticated heart rate variability (HRV) measurement system using the BeagleBoard as a computing platform. The HRV is the measurement method of heart rate for a long period of time and gives significant information about the person under test.

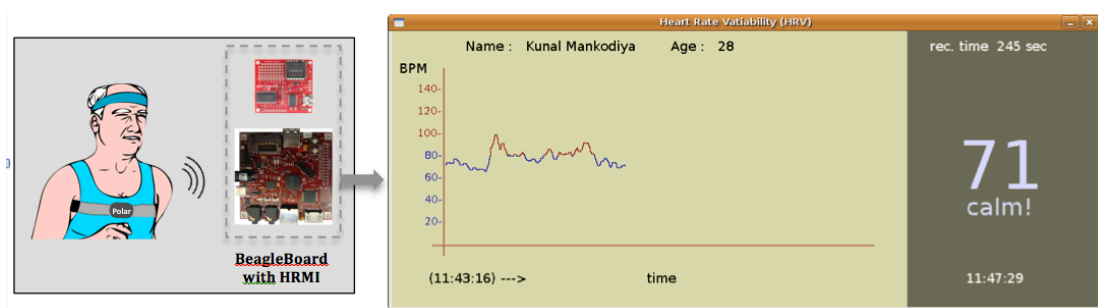


Fig. 3-7: An illustration of the HRMI-BeagleBoard interface. The display panel is 10 min. time window plotting the user’s HR.

Thus, the BeagleBoard successfully passed the test of continuously monitoring the

HR of the person wearing the polar chest belt. The test also confirmed the functionality of the development environment and the integration of the SDL libraries to plot the HR data in real-time. The next experiment will show the use of the SDL libraries in designing embedded algorithms with the alarm sounds.

3.6 FEASIBILITY TEST II – PATIENT MONITOR INTEGRATION

Audible alarms in monitors play an important role in providing information during patient monitoring. However an overabundance of separately informative alarm sounds produces unpleasant noise and becomes a nuisance to medical personnel. Consequently, a new approach to alarm sounds has to be taken, which is both informative and not annoying, even in a chorus of different monitoring systems. In order to research this question, a BeagleBoard-based interface has been developed in order to present choosable audible outputs from a set of commercially available monitors. As a proof of principle, a capnograph and a cerebral oximeter are chosen to connect with a dual-core embedded processor in order to display EtCO₂ and rSO₂ values, respectively in an audible form. The output is frequency coded into distinct harmonies, with optimal sound synthesis to be researched in the future.

Alarm Scenario in the Patient Monitoring

Intensive care units (ICU) and operating rooms are full of sophisticated patient monitoring technology (see Fig. 3-8). Even though, the medical alarms are standardized by IEC 60601-1-8, overabundance of them emits harsh and unpleasant noise, which is gradually becoming a nuisance to the clinical personnel [9, 10]. Pulse beep audible alarm is widely used and highly undistinguishable during multi-parametric patient monitoring. It has been observed that the medical staffs frequently disable the pulse beeps [11]. Standardization of alarm sounds for patient parametric changes is one of the alternatives to resolve the problems currently encountered with the use of alarms. [12]

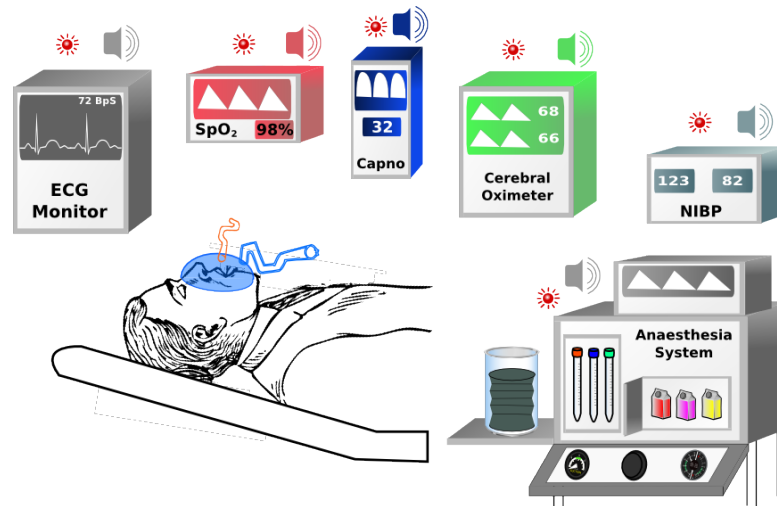


Fig. 3-8: A general scenario in patient monitoring.

Concept of Patient Monitor Integration

Fig. 3-9 represents an interface, which unifies the patient monitors in a single platform. The objective of the interface is to produce distinguishable and non-annoying alarm sounds along with the real-time patient data plotting. Nowadays, many of the commercial patient monitors facilitate a real-time digital data-out at serial or USB port. The endeavor is to utilize the benefits of these interfaces and integrate several monitors into one single platform, which is required to be small and to have high-performance capabilities. Thus, the ultimate goal is to produce distinct alarm for each patient parameter and also visualize them simultaneously.

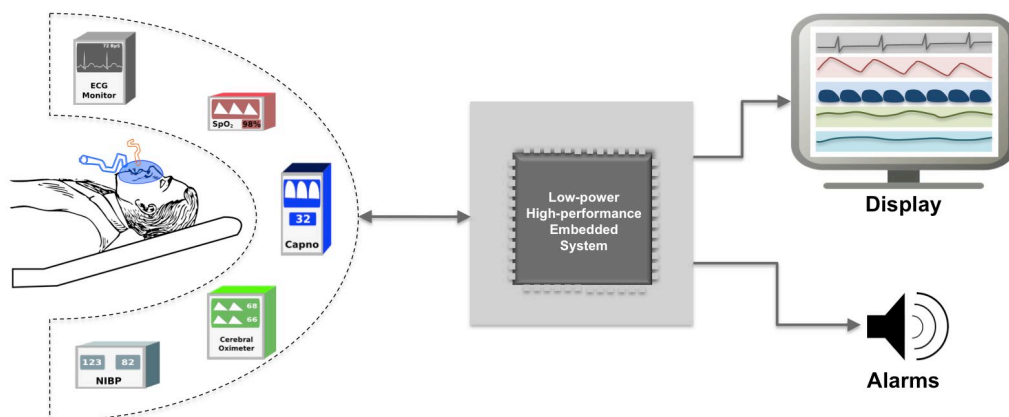


Fig. 3-9 : A conceptual diagram of patient monitor integration.

Patient Monitors with Serial Output

To demonstrate the unification of the patient monitors, two of such commercial patient monitors, a capnograph and a cerebral oximeter were chosen

A microstream portable capnograph, MicrocapPlus (Oridion Capnography Inc., USA), which provides EtCO₂ data of intubated or non-intubated patients, was used in this application. This capnograph shows instantaneous EtCO₂ value and real-time plot on its screen. A communication adaptor kit provided with this monitor facilitates data output via serial port with 50msec time-lag [13].

An INVOS 4100 (Somanetics, USA) cerebral oximeter, which is a dual-channel continuous wave spatially resolved spectrometer, is used as one of the patient monitors. The cerebral oximeter monitors regional oxygen saturation (rSO₂) from the forehead of the patient and also facilitates the data at its serial output every 5sec [14].

Integration of the Monitors with the BeagleBoard

As shown in Fig. 3-10, the capnograph and the cerebral oximeter are physically connected to a USB host port of the BeagleBoard. The rest of the BeagleBoard setup is the same as mentioned previously in this section. Two separate embedded applications CapnoPlot and Cereplot have been designed to communicate with the individual monitors.

A C++ program called CapnoPlot on BeagleBoard initiates the communication with Capnograph by inquiring a device ID and software version after the serial communication parameters are set. The EtCO₂ values are sent every 50msec to the BeagleBoard by the capnograph [13]. Using the SDL libraries, CapnoPlot also produces informative alarm sounds when the EtCO₂ value crosses the set-limits.

Similarly, a C++ program called CerePlot on the BeagleBoard executes the data transfer with the INVOS 4100. The rSO₂ values are sent every 5 seconds from the

INVOS 4100 to the BeagleBoard [14]. CerePlot not only plots the data but also triggers the alarm in order to inform clinical staff.

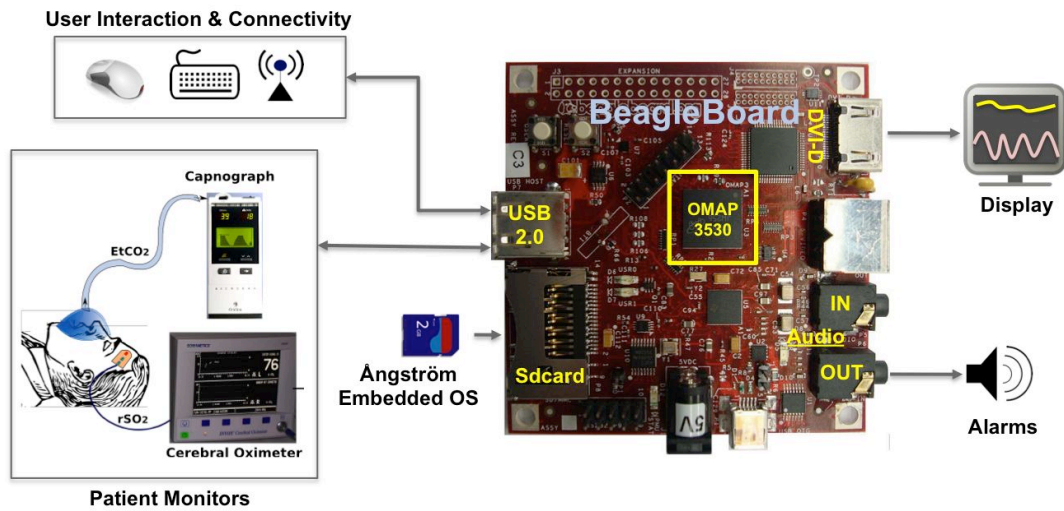


Fig. 3-10: An illustration of the patient monitor integration using the BeagleBoard as a processing unit.

Realization of Patient Monitor Integration

Fig. 3-11 shows the BeagleBoard set-up with the monitors. The CapnoPlot and CerePlot applications display the values of EtCO₂ and rSO₂ respectively on a single monitor simultaneously. The CapnoPlot requires no trigger from the capnograph to receive instant EtCO₂ values, while for the CerePlot, the digital out has to be set on the cerebral monitor.

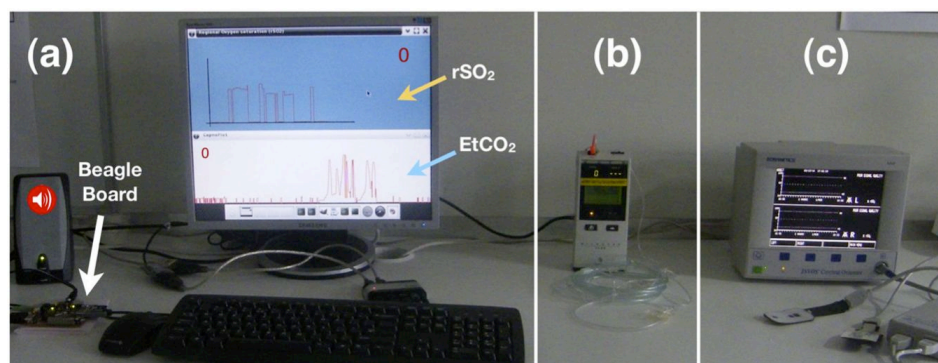


Fig. 3-11: An original practical setup of the patient monitor integration.

(a) A BeagleBoard with the peripheral connections and display, connected to (b) the Micro-cap®Plus and (c) the INVOS 4100 with the SomaSensor.

CapnoPlot

Fig. 3-12a shows the screen capture of Microcap⁺Plus. Although the capnograph does store patient's long-term EtCO₂ data, it displays the current capnogram only briefly. The EtCO₂ value alone is updated every 5 seconds. The monitor sounds for security reasons a beep alarm when the EtCO₂ value is zero for a finite time period.

Fig. 3-12b shows collected EtCO₂ data plotted by the CapnoPlot. Quantisation steps in the plot indicate that instant EtCO₂ value was sent to BeagleBoard every 50ms. Our EtCO₂ graph shows consecutive patient's data for 5min before it is updated. Currently three different types of audio output are enabled related to the EtCO₂ level (Fig. 3-12c). For EtCO₂ values below the lower limit, no sound is given, in order to reduce the noise. For intermediate levels the base frequency of 100Hz (sinusoidal) is presented. This sound is varied proportional to the gathered EtCO₂ value, according to the following formula:

$$\text{sound}(\text{output}) = 0.25 \times \text{EtCO}_2 \times 100\text{Hz} \quad \text{Eq. 3-1}$$

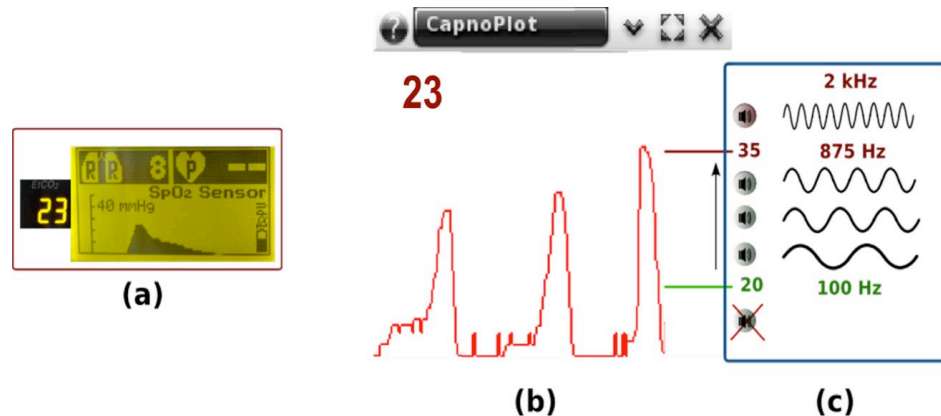


Fig. 3-12: The performance of the CapnoPlot.

(a) Microcap-Plus screen capture, (b) corresponding CapnoPlot screenshot over several breathing cycles, and (c) illustration of CapnoPlot audio profile.

The third level is a classical alarm to inform the anesthesiologist that the EtCO₂ value is currently above the upper limit. This alarm is a continuous sinusoidal audio output with 2 kHz. The upper and lower limits of the EtCO₂ trend can be changed in the CapnoPlot program, but will be integrated in the display panel in the future. The

current output proves the principle of the audible presentation of the monitoring data. Our audio module is under constant improvement until finally the most ergonomic path to convey information will be found for the ICU.

CerePlot

A comparison of visual outputs for the cerebral oximetry is shown in Fig. 3-13. Subplot 3-9b shows the screen capture of the commercial INVOS 4100. It displays the patient's forehead rSO_2 value every 5sec and marks it in a plot over two hours. It sounds a continuous alarm in case no signal is detected for some minutes.

Subplot 3-9a shows the gathered rSO_2 value plotted by CerePlot. The rSO_2 value is updated every 1sec and the trend plots the patient's data for 10 minutes before it updates. Glitches in the CerePlot trend are caused by faulty digital data sent by the INVOS port.

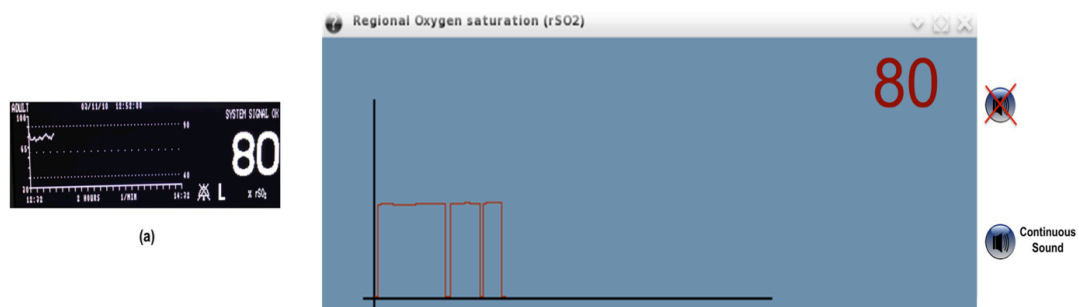


Fig. 3-13: The performance of the CerePlot.

(a) A screenshot of the INVOS 4100 and (b) a corresponding CerePlot screenshot.

The audible alarm scheme of CerePlot is currently set to intermittent, but will be designed for pleasant sound bursts, to distinguish them from the CapnoPlot alarm.

The programs CapnoPlot and CerePlot successfully performed the collection of the real time data from the patient monitors and displayed the values on a single display screen. Moreover, the programs provided the data-driven audio output on the speakers connected to the BeagleBoard. Thus, this exemplary patient monitor integration

with the BeagleBoard was a successful proof-of-the-concept design and opened a new window for how to utilize the existing monitors in a more efficient manner.

Hardware interfacing with the Beagleboard

Feasibility tests I and II proved the BeagleBoard's eligibility in building embedded applications in the field of medical technology. Now, it is to see that how the BeagleBoard is able to talk to novel analog front-ends instead of the commercial patient monitors. The next chapter will show an embedded setup, in which the BeagleBoard communicates with the analog-to-digital converter via fast interface protocol. The analog front-end interfacing will allow the health monitoring signals to be processed in the OMAP3530.

3.7 REFERENCES

- [1] BeagleBoard diagnostics.
<http://code.google.com/p/beagleboard/wiki/BeagleBoardDiagnostics>. Web 22 Apr. 2010.
- [2] Ångström- Distributions. <http://linuxtogo.org/gowiki/Angstrom>. Oct. 2009. Web 22 Apr. 2010
- [3] TI DSP/BIOS Link 2005: Texas Instruments. DSP/BIOS LINK, November 22 2005.
- [4] How to get Angstrom running,
<http://code.google.com/p/beagleboard/wiki/HowToGetAngstromRunning>
Web 22 Apr. 2010.
- [5] <http://www.codesourcery.com>. *Sourcery G++ light*. 2009 [cited 2009 2.3.2009].
- [6] <http://www.codeblocks.org/>. Code::Blocks -The open source, cross platform, free C++ IDE. . 2009 [cited 2009 2.3.2009].
- [7] <http://www.eclipse.org/>. Eclipse website: Open source IDE. 2009 [cited 2009 2.3.2009].
- [8] HRMI user manual, www.sparkfun.com, USA.
- [9] AJ Cropp, LA Woods, „Name that tone: the proliferation of alarms in intensive care units“, *Chest*. 105(4), 1994, 1217-1220.
- [10] Y Donchin, FJ Seagull. „The hostile environment of the intensive care unit“, *Curr Opin Crit Care*. 8, 2002, 316–20.
- [11] R.M. Craven and A.K. Mcindoe, "Continuous auditory monitoring — how much information do we register?," *British Journal of Anaesthesia*, vol. 83, 1999, pp. 747-749.
- [12] Osinaike B. B., Amanor-Boadu S. D., Oyebamiji E.O., Tanimowo A, Dairo M.D., "Audile Monitor Alarm : Friend or Foe ?," *Anaesthesia online*
- [13] Communication Interface-Microstream[®] portable capnographs, Oridion Inc. 2004
- [14] Instruction Manual - INVOS Monitors, Somanetics, 2004

4. NOVEL HARDWARE INTERFACING WITH THE OMAP3530

Since the focus of the presented work is to design a multimodal system, it is highly important to consider the hardware requirements. This section overviews the system layout with individual component details. Among all the components, an ADC, which is an essential element, plays a major role in terms of signal quality. In this work, the ADC is an interface between the multimodal analog hardware (see the following sections) and the OMAP3530 processor. The high-resolution delta-sigma ADC is chosen in order to cover all the health monitoring parameters.

Enabling communication between the chosen ADC and the OMAP3530, which is a challenging task, has been elaborated in the later part of this section. The section will explore the expansion pins of the OMAP3530 and describe how to configure the pin multiplexer for the SPI port on the BeagleBoard. At the end, the OMAP3530's SPI port will give an access to the ADC. This chapter sets foundation for the following sections for developing the continuous and unobtrusive health monitoring with the OMAP3530-based system.

4.1 GENERALIZED BIOSIGNAL ACQUISITION SYSTEM

Without exception, all biosignals are analog signals. Biosignals have amplitudes in the microvolt to millivolt range and spectral components of interest occur in the frequency range from 0.01 Hz to 10kHz [1].

Fig. 4-1 shows a general overview of a biosignal preprocessing system. The analog hardware fulfils the need of amplification and also filtering by selection of cut-off

frequencies (see detailed explanations in the following sections). Consecutively, the amplified biosignals need to be discretised before they go into the processor or a computer for further processing. The selection of the individual components is highly dependant on the signal of interest.

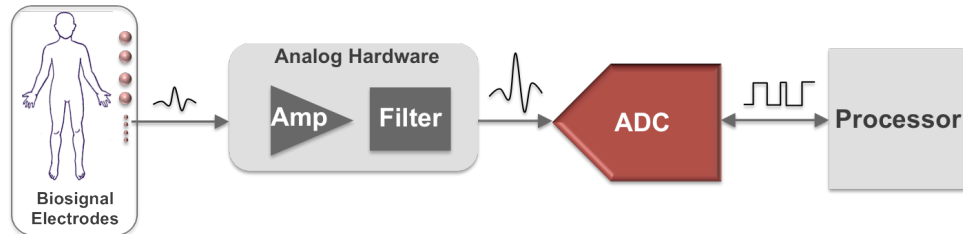


Fig. 4-1: A generalized biosignal acquisition system.

Biopotential signals and their impact on the system hardware design

Table 4-1 lists some of the biosignals having a diagnostic significance in major diseases. The signals range from a very few microvolt to hundred millivolt. Further more, they possess a vast frequency range from DC to 5kHz. To scale them to 3-5V range, there is a need of variation in amplification as well as the resolution bits. In order to cover the whole range of the biosignals into a single ADC, a high bit-resolution is recommended in order to handle the varieties of frequencies and amplitudes [2]. The ADC plays a vital role and quantifies the biosignals before they enter into the processor for further computing. The quality of a signal and its processing in the processor is highly dependent on the type of ADC used. A high bit resolution e.g., 24-bit allows the unification of the gain factor and hence minimizes the cost and size of the system.

Table 4-1: Typical system characteristics of the biosignals [3].

Type	Amplitude	Resolution [bits]	Bandwidth [Hz]	min. SR [s/sec/ch]	No. of channels	max. Gain
EEG	5-300 μ V	9-24	0.05-5k	10k	1-100	10000
ECG	0.5-4mV	8-18	0.05-250	500	1-13	1000
EMG	5 μ V – 100mV	8-16	1-1k	2k	1-2	1000
EOG	10 -100mV	8-16	DC-40	100	1-4	1000
SpO ₂	1-100mV	8-16	0.05-250	400	1	1000
rSO ₂	1-50mV	8-16	0.05-10	100	2	1000

There are two popular ADC architectures: Successive Approximation Register (SAR) and Delta-Sigma ($\Delta\Sigma$). The SAR architecture is one of the most popular ADC architectures used in precision applications. The precision in the SAR architecture is primarily due to the precision and analog performance of the components of the ADC - capacitor matching, DAC settling time, and comparator accuracy and speed [3]. However, the disadvantages for SAR ADCs include the need for trimming to achieve good performance and more stringent front-end filtering for anti-aliasing [3].

The other popular architecture, delta-sigma architecture differs from the SAR in that it relies more on digital processing techniques than on component matching and analog precision to achieve high performance. The delta-sigma ADC offers the following advantages over other architectures [3]:

- The sampling rate is typically much higher.
- It simplifies the analog-front-end
- The architecture is inherently linear.
- The sophisticated digital processing techniques and filtering used provide for a very high dynamic range.

Delta-sigma ADC

The key feature of a Delta-Sigma ($\Delta\Sigma$) converter is that it is the only low cost conversion method, which provides both high dynamic range and flexibility in converting low bandwidth input signals. As, many of the interested biosignals considered in this work have very low frequency component, the delta-sigma architecture is very suitable.

As in the block diagram shown in Fig. 4-2, the input analog signal is oversampled at high frequency and is then sent to the digital decimator filter. By averaging over multiple samples at a decimator, Delta-Sigma converters reach a much better signal-to-noise ratio than SAR or pipeline converters. The averaging performed by the converter usually occurs in the form of a Finite Impulse Response (FIR) or Infinite Impulse Response (IIR) digital filter [4]. As a result, the acquisition time is longer than it is with a Successive Approximation Register (SAR) or Pipeline converters, which only samples the signal once for each conversion [4].

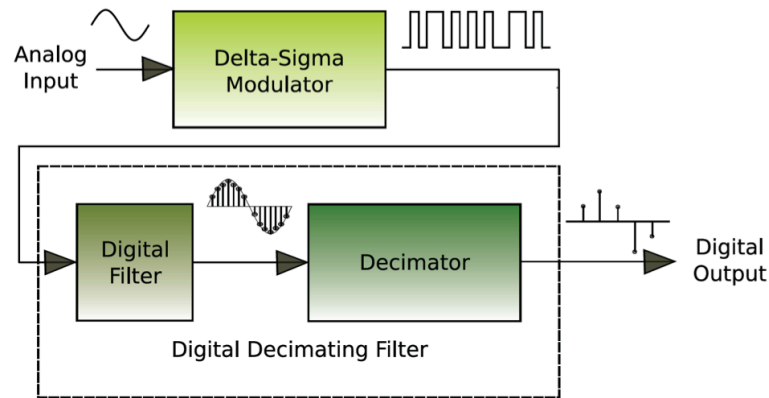


Fig. 4-2: A block diagram a Delta-Sigma converter [4].

At the time of selecting the Delta-Sigma ADC for our applications, several requirements were to be met:

- The ADC needs to provide multiple single and differential analog input channels.
- High sampling rate per channel upto 10kSps is preferred.
- The bit resolution is required to be more than 20-bit.
- It must provide fast communication protocol.
- It should come with evaluation board in order to speed up the prototyping.

After thorough analysis on available Delta-Sigma ADCs in the market, ADS1258 (Texas Instruments inc., USA) was chosen due to its high suitability to the above requirements.

4.2 ADS1258 – 16-CHANNEL ADC

The ADS1258 is a 16-channel (multiplexed), low-noise, 24-bit, Delta-Sigma ADC. The functional components of the ADS1258 shown in Fig. 4-3 are described as following [5]:

- A flexible input multiplexer accepts combinations of eight differential or 16 single-ended inputs with a full-scale differential range of 5V or true bipolar range of $\pm 2.5V$ when operating with a 5V reference.

- The fourth-order delta-sigma modulator is followed by a fifth-order sinc digital filter optimized for low-noise performance.
- The differential output of the multiplexer is accessible to allow signal conditioning prior to the input of the ADC.
- Internal system monitor registers provide supply voltage, temperature, reference voltage, gain, and offset data.
- The ADS1258 operates from a unipolar +5V or $\pm 2.5\text{V}$ analog supply and a digital supply compatible with interfaces ranging from 2.7V to 5.25V.
- Serial digital communication is handled via an SPI™-compatible interface. A simple command word structure controls channel configuration, data rates, digital I/O, monitor functions, etc.

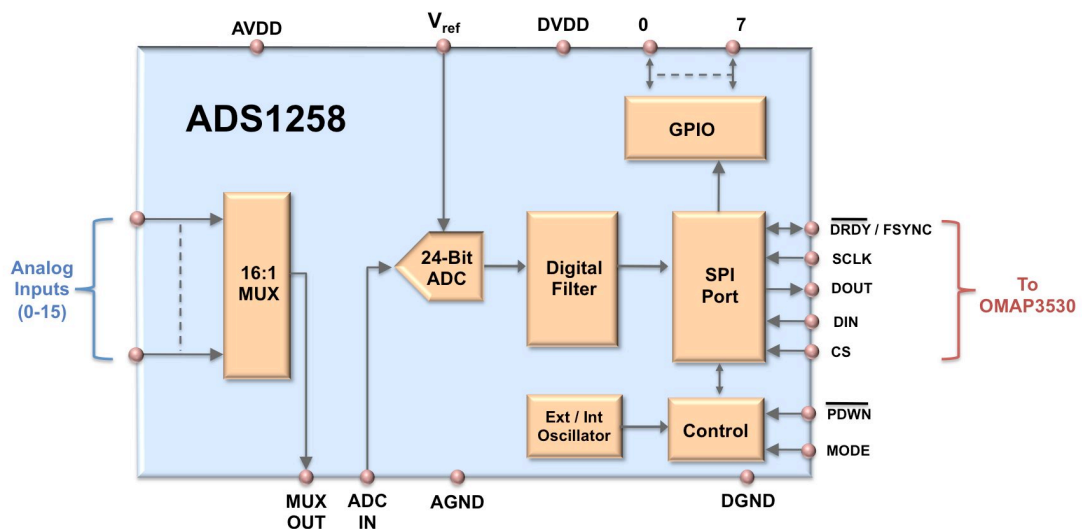


Fig. 4-3: A system block diagram of the ADS1258.

ADS1258EVM

The ADS1258 comes with an evaluation module called ADS1258EVM (Texas Instruments Inc., USA), which is specially designed for rapid prototyping and hardware interfacing. The ADS1258EVM is chosen as a stand-alone printed circuit board (PCB), instead as part of the ADS1258EVM-PDK [6]. For maximum flexibility, the ADS1258EVM is designed for easy interfacing to multiple analog sources. Fig. 4-4 reveals that the ADS1258EVM contains the ADS1258 along with the necessary

components required for connections and interfacing. The analog input header provides access to 16-channel of the ADS1258. The analog and digital power supply can be connected to the power header. The SPI header is also available to connect the ADS1258 to the processor, the OMAP3530 in our case.

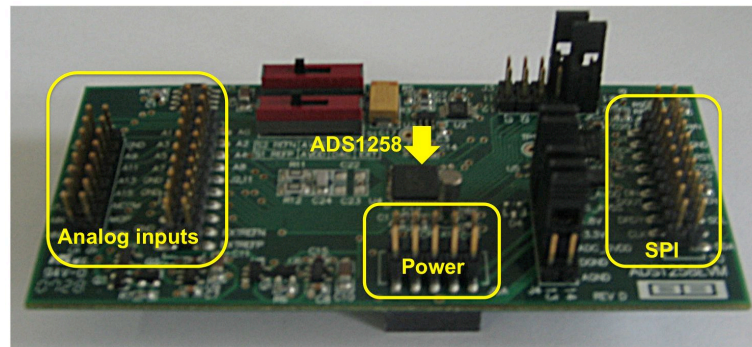


Fig. 4-4: An image of the ADS1258EVM.

4.3 SERIAL PERIPHERAL INTERFACE (SPI) ON THE ADS1258

The ADS1258 is operated via a SPI-compatible serial interface, which is a four-wire serial interface.

SPI Communication Protocol

The Serial Peripheral Interface Bus or SPI bus is asynchronous serial data link standard named by Motorola that operates in full duplex mode [7]. As shown in Fig. 4-5, devices communicate in master/slave mode where the master device initiates the data frame [7]. Multiple slave devices are allowed with individual slave select (chip select) lines. The SPI bus can operate with a single master device and with one or more slave devices. Sometimes SPI is called a "four wire" serial bus, since it SPI bus specifies four logic signals [7].

- SCLK — Serial Clock (output from master)
- MOSI/SIMO — Master Output, Slave Input (output from master)
- MISO/SOMI — Master Input, Slave Output (output from slave)
- CS — Chip Select (active low; output from master)

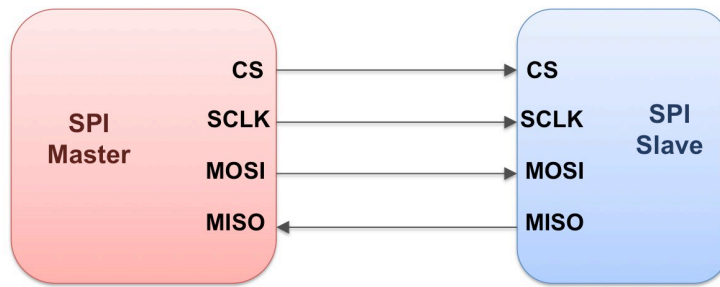


Fig. 4-5: An SPI master-slave communication protocol

To begin a communication, the master first configures the clock, using a frequency less than or equal to the maximum frequency the slave device supports. Such frequencies are commonly in the range of 1-70 MHz.

The master then pulls the chip select low for the desired chip. If a waiting period is required (such as for analog-to-digital conversion) then the master must wait for at least that period of time before starting to issue clock cycles.

During each SPI clock cycle, a full duplex data transmission occurs [7]:

- The master sends a bit on the MOSI line; the slave reads it from that same line.
- The slave sends a bit on the MISO line; the master reads it from that same line.

SPI on the ADS1258

SPI-compatible serial interface on the ADS1258 writes data to the configuration registers, using commands to control the converter and finally reading back the channel data [5]. As shown in Fig. 4-3, the interface consists of four signals: CS, SCLK, DIN, and DOUT, which are analogous to the SPI protocol signals CS, SCLK, MOSI and MISO respectively.

CS

CS is an input that is used to select the device for serial communication. CS is active low [5]. When CS is high, read or write commands in progress are aborted and the serial interface is reset.

Serial Clock (SCLK) Operation

The serial clock (SCLK) is an input which is used to clock data into (DIN) and out of (DOUT) the ADS1258 [5].

Data Input (DIN/) and Data Output (DOUT) Operation

The data input pin (DIN) is used to input data to the ADS1258 [5]. The data output pin (DOUT) is used to output data from the ADS1258 [5].

4.4 ADS1258 COMMUNICATION PROTOCOL

Communicating to the ADS1258 involves shifting data into the device (via the DIN pin) or shifting data out of the device (via the DOUT pin) under control of the SCLK input.

Reading Data

DRDY goes low to indicate that new conversion data is ready [5]. The data may be read via a direct data read (Channel Data Read Direct) or the data may be read in a register format (Channel Data Read Register).

Channel Data Read Direct

The DIN input pin is held inactive (high or low) for at least the first three SCLK transitions. When the first three bits are 000 or 111, the device detects a direct data read and channel data is output. A total of 24 or 32 SCLK transitions complete the data read operation. The number of shifts depends on whether the status byte is enabled. The data must be completely shifted out before the next occurrence of DRDY or the remaining data will be corrupted. It is recommended to monitor DRDY to synchronize the start of the read operation to avoid data corruption. Before DRDY asserts low, the MSB of the Status byte or the MSB of the data is output on DOUT (CS = '0'), as shown in Fig. 4-6.

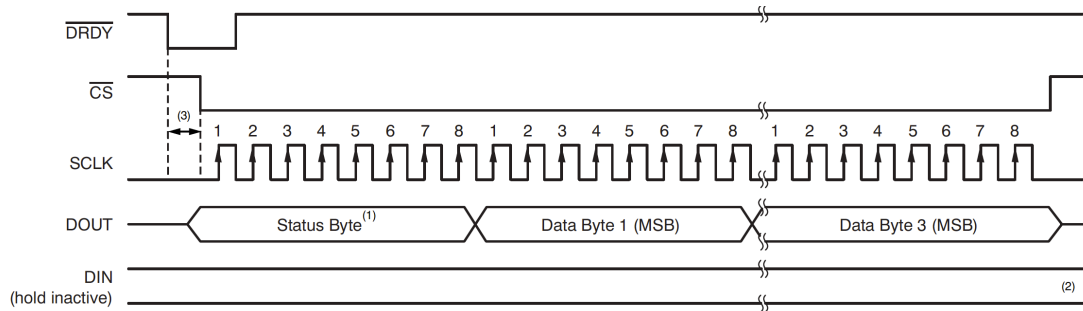


Fig. 4-6: The timing diagram of the channel data read direct [5]

Channel Data Read Register

To read channel data in this mode (register format), the first three bits of the command byte to be shifted into the device are 001. The MUL bit must be set because this command is a multiple byte read. Beginning with the eighth SCLK falling edge (command byte completed), the MSB of the channel data is restarted on DOUT. Unlike the direct read mode, the channel data can be read during a DRDY transition without data corruption. This option avoids conflicts with DRDY, as shown in Fig. 4-7.

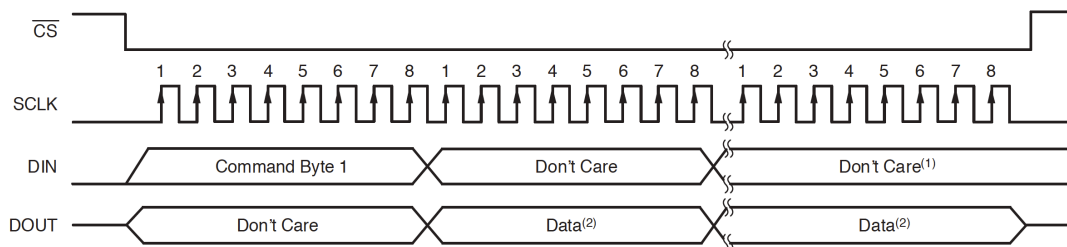


Fig. 4-7: The timing diagram for the channel data read register [5].

Register Read/Write Command

To read register data, the first three bits of the command byte to be shifted into the device are 010. These bits are followed by the multiple register read bit (MUL). If MUL = '1', then multiple registers can be read in sequence beyond the desired register.

To write register data, the first three bits of the command byte to be shifted into the device are 011. These bits are followed by the multiple register read bit (MUL). If MUL = '1', then multiple registers can be written in sequence beyond the desired register.

Channel Data Format

The data read operation outputs either four bytes (one byte for status and three bytes for data), or three bytes for data only. The MSB of the data is shifted out first. The stats byte provides the certain information regarding data, which includes new data coming, over flow, analog supply limit channel ID (0-4).

Commands

Commands are used to control the communication with the ADS1258. These commands are sent to the command byte register of the ADS1258. The command byte consists of three fields:

1. Command Bits(C[2:0]) are used to read channel data.
2. Multiple register access bit (MUL) is used to access the configuration register.
3. Register Address Bits (A[3:0]) are used to control the conversion process.

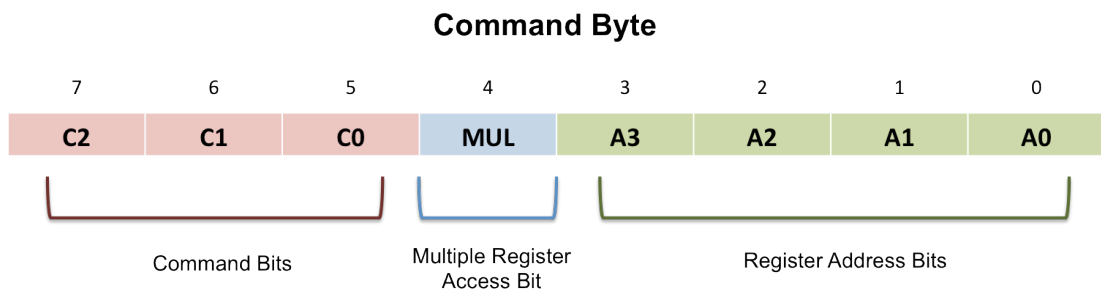


Fig. 4-8: The command byte and its three parts [5].

The SPI communication between the ADS1258 and the OMAP3530 can be enabled by connecting the four logic signals of the ADS1258EVM to the expansion header of the BeagleBoard. The communication protocol of the ADS1258 has to be considered in designing an algorithm on the BeagleBoard, which acts as a master. The BeagleBoard's expansion header contains multi-functional pins for several serial protocols, which are discussed in the following topic.

4.5 EXPANSION HEADER ON THE BEAGLEBOARD

The expansion header is provided to allow a limited number of functions to be added to the BeagleBoard via the addition of expansion hardware, which is the ADS1258 in this case [8]. The main purpose of the expansion connector is to route additional signals from the OMAP3530 processor. Fig. 4-9 shows all of the signals that are on the expansion header. The expansion header consists of 28 pins, which provide power (+5V and +1.8V), ground and multiple serial ports such as multi-channel SPI (McSPI), Multi-channel buffered serial port, multi-memory controller (mmc), universal asynchronous receiver/transmitter (UART) and general-purpose input/output (GPIO). Among all of these ports, the McSPI and McBSP are SPI compatible interfaces and hence either of them can be used for communicating with the ADS1258.

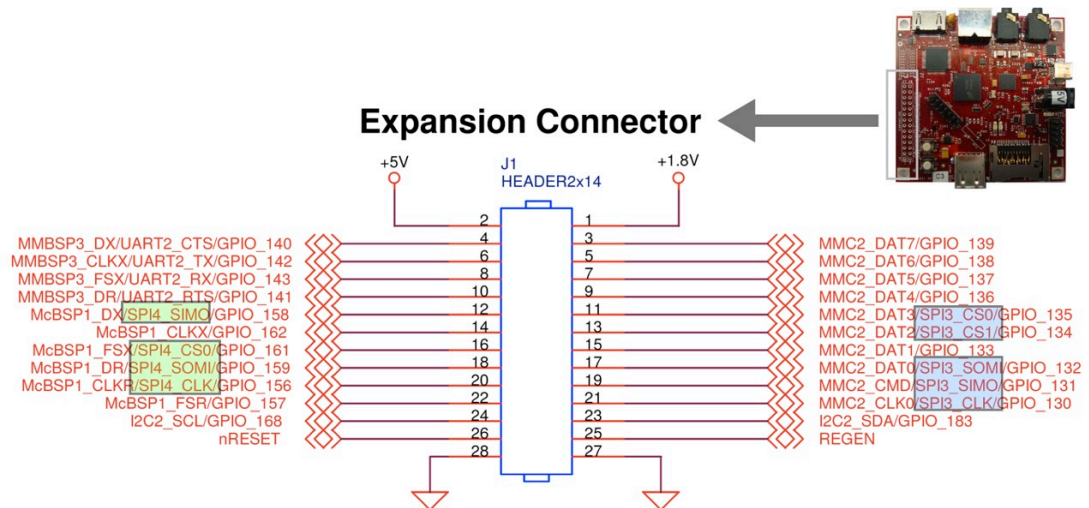


Fig. 4-9: A layout of the expansion connector of the BeagleBoard with SPI ports highlighted [8].

The McBSP interface provides interrupt functionality along with the SPI protocol, which decreases the data corruption during communication. However, the McBSP is very difficult option to implement due to limited resources e.g., device driver, technical manuals, etc. Development of our own device driver is not in the course of this work. On the other hand, the McSPI is provided with the driver software and example templates, which shortens the development process. Although the McSPI doesn't facilitate the interrupt handling, it has been chosen in this work due to ease in development. As can be seen from, Fig. 4-9, there are two McSPI ports 3 and 4 available on

the expansion connector and hence either of them can be used in communicating with the ADS1258.

As the OMAP3530 has a multiplexing feature, multiple signals can be connected to certain pins to add additional options as it pertains to the signal available. There are seven mux modes listed in Table 4-2, which categories the functionality of the particular pin. Each pin can be set individually for a different mux mode. This allows any of the mux modes to be set on a pin by pin basis by writing to the pin mux register in software. By default, the GPIO pins are made available on the expansion header. At the time of changing the functionality of the pins, the PINMUX register of the OMAP3530 was set.

Table 4-2: The BeagleBoard's expansion connector signals [8, 9].

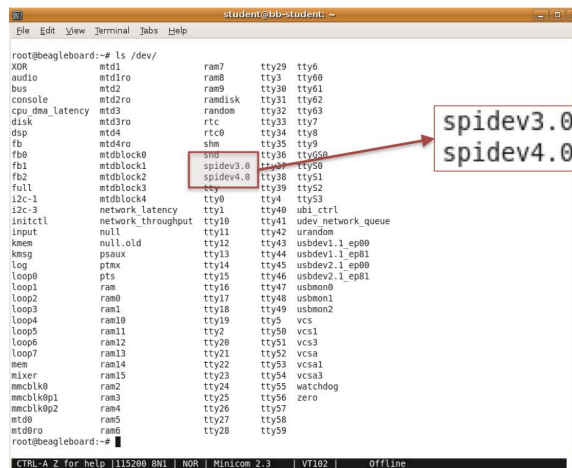
EXP	OMAP	0	1	2	3	4	5	6	7
1		VIO 1V8							
2		DC 5V							
3	AE3	MMC2_DAT7	*	*	*	GPIO 139	*	*	Z
4	AB26	UART2_CTS	McBSP3_DX	GPT9_PWMEVT	X	GPIO 144	X	X	Z
5	AF3	MMC2_DAT6	*	*	*	GPIO 138	*	X	Z
6	AA25	UART2_TX	McBSP3_CLKX	GPT11_PWMEVT	X	GPIO 146	X	X	Z
7	AH3	MMC2_DAT5	*	*	*	GPIO 137	*	X	Z
8	AE5	McBSP3_FSX	UART2_RX	X	X	GPIO 143	*	X	Z
9	AE4	MMC2_DAT4	*	X	*	GPIO 136	X	X	Z
10	AB25	UART2_RTS	McBSP3_DR	GPT10_PWMEVT	X	GPIO 145	X	X	Z
11	AF4	MMC2_DAT3	McSPI3_CS0	X	X	GPIO 135	X	X	Z
12	V21	McBSP1_DX	McSPI4_SIMO	McBSP3_DX	X	GPIO 158	X	X	Z
13	AG4	MMC2_DAT2	McSPI3_CS1	X	X	GPIO 134	X	X	Z
14	W21	McBSP1_CLKX	X	McBSP3_CLKX	X	GPIO 162	X	X	Z
15	AH4	MMC2_DAT1	X	X	X	GPIO 133	X	X	Z
16	K26	McBSP1_FSX	McSPI4_CS0	McBSP3_FSX	x	GPIO 161	X	X	Z
17	AH5	MMC2_DAT0	McSPI3_SOMI	X	X	GPIO 132	X	X	Z
18	U21	McBSP1_DR	McSPI4_SOMI	McBSP3_DR	X	GPIO 159	X	X	Z
19	AG5	MMC2_CMD	McSPI3_SIMO	X	X	GPIO 131	X	X	Z
20	Y21	McBSP1_CLKR	McSPI4_CLK	X	X	GPIO 156	X	X	Z
21	AE2	MMC2_CLKO	McSPI3_CLK	X	X	GPIO 130	X	X	Z
22	AA21	McBSP1_FSR	X	*	Z	GPIO 157	X	X	Z
23	AE15	I2C2_SDA	X	X	X	GPIO 183	X	X	Z
24	AF15	I2C2_SCL	X	X	X	GPIO 168	X	X	Z
25	25	REGEN							
26	26	nRESET							
27	27	GND							
28	28	GND							

PINMUX configuration

At the time of this work, there were two available methods to set the PINMUX:

- OpenEmbedded (OE) repository approach
- Non-OE approach

The OE repository method was followed due to its ease of use with the Ångström-distribution. As mention in the previous section, the Ångström images are built using OE repository. The OE repository allows building a customized Ångström image, which requires installation and BitBake.



```

student@bb-student:~$ ls /dev/
XDR          mt01          ram7          tty29         tty6
audio        mt03ro       ram8          tty3          tty60
bus          mt02         ram9          tty30         tty61
console      mt02ro       ramdisk      tty31         tty62
cpu_dma_latency mt3          random       tty32         tty63
disk         mt03ro       rtc          tty33         tty7
dsp          mt04         rtco         tty34         tty8
fb           mt04ro       shm          tty35         tty9
fb0          mtblock0     slm          tty36         tty60
fb1          mtblock1     spidev3.0    tty37         tty50
fb2          mtblock2     spidev4.0    tty38         tty51
full         mtblock3     tty          tty39         tty52
i2c-1        mtblock4     tty0         tty4          tty53
i2c-3        network_latency tty1         tty40         ubi_ctrl
initctl      network_throughput tty10        tty41         udev_network_queue
input        null         tty11        tty42         urandom
kmem        null.old     tty12        tty43         usbdev1.l_ep00
kmsg        psaux       tty13        tty44         usbdev1.l_ep01
log          ptmx        tty14        tty45         usbdev2.l_ep00
loop0       pts         tty15        tty46         usbdev2.l_ep01
loop1       ram         tty16        tty47         usbmon0
loop2       ram0        tty17        tty48         usbmon1
loop3       ram1        tty18        tty49         usbmon2
loop4       ram10       tty19        tty5         vcs
loop5       ram11       tty2         tty50         vcs1
loop6       ram12       tty20        tty51         vcs3
loop7       ram13       tty21        tty52         vcsa
mem         ram14       tty22        tty53         vcsa1
mixer       ram15       tty23        tty54         vcsa3
mmcblk0     ram2        tty24        tty55         watchdog
mmcblk0p1   ram3        tty25        tty56         zero
mmcblk0p2   ram4        tty26        tty57
mt00        ram5        tty27        tty58
mt00ro      ram6        tty28        tty59
root@beagleboard:~#

```

Fig. 4-10: A screenshot of the BeagleBoard’s terminal program showing the existence of the SPI ports 3 and 4.

The OE repository permits to make changes in the software setting of the bootloader and linux-kernel. In this work, the software settings were made to edit the PINMUX configuration and change the pin functions from GPIO to SPI port and 4. The pins 11-13 and 16-21, which were previously set as a default GPIO, were changed to SPI functionality. After making such changes, there existence was also confirmed by running the new Ångström image on the BeagleBoard and checking the available device tools “/dev” in the terminal program (see Fig. 4-10).

SPI Port Testing on the BeagleBoard

There is a driver program for testing SPI port written in C. The program named as “spidev-test.c” can be used in connection to any embedded board or processor with SPI port. The structure of the test program shown in Fig. 4-11a is very simple. The program sets the communication parameters before opening the SPI port. First few bytes of data is sent by using the SPI write command. Consecutively, the program waits to receive the data in return. At the end, the program displays the received

bytes.

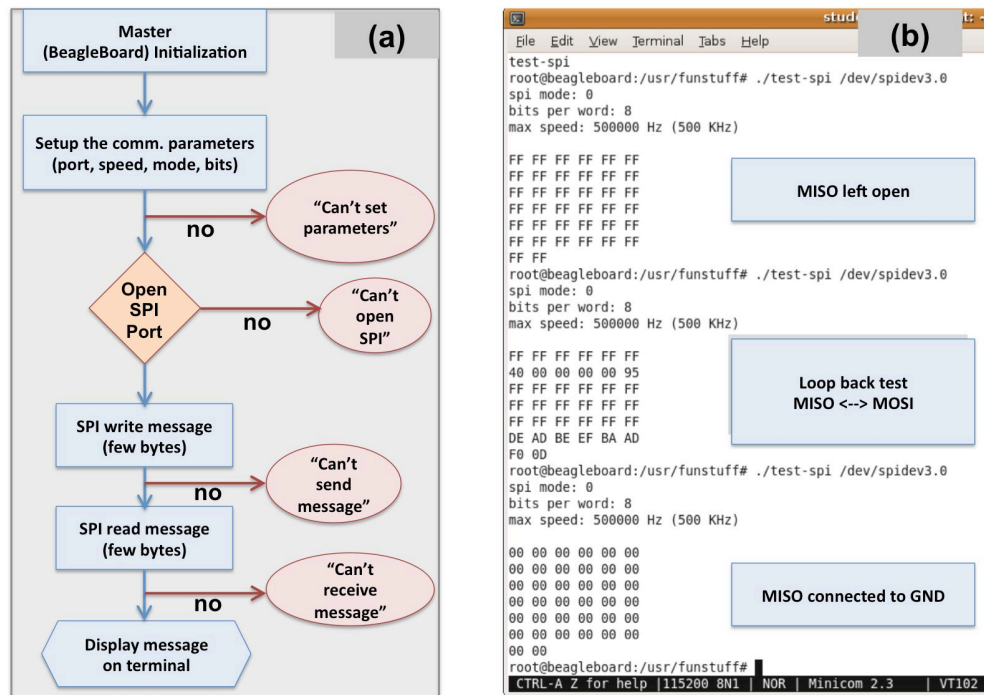


Fig. 4-11: (a) A flowchart of the spidev-test program and (b) a loop-back test with spidev-test program on the BeagleBoard

Look-back test on SPI port of the BeagleBoard

The spidev-test.c program was cross-compiled for the BeagleBoard to execute on the ARM Cortex-A8 core. The execution of the program yields the results shown in Fig. 4-11b. In the first run, the MISO pin was left open and showed all HIGH (FF) values, since the expansion header pins are active HIGH. Second run shows the loop back test, in which the MISO was connected to MOSI. In other words, the program receives the same data what is being sent. It is clear that the received data are different than the first run. The received data showed the same value as the sent data when it was compared. Finally, the last run shows all zero values when the MISO pin was connected to the ground. Thus, the spidev_test program was successfully implemented on the BeagleBoard and also set the basic architecture for communication between the ADS1258EVM and the BeagleBoard.

4.6 COMMUNICATION BETWEEN THE ADS1258 AND THE OMAP3530

SPI Bridge PCB

The ADS1258EVM and the BeagleBoard were required to link to each other with appropriate SPI pin-pin connection. In order to do so, the SPI bridge PCB was designed which connects the ADS1258 pins CS, SCLK, DIN and DOUT to the McSPI3_CS, McSPI3_SCLK, McSPI_MOSI and McSPI_MISO respectively. The bridge PCB shortens the connection and reduces the capacitive effects during the data communication. In the case of long connections, the capacitive effect may increase the data transfer error, which occurred in the beginning of the SPI communication between the BeagleBoard and ADS1258.

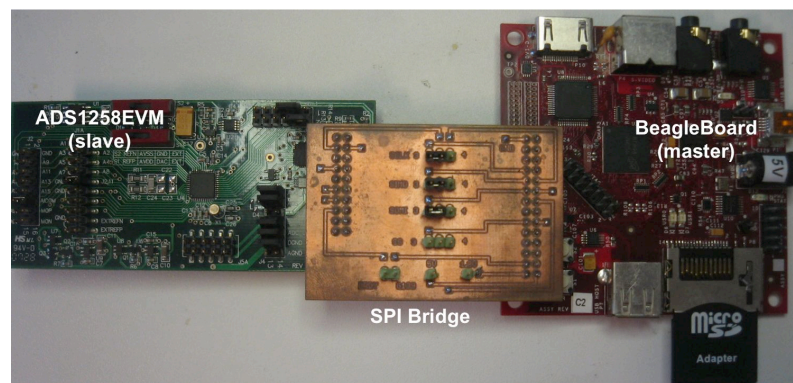


Fig. 4-12: The connection between the ADS1258EVM and the BeagleBoard.

SPI-data Transfer Program

A program named “spi-ads”, which integrates the ADS1258 SPI protocol parameters into the spidev-test program, was designed. A header file ads1258.h was written, that contains the constants to control the ADS1258’s registers. It also includes some masks for the status byte, which is sent with every sample from the ADS1258. As shown in Fig. 4-13a, the spi-ads program initializes the SPI port similar to the spidev-test. Then, the control word is sent to the ADS1258’s register. Consecutively, the register data is read and displayed to confirm the control word transfer. The control word selects the channel and sampling rate. The channel data is read and dis-

played on the screen. Fig. 4-13b shows the actual logic signals exchanged between the ADS1258 and the OMAP3530. DRDY signal goes high and signals the data availability. The master (OMAP3530) writes the control word, which can be seen as MOSI. In sequence, the slave (ADS1258) sends the data shown as MISO. During the data transfer process, the master generates the clock signal SCLK.

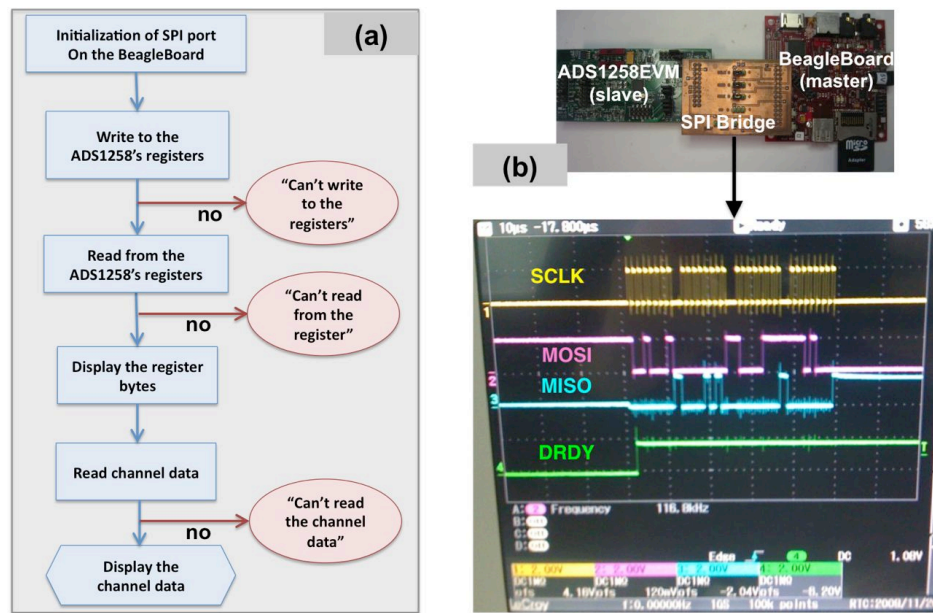


Fig. 4-13: (a) A flowchart of the spi-ads program and (b) the screenshot of the spi-data transfer between the ADS1258EVM and the BeagleBoard.

Hexadecimal-Decimal Conversion & Plotting

The digital channel data, which arrives at OMAP3530, is coded in hexadecimal values. The hexadecimal values are required to be converted into the decimal values at each sampling point. The flow chart of the program “spi-ads-plot” shown in Fig. 4-14a provides the process of converting the hexadecimal values into decimal and of plotting the decimal values. The digital data is consisted of 4 bytes: status, HB, MB and LB [5]. As mentioned before the status byte gives the additional information regarding the current data and new coming data. Therefore, the status byte needs to be separated from the other data. The rest of data is required to be merged to construct a hexadecimal value. The hexadecimal values are converted into decimal. Finally, the decimal values are plotted on the Angström desktop environment using the SDL libraries.

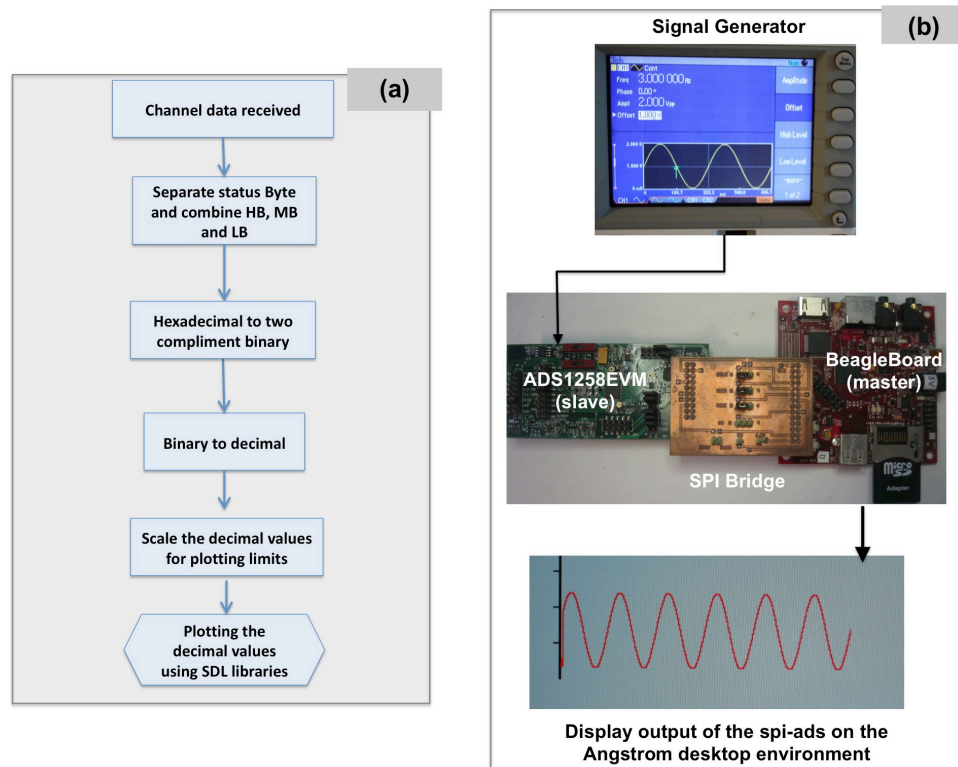
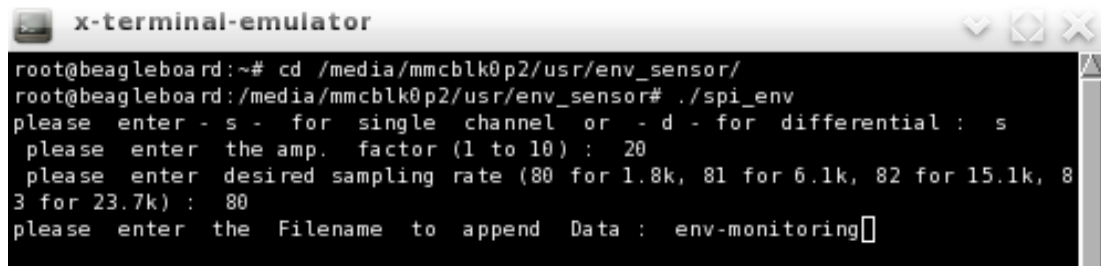


Fig. 4-14: (a) A flowchart of the D-to-A data conversion and plotting and (b) a picture of real-time data plotting.

The spi-ads-plot program was tested by providing an analog sinusoidal 3Vpp signal to the analog input channel of the ADS1258 (see Fig. 4-14b). The analog data was digitized by the ADS1258 at sampling rate of 23 kps and resolution of 24-bit. The program running on the BeagleBoard received the digitized data through SPI communication and converted the hexadecimal values into decimal. When the decimal values was plotted in real-time, it clearly showed the sinusoidal signal on the desktop screen. Thus, the experiment confirmed the success of not only SPI communication but also the SDL libraries in plotting the signal in real-time.

As shown Fig. 4-15, the spi-ads-plot program (also known as “spi_env” for body-environment monitoring) facilitates the selection of certain parameters such as channel type, amplification factor, sampling rate and the excel file name for saving the data. After providing the desired parameters, the program brings the plotting window and plots the received data as shown in Fig. 4-14b.



```

x-terminal-emulator
root@beagleboard:~# cd /media/mmcblk0p2/usr/env_sensor/
root@beagleboard:/media/mmcblk0p2/usr/env_sensor# ./spi_env
please enter - s - for single channel or - d - for differential : s
please enter the amp. factor (1 to 10) : 20
please enter desired sampling rate (80 for 1.8k, 81 for 6.1k, 82 for 15.1k, 83 for 23.7k) : 80
please enter the Filename to append Data : env-monitoring

```

Fig. 4-15: A screenshot of the terminal application showing the execution of the spi-ads-plot program (here known as a “spi_env”).

Interfacing Novel Body Sensor Modules with the OMAP3530

Successful implementation of communication between the ADS1258 and the OMAP3530 has been shown in this section. The program for the OMAP3530 has been developed to receive, process and plot the digitized data in real-time. The digital part of the multimodal, wearable health monitoring is now ready to link with novel body sensor modules. Before beginning with novel sophisticated analog frontends, the digital module was tested for its feasibility in the real-time data handling from a sensor. The following section will present a design of novel personal environment monitoring module and its performance with the OMAP3530-ADS1258 system.

4.7 FEASIBILITY TEST – PORTABLE PERSONAL ENVIRONMENT MODULE

Early during the defining the objectives of the research work, it was discussed that the individual’s health is influenced by the body surrounding environment and its quality. Even change in environment humidity and temperature may cause the severe health problems. WHO advises to maintain the body environment in the moderate condition to sustain a good health. To achieve this, one requires a wearable or portable module to monitor his personal environment parameters in a continuous manner. The following presents a portable personal environment monitoring module as an front-end to the OMAP3530 smartphone processor. The presented laboratory prototype contains air humidity and atmospheric temperature sensors with the analog output voltage. The analog voltage is directly fed to the ADS1258 for digitization.

And finally the data is processed and displayed by the BeagleBoard on its desktop environment. Although the module is developed as an integral part of the multimodal system, it also serves as an individual device for body environment data monitoring.

Personal Environment Monitoring

The environment is an integral part of human life, the quality of which plays a critical role in human health. Human health is very closely linked to environmental quality, as the etiology of most of the human diseases being related to the status of the living environment of man [10]. Globally, there are many events happening, which affect the environment quality and hence influence the individual's health and quality of life.

One of such events occurred in 2003 in Paris, France. Two weeks of devastating heat wave claimed at least 300 lives of healthy humans [11]. The temperature rose beyond 40C and became intolerable for French residents [11]. On the other hand, the studies have found that the cold surrounding environment increase the risk of cardiovascular diseases and may cause death [12]. Therefore, the cardiovascular mortalities are common in northern Europe [12]. These two extreme cases of the temperature change suggest that the body environment temperature should be maintained in moderate limits (15-25 C) and exposure to the extreme temperature should be avoided [13]. In the similar manner, the environment humidity is also an influential factor. Greek studies have found that the higher humidity level increases heart attack risk [14].

Above examples show the importance of the personal environment and its impact on one's health. To sustain good health, monitoring a surrounding environment seems a good practice and requires a set of sensors to be incorporated in the vicinity of the body in a wearable manner. The presented work shown in Fig. 4-16 demonstrates such portable, real-time monitoring of a personal environment using the OMAP3530 smartphone processor as a processing unit. For this work, two environment parameters, temperature and humidity are selected for monitoring due to ease of prototyping the sensor hardware along with the digital module.

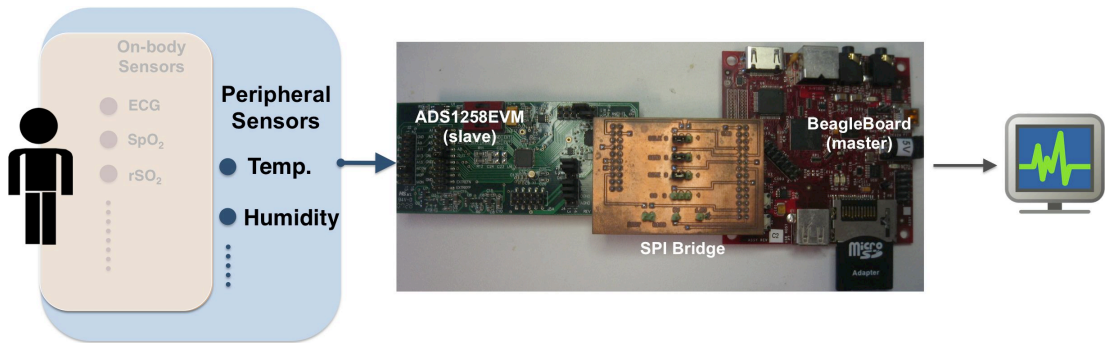


Fig. 4-16: A concept of the body environment monitoring with peripheral sensors and the OMAP3530-ADS1258 system.

System Components

The analog part of the system consists of two sensors: humidity sensor and temperature sensor.

Humidity Sensor

HIH4030 (Honeywell, USA) was selected for humidity measurements [15]. It is an SMD sensor with three terminals, providing the analog voltage proportional to the environment relative humidity. It provides linear proportionality between the relative humidity (RH) and the output voltage (see Fig. 4-17). Its application areas also include medical environment monitoring.

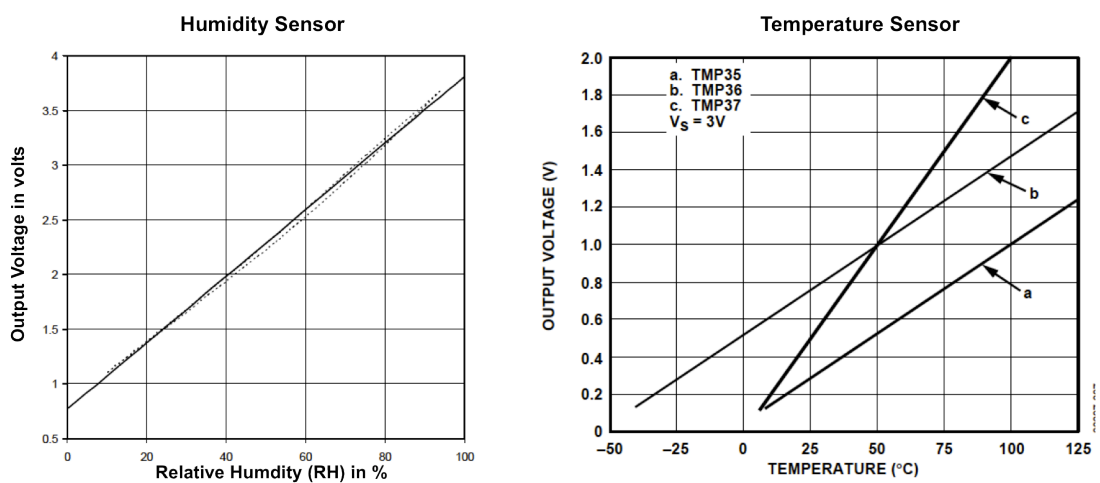


Fig. 4-17: Output voltage proportionality graphs of the humidity and temperature sensors [15, 16].

Temperature Sensor

The TMP36 (Analog Devices, USA) is selected for temperature sensing and is low voltage, precision and centigrade temperature sensor [16]. The low output impedance of the TMP36 and its linear output and precise calibration simplify interfacing to any A/D converter [16]. The sensor is intended for single-supply operation from 2.7 V to 5.5 V maximum. The supply current runs well below 50 μA , providing very low self-heating—less than 0.1°C in still air. It also provides a linear relationship between output voltage and the measured (see Fig. 4-17).

Digital Module

The sensors HIH4030 and TMP36 mounted on a single PCB are linked to the digital module, which consists of ADS1258EVM and the OMAP3530-based BeagleBoard (see Fig. 4-18). The analog data are fed to the ADS1258 for digitation and the SPI communication provides the data to the BeagleBoard at sampling rate of 1.8ksps. The BeagleBoard by running embedded program processes and displays the real time data on the plotting window.

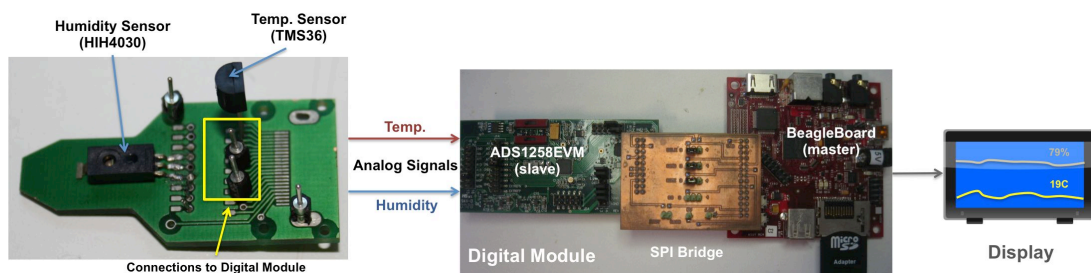


Fig. 4-18: A complete system of a personal environment monitoring module.

System Firmware

The system firmware is similar to the spi-ads algorithm mentioned earlier. The firmware is customized for plotting the values of the humidity and the temperature. 500 samples of decimal values are averaged before plotting to widen the window timing.

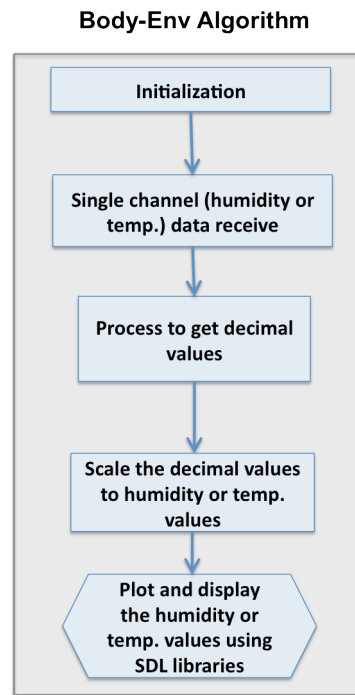


Fig. 4-19: A flowchart of a simple Body-Env Algorithm

Experiments & Results

The humidity and temperature sensors feed the corresponding environment parameter values to the ADS1258 in analog voltage form. The body environment algorithms running on the BeagleBoard fetch the digital data coming from the ADS1258. The processed signal is plotted on the desktop environment. The humidity plot in Fig. 4-20 shows that there is a delay of 1-2 seconds in detection of the humidity change during opening and closing of the window. This occurs due to the slow response time of the humidity sensor.

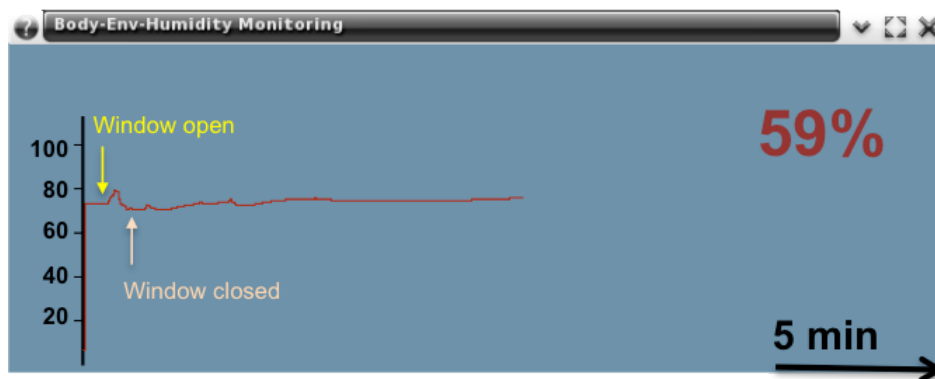


Fig. 4-20: A screenshot of the Body-Env-Humidity monitoring.

Similarly, the temperature plot in Fig. 4-21 reveals 2-3 seconds of delay in responding to the temperature change. Another factor impacting the delay is the averaging of the 500 samples during the program execution.

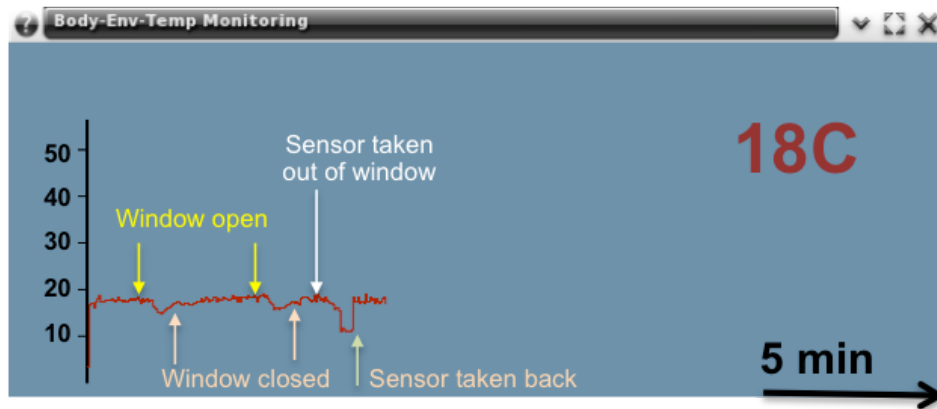


Fig. 4-21: A screenshot of the Body-Env-Temp monitoring.

Thus, the humidity and temperature sensor were successfully implemented along with the digital module to monitor a personal environment.

Conclusions

The surrounding environment indeed impacts the human health and in severe condition may cause death. It has been suggested that the human health can be sustained better if the surrounding environment is in moderate condition. Therefore, it is necessary to monitor personal environment especially during the chronic diseases or allergic reactions. The presented work demonstrates the portable module for monitoring the body environment. In the laboratory prototype, humidity and temperature sensors were chosen and mounted together on a single PCB to connect the digital module consisting the ADC and the OMAP3530. The embedded application running on the OMAP3530 successfully collected the data and plotted them in real-time. The personal environment monitoring module will further discussed in next section as an integral part of multimodal system.

4.8 REFERENCES

- [1] Bronzino (2006) *The Biomedical Engineering Handbook: Medical Devices and Systems* CRC Press.
- [2] D. Berry, F. Duignan, and R. Hayes, "An Investigation of the use of a High Resolution ADC as a “ Digital Biopotential Amplifier ”," ECIFMBE 2008, Heidelberg: Springer, 2008, pp. 142-147.
- [3] Robert Schreiber, Texas Instruments.
<http://archive.chipcenter.com/analog/c078.htm>. Web 12 Sept. 2010.
- [4] Bonnie Baker. A glossary of analog-to-digital specifications and performance characteristics. Technical report, Texas Instruments, August 2006-2008.
- [5] Texas Instruments. Datasheet for ADS1258, 2008.
- [6] Texas Instruments. User’s guide for ADS1258EVM, 2008
- [7] David Kalinsky and Roe Kalinsk, Introduction to Serial Peripheral Interface, www.eetimes.com, Jan. 2002.
- [8] BeagleBoard C4 Reference Manual, www.beagleboard.org. Dec. 2009.
- [9] OMAP35x technical reference manual, www.ti.com, SPRUF98D, Oct. 2009.
- [10] Report on “Environment pollution and impacts on public health”, Urban Environment Unit, UNEP, Kenya.
- [11] http://english.peopledaily.com.cn/200308/26/eng20030826_123075.shtml
- [12] P. Wilmshurst, Temperature and cardiovascular mortality. *BMJ*. 1994 October 22; 309(6961): 1029–1030.
- [13] Anderson TW, Le Riche WH. Cold weather and myocardial infarction. *Lancet* 1970;i:291-6.
- [14] <http://www.webmd.com/heart-disease/news/20060712/high-humidity-boosts-heart-attack-risk>
- [15] Datasheet, HIH-4030, www.honeywell.com.
- [16] Datasheet, TMP36, www.analog.com

5. WEARABLE ECG BELT FOR CONTINUOUS MONITORING

Life-threatening cardiovascular diseases require early detection or diagnosis. A standard procedure, long-term ECG monitoring of cardiac patients is currently the best way to reduce the number of heart failures. In comparison to conventional gelled ECG electrodes, dry and washable textile electrodes embedded in comfortable garment or in a wearable chest belt have been proven very effective for a long-term ECG monitoring. This section presents an implementation of wearable ECG belt called “Active Belt” which contains the stitched textile electrodes for ECG detection and analog pre-processing circuit embedded in tiny cell-phone plug. With them, ECG processing and display have been achieved using the smartphone processor OMAP3530. The embedded programs running on the OMAP3530 display the real-time ECG and heart rate extracted from the detected ECG signal. The experiments with the Active Belt have shown promising results in conveying a better ECG signal quality with a clinical significance and hence enabled long-term ECG recording in a daily life.

5.1 INTRODUCTION

Physiological sensors were initially designed to be used in a hospital or laboratory. The patients were generally seriously ill and stationary on the hospital beds. Sensors were carefully applied on clean skin by trained technicians and gels and adhesives were also applied for a guaranteed connection between the skin and the electrode. Without choice, the patients generally had to wear the sensors and to often face serious consequences like itchy electrode patch or bacterial infection. But in today’s world with tremendous technological advancement, the rigid procedure of applying

sensors on the skin can be overcome by embedding textile electrodes in the daily garments. The smart textiles could help in detecting the symptoms prior to the serious illness and hence enable the preventive measures for the disease.

Now-a-days, there is a move towards developing a wearable physiological recording systems where the essential element is textile electrode that senses the physiological parameters from the patient's body during one's daily activity. Cardiovascular diseases are the main cause of death in the middle-to-old aged people globally. In Germany, more than 300000 people experience a heart attack annually [1]. Early detection of symptoms in the risk group (patients with recent bypass surgery or angioplasty) by recording ECG in a long-term manner can significantly reduce the number of heart failures or sudden deaths [1, 2, 3]. The wearable ECG system could furnish a quality long term ECG recording of the patient along with intelligent symptom detection and could also alert the hospital or cardiologist for the upcoming cardiac event for taking some preventive steps in time.

State-of-the-Art Technologies in Wearable Physiological Monitors

Wearable ECG recorder is not a very new trend in medical technology, but is there since last decade. It all started from evolution of the wearable electronics in the last three decades. The advancements in textile technology have speeded up the wearable medical devices and enabled the sensors to be mounted or stitched on the daily clothes.

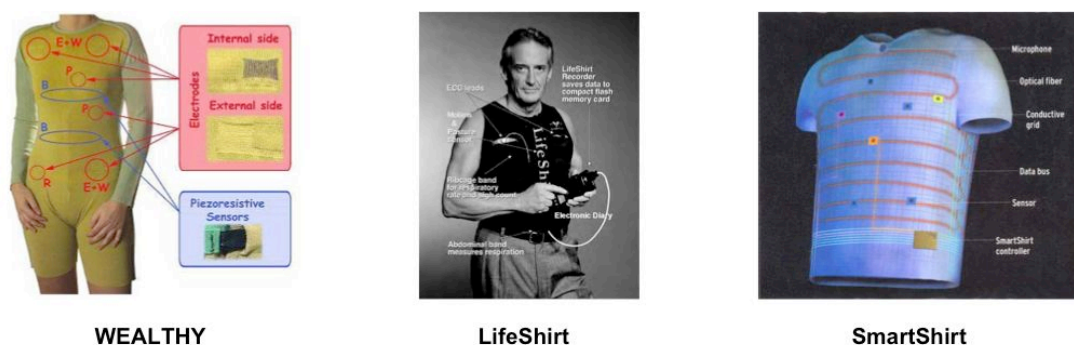


Fig. 5-1: The state-of-the-art technologies in wearable physiological monitoring

The following are some of the pioneering wearable physiological monitoring systems accomplished by stitching or weaving the textile sensors in the garments (see Fig. 5-1):

- A European consortium has designed WEALTHY, the wearable healthcare system which senses temperature, respiration and movement in its beta version [4].
- Sensors in the LifeShirt (Vivometrics, Inc., Ventura, CA, U.S.A.) garment continuously monitor respiration, the electrocardiogram, activity and posture [5].
- The SmartShirt (Sensatex Inc., USA) can remotely monitor a wearer's movement, heart rate, and respiration rate in real-time through a nanotechnology conductive fibre grid [6].

Prerequisites for the Wearable Physiological System Design

During the past few years, a number of wearable physiological monitoring systems have been in practice for health monitoring of the patient in hospital and real life situations and their performances have been reported [7]. Some prerequisites for such wearable systems are their small size, low-power consumption, low weight, real-time signal processing and most importantly wireless connectivity [8].

Active Belt - On-Body ECG Diagnosis System

Having considered above prerequisites, a single channel long-term ECG belt called Active Belt developed has been designed (see Fig. 5-2). Textile electrodes are stitched on the skin-contact side of the belt. The electrodes are wired to analog processing circuits confined into two small cell-phone plugs. At the end, the digital ECG signal enters into a dual-core OMAP3530-based BeagleBoard for ECG processing and display. A dual-core functionality (ARM+DSP) of the OMAP3530 is suitable for wearable health monitoring applications [9].

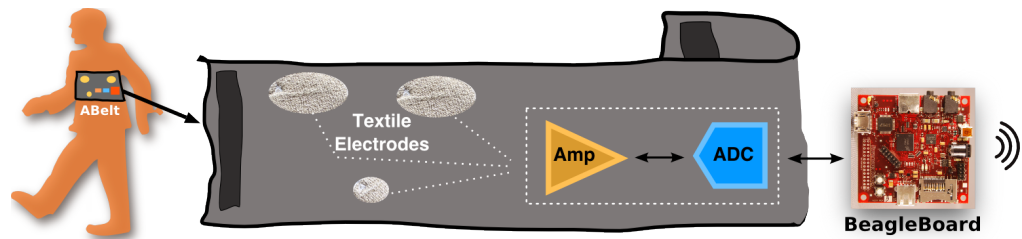


Fig. 5-2: A conceptual diagram of textile-based ECG detection.

The Active Belt's ultimate goal is to provide prototype wearable and high performance system, which can enable the on-site ECG signal processing in order to detect early signs and symptoms. The Active Belt is further discussed in detail later in this section.

5.2 BACKGROUND THEORY

The human heart serves as a four-chambered pump for circulatory system. The upper two chambers are called the atria, and the lower two chambers are called the ventricles. The smooth, rhythmic contraction of the heart chambers has an underlying electrical precursor in the form of a well-coordinated series of electrical events that takes place within the heart.

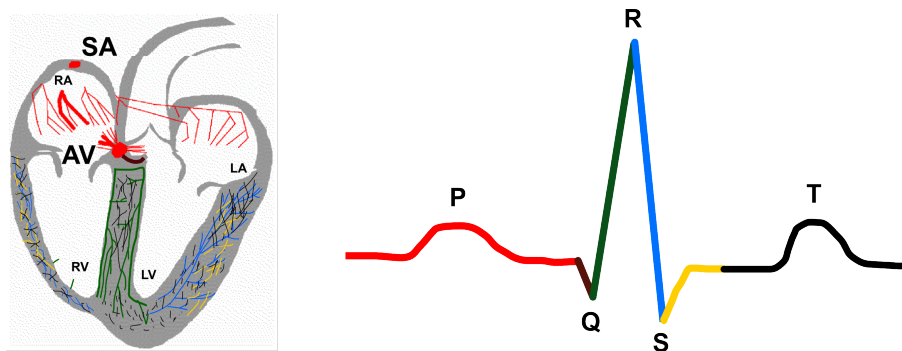


Fig. 5-3: The electrical activity of a heart. Representation of an electrical activity of various heart regions (in right) along with a scalar ECG (in left)

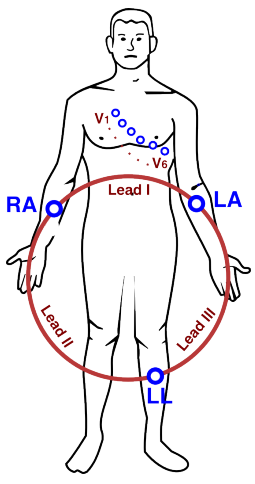
As shown in Fig. 5-3, the sinoatrial (SA) or sinus node, located at the right atrium rhythmically generates an electrical stimulus which travels down through the conduction pathways and causes heart's chambers to contract and pump the blood out.

Consecutively, the electrical stimulus halts for a very short period at atrioventricular (AV) node and then continues down to the conduction pathways via the bundle of His into the ventricles [10]. Since the body acts as a purely resistive medium, the electrical stimulus generated by heart extends to the body surface [11].

Table 5-1: The origins of various ECG segments [11].

Segments	Representation
P wave	Activation of the atria
QRS complex	Excitation of the ventricles
T wave	Ventricular repolarization
U wave (rarely found)	Slow repolarization of ventricular papillary muscles [10]

Table 5-2: Standard 12-lead ECG configuration [10].

	Polarity	Type	Lead	Connections
 <p>Fig. 5-4: Graphical illustration of standard 12-lead connection [10].</p>	Bipolar	Standard Limb Leads	Lead I	Left arm (LA) and right arm (RA)
			Lead II	Left leg (LL) and RA
			Lead III	LA and LL
	Unipolar	Augmented Limb Leads	aVL	LA - positive RA and LL - negative
			aVR	RA - positive LA and LL - negative
			aVF	LL - positive RA and LA - negative
		Precordial Leads	V ₁ -V ₆	Starting from the right of the sternum Ending at below middle of armpit

ECG Measurement Principle

As shown in Fig. 5-4, the ECG signals can be detected by placing a transducer on the skin [10]. The transducer consists of a pair of electrodes, which convert the ionic potentials from the body into the electronic potentials for implementing analog signal processing. 12-lead ECG system is most commonly used and standardized for clinical practice [12]. The leads are categorized according to the location and combination of the electrodes placed on the body surface. The bipolar leads are derived from the various permutations of pairs of limb electrodes. On the other hand, the unipolar leads are based on the signals obtained from more than one pair of electrodes [10].

ECG Electrodes

Detection of ECG requires the use of electrodes designed to be in contact with the human body where these electrodes measure the biopotentials emanating from the heart. The most common types of electrodes that are used in the clinical setting are wet Ag/AgCl electrodes. Recently, the dry electrodes made of conductive yarns have been of an upcoming research interest for biopotential measurements. Both kinds of electrodes including their pros and cons are thoroughly discussed in the following subsections.

Wet Ag/AgCl Electrodes

The electrode is the floating silver/silver chloride (Ag/AgCl) electrode, which is formed by electrochemically depositing a very thin layer of AgCl onto an Ag electrode [13]. The electrode is imbedded in a foam-soaked with an electrolyte gel to provide good electrical contact with the skin [13]. These electrodes highly rely on a gel with a high ionic concentration, which acts as a transducer at the skin-electrode interface [14].

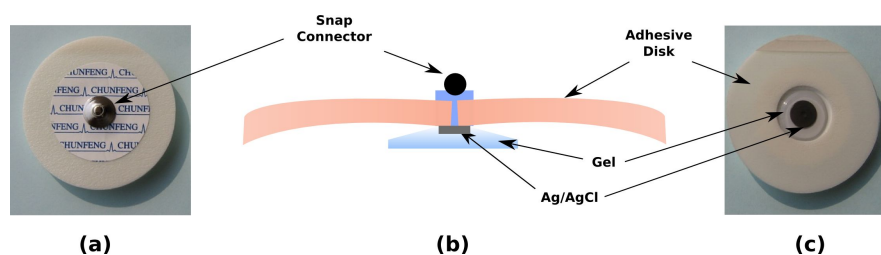


Fig. 5-5: A commercial Ag/AgCl ECG Electrode.

(a) A connection side, (b) a cross-sectional graphical illustration and (c) a skin contact side.

Despite preferable in the clinical ECG recording, the wet electrodes are associated with some serious disadvantages, which discourage to use them in a long-term monitoring.

- Gel dehydration over time modifies the electrode impedance, which may cause noise and other artifacts.
- In long-term applications, the gel may cause skin irritations and eventually result in dermatitis [15].

Dry Textile Electrodes

Textile electrodes and conductors are being developed and used in different physiological monitoring such as ECG, EMG, EEG, respiratory rate, bioimpedance spectroscopy, etc. [16]. The textile electrodes are widely used in the health monitoring, because they are easy to fabricate and integrate into the daily clothing. Knitting, embroidering, weaving and sewing are all fabrication techniques to produce the textile electrodes. The textile electrodes can be categorized into three types based on their content materials:

- Conductive yarns: The yarns contains conductive fibers like stainless steel, Ag/AgCl coated polyester or silver coated polyamide.
- Conductive rubbers: The rubber filled with carbon, nickel-coated carbon or silver.
- Conductive ink: The ink is silver filled paste.

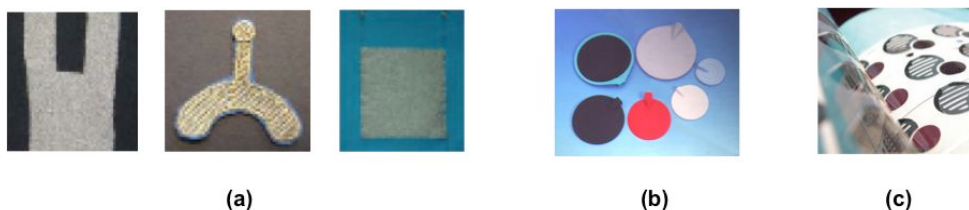


Fig. 5-6: Different types of the dry electrodes.

(a) The knitted, embroidered and woven electrodes (left to right) made of polyamide threads (26-Greiz, Germany), (b) the silicone conductive rubber pads (Wandy

Rubber Industrial Co. Ltd., Taiwan) and (c) biosensors for ECG made of printed electronic ink (Henkel Corporation, USA).

Among all the types, the conductive yarns are the most popular and hence are used in this research work, because the knitted yarn electrodes offer several advantages:

- The conductive yarns are biocompatible material and do not produce any skin allergenic reaction or dermatitis during long term skin-contact.
- The electrodes are robust, reusable and washable.
- The electrodes can easily be embedded into the clothes.
- A single production process can fabricate the electrodes and interconnects and hence saves the time and cost [4].

Skin-Electrode Impedance

In long-term surface biopotential recordings, the skin-electrode impedance plays a major role in the quality of signals. The body impedance depends on several factors such as size and location of the contact electrode as well as the skin hydration. Moreover, the contact force is an important factor influencing the contact impedance and is difficult to control when taking measurements on a human subject [16].

When using conventional electrodes, an electrode gel is placed as a contact medium between the skin and the electrode. The electrolyte and the electrode generate a galvanic cell with a half-cell polarization potential, which adds to the original potential difference. The charge is distributed and the electrical double layer appears [10]. The double layer forms a potential difference ($\Delta\psi$), which can be described by the Nernst equation [17]:

$$\Delta\psi = \frac{RT}{zF} \ln \frac{a_2}{a_1} \quad \text{Eq. 5-1}$$

Where, R = the universal gas constant

T = the temperature

z = number of electrons transferred in the reaction

F = the Faraday constant

a_1 and a_2 = the ions activity

The electrode–skin system is stabilized based on the assumption of time independent electrode potential [18]. If a current is injected through the electrode, the electrode potential will change. The electrode potential will change proportional to the current, when the current and the voltage in the electrode are small.

The equivalent electrical circuits for the conventional Ag/AgCl as well as textile electrodes skin interface and their models are shown in Fig. 5-7.

Electrode Layer:

In the equivalent circuits, C_d represents the double layer, while E_{el} is the electrode potential. R_d represents the charge transfer resistance (or leakage resistance), which occurs at the interface [19].

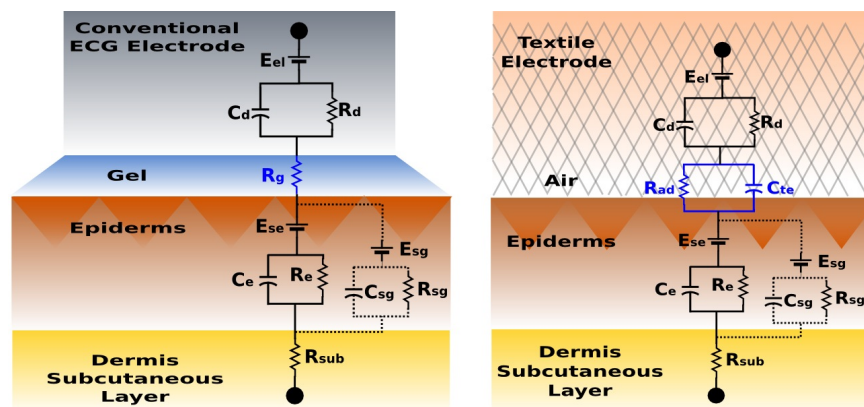


Fig. 5-7: Skin-electrode models.

The model for conventional Ag/AgCl ECG electrodes (left) [5] and for textile electrodes (right) [8]

Skin Layer:

Lower half of the equivalent circuits represent the electrical model of the skin. The human skin consists of several layers (e.g. epidermis, dermis, subcutis), which can be simulated by a capacitor C_{sg} . The numerous channels, perspiratory glands and hair follicles within the skin connect the layers and are represented by the resistance R_e . The subcutis layer is well supplied with blood and may therefore be represented as a resistance R_{sub} . The layered structure of the stratum corneum leads to semipermeable membranes and differences in the ion concentration, which result in a potential E_{se} .

For Conventional Ag/AgCl Electrode:

For the conventional electrode, R_g represents the resistance of the gel and the leads.

Thus, the equivalent impedance for the conventional electrode model is given by:

$$Z_{conventional} = \frac{R_d}{1 + j\omega R_d C_d} + R_g + \frac{R_E}{1 + j\omega R_E C_{SG}} + R_{sub} \quad \text{Eq. 5-2}$$

For Dry Textile Electrodes:

In comparison to standard metal electrodes, the dry textile electrodes show a strong capacitive behavior (C_{te}) at the interface due to lack of the hydrogel, which is often used as an electrolyte layer. Sweat and skin humidity result in an additional conductive path (R_{ad}) parallel to the capacitance [20, 21]. Thus, for textile electrodes an equivalent circuit can be reshaped as shown in the Fig. 5.7 and the overall impedance for the circuit can be calculated as following:

$$Z_{textile} = \frac{R_d}{1 + j\omega R_d C_d} + \frac{R_{ad}}{1 + j\omega R_{ad} C_{te}} + \frac{R_E}{1 + j\omega R_E C_{SG}} + R_{sub} \quad \text{Eq. 5-3}$$

In long-term measurements, R_g reduces the over-all interface impedance due to dehydration of the gel and also makes the conventional electrode more susceptible to the noise. In case of dry textile electrodes, the impedance, $R_{ad}||C_{te}$ decreases as the electrode location is moisturized due to sweat. Although the sweat has a lower ion conductivity compared to a gel, the interface impedance will gradually decline in a long run for effective signal detection [1]. Moreover, due to the flexible nature of textile, the electrode can adapt itself on the hairy skin and make a firm skin contact by maintaining sufficient pressure acting on them.

ECG Instrumentation

After detection of the ECG signals at the electrodes, the signals are passed to the different stages of the analog circuits for signal conditioning and are finally fed to the processor for signal analysis and processing (see Fig. 5-8). In order to stick to the

application, wearable ECG monitoring is only taken into consideration for the description of the ECG instrumentation.

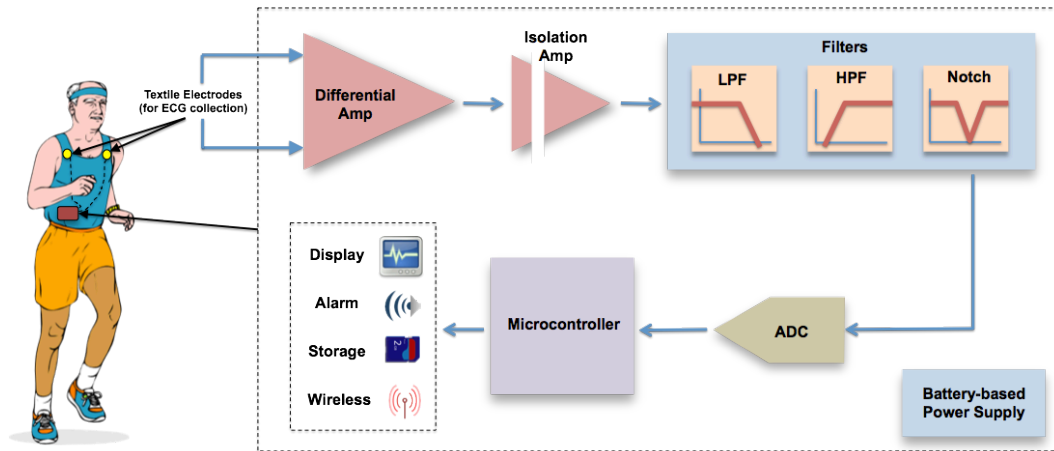


Fig. 5-8: A generalized block diagram of the wearable ECG system.

Differential Amplifier

Surface ECG signals are in the range of 1-5 mV and thus too easily absorb the interference of environmental noise (especially power-line noise). As shown in Fig. 5-9, the in-phase noise appears simultaneously at the two input lead terminals. If these terminals are used as the differential input, the noise present at both terminals can be minimized or completely cancelled. The signal of interest (ECG) will be amplified. In brief, a differential amplifier provides a functionality of common mode rejection (CMR).

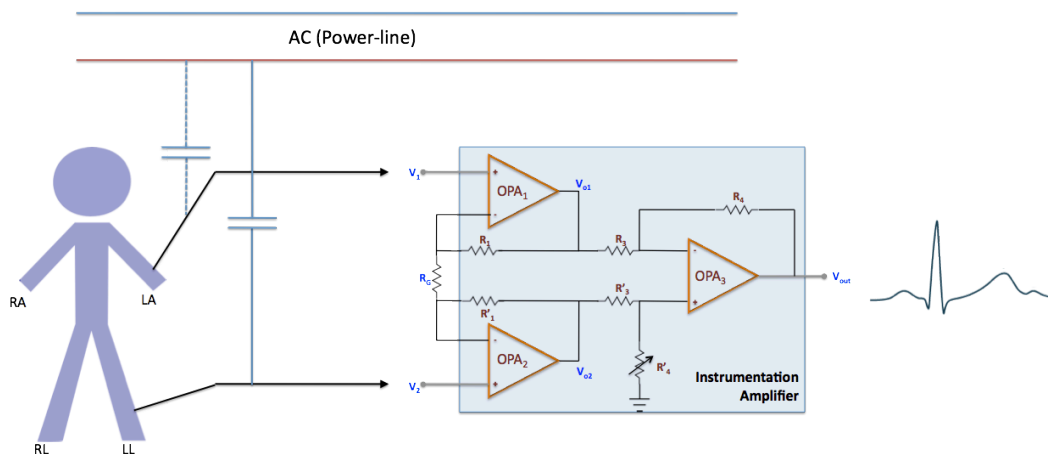


Fig. 5-9: A concept of the power-line interference in the ECG signal.

An instrumentation amplifier (IA) with high CMRR minimizes this interference. In the block diagram, R_G sets the gain and R'_4 sets the CMRR of the IA.

Moreover, a differential amplifier provides a good signal-to-noise ratio (SNR) as well. However, a single differential amplifier has a small gain and a small CMRR and thus is not suitable for the small amplitude signals such as ECG. In solution to this problem, an instrumentation amplifier (IA), which incorporates a multistage differential amplifier, improves the amplification, CMRR and input impedance. The gain of the IA can be given by:

$$\frac{V_{out}}{V_{id}} = A_d = \left(\frac{R_4}{R_3}\right) \left[\left(2 \times \frac{R_1}{R_f}\right) + 1 \right] \quad \text{Eq. 5-4}$$

Where,

V_{out} = Output voltage

$V_{id} = V_1 - V_2$ = Difference of input voltages

A_d = Differential gain

Thus, IA is the backbone for the most physiological signal devices due to its versatile functionality [22].

Isolation Amplifier

The isolation amplifier is for a patient's safety and a barrier to the passage of current from the power line. For example, if the patient comes in contact with a 220 V, this barrier would prevent the current flowing from the patient through the patient to the ground of the system. In biopotential recording applications, opto-couplers are generally in use for providing isolation.

Filter Circuits

The electrophysiological signals have different frequency components and are in practice contaminated by the environment and electromagnetic noise. The graph in Fig. 5-10 depicts that the spectrum of the four physiological signals lie at low frequency band, therefore, the active analog filters are deployed after the IA for eliminating the unwanted signals.

High-pass Filter (HPF) for DC blocking

The baseline wander is an extraneous, low-frequency activity in the ECG which may interfere with the signal analysis, making the clinical interpretation inaccurate. Baseline wander in ECG monitoring can be caused by respiration, electrode impedance change and importantly body movements [23]. The spectral content of the baseline wander is usually in the range between 0.05-1Hz [28]. A high-pass filter is placed following IA to eliminate such very low frequency base-line wander and also DC components. Typical range for corner frequency of high pass filtering is from 0.05Hz to 0.5Hz [24].

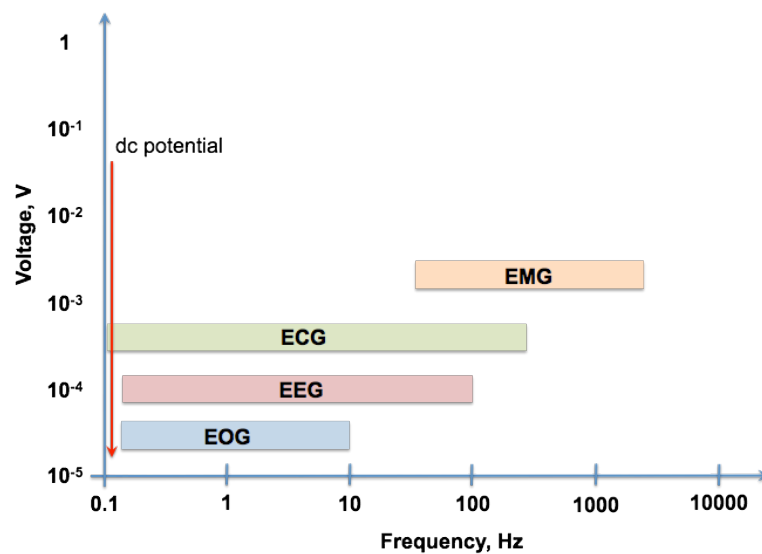


Fig. 5-10: Electrical properties of the electrophysiology signals [29].

EOG is the electrooculogram, EEG is the electroencephalogram, ECG is the electrocardiogram and EMG is the electromyogram.

Notch Filter (NF)

50/60 Hz power line noise pervades the ECG waveform because of magnetic induction in wires, displacement currents in the electrode leads, displacement currents in the body, and equipment interconnection and imperfection. It is an universal approach to implement a band reject or notch filter to eliminate the noise for achieving good quality of the ECG signals. Twin “T” notch filter is commonly used for this purpose.

Higher Order Low-pass Filter (LPF)

ECG signal confines within 250 Hz. Beyond this frequency, ECG loses its diagnostic value and degrades the visual form. Therefore, higher order low-pass filter is cascaded in the ECG instrumentation, which not only limits the ECG signal in frequency but also helps in deciding the analog to digital converter. 3rd order Butterworth filter is the most common for ECG recording due to its flat response.

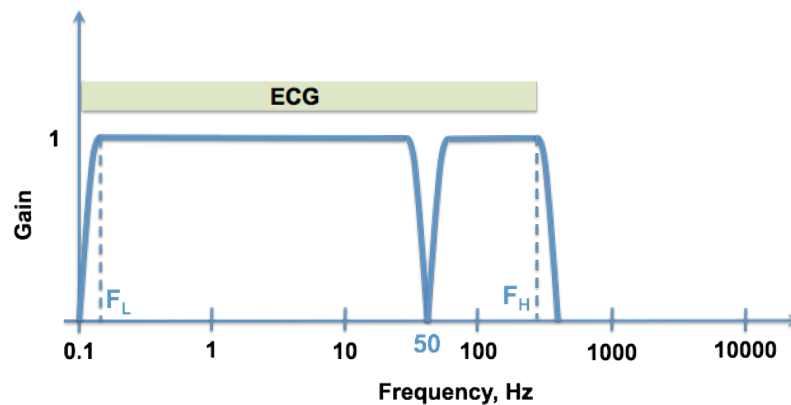


Fig. 5-11: The response of HPF, NF and LPF cascaded in ECG instrumentation.

F_L represents the cutoff frequency for high-pass filter, F_H represents the cutoff frequency for low-pass filter. 50 Hz is the cutoff frequency for notch filter.

The combination of high-pass and low-pass filters constructs a bandpass-filter, which can be implemented with less number of components for the same performance. Fig. 5-11 shows the response of the filters in cascaded form for ECG measurements.

Analog to Digital Converter

When it comes to process and analyze the detected ECG signal into computer or microprocessor, it has to be converted from analog to digital form. The ADC performs the conversion and produces the ECG into coded form interpretable by the computer. Post-processing of ECG data is not only used for detection of abnormalities but also sometimes for further noise and artifact removal, specially in portable monitoring devices [25]. Therefore, the selection of ADC depends on the resolution requirement and the application. Resolution upto 24 bit and sampling rate upto 2k samples/s are used when sophisticated post processing like ST-T micro-variability need to be

detected [25]. Delta-sigma ADCs have become common in ECG application since they provide higher resolution and faster data throughput.

Microcontroller

In standard monitoring, signal processing task is not sophisticated and hence can be handled by a low-power microcontroller. However, diagnostic monitoring requires advanced and very accurate DSP algorithms to be embedded into the device. Hence the wearable ECG device for diagnostic application contains the following digital modules:

- Microcontroller
- Clock generator
- Memory modules
- Screen for display
- Speaker for sound output
- Data transfer interface (USB or serial)
- Data transmission interface (bluetooth module or WLAN adaptor)

Above list of components suggests the fully-functioning embedded system board. Therefore, the OMAP353-based BeagleBoard is very suitable for this application and hence has been explained thoroughly in the previous sections.

5.3 ACTIVE BELT COMPONENTS

Textile Electrodes

The textile electrodes used in the wearable Active Belt system are manufactured by the Institute for Special Textile and Flexible Materials (TITV-Greiz, Germany). The electrodes are made of polyamide threads coated with pure silver with a thickness of 1-2 μ m and a resistivity of 20 Ω /m [26]. The threads, which are commercially called ELITEX[®], are undergone an electro-deposition procedure to coat pure silver on top

of polyamide material. Each thread can be stretched up to 7% of the original length without compromising the conductivity [26].



Fig. 5-12: The textile electrodes used for the Active Belt system. (a) An elliptical electrode, (b) a circular electrode and (c) a microscopic (40x) view of ELITEX[®] threads.

As shown in Fig. 5-12, two shapes of the electrodes are used in the Active Belt system: two elliptical electrodes (6.5cm x 3.5cm) for ECG collection and a circular electrode (Ø2.5cm) for ground. The technical details of the textile electrodes and the ELITEX[®] threads is listed in the Appendix.

Chest Belt

A stretchable and breathable chest belt (34.5cm x 84.5cm) was fabricated from neoprene material (SEDO Chemicals Neoprene GmbH, Germany) with velcro on the closing ends. Three textile electrodes, two elliptical for ECG collection are stitched on two sides of the torso on the belt and a circular electrode for ground (Ø2.5cm) next to the navel as shown in Fig. 5-13.



Fig. 5-13: The chest belt of the Active Belt System. (a) A skin contact side view of the belt and (b) an image of the chest belt worn by a subject.

Amp Plug

The raw ECG signal detected by the textile electrodes on the chest belt needed to be processed in the proximity to the electrode locations. The following factors were considered in designing a front-end circuit for the Active Belt system:

- Smaller in size
- Mountable in proximity to the electrode locations on the chest belt
- Easily detachable from the belt
- Functionally expandable for the other vital signals electromyogram (EMG), respiration rate, activity, sweating rate, etc. (In other words, multichannel inputs)
- High input impedance to overcome initial high electrode contact impedance
- Incorporating in-built multiplexer, and ADC if feasible
- low power consumption

The above requirements can be fulfilled by using a single CMOS IC, which can serve as a multi-channel biopotential amplifier with in-built filters and mux. Several options were considered before arriving to a CMOS IC RHA1016, which is a 16-channel biopotential amplifier and fits to the prerequisites.

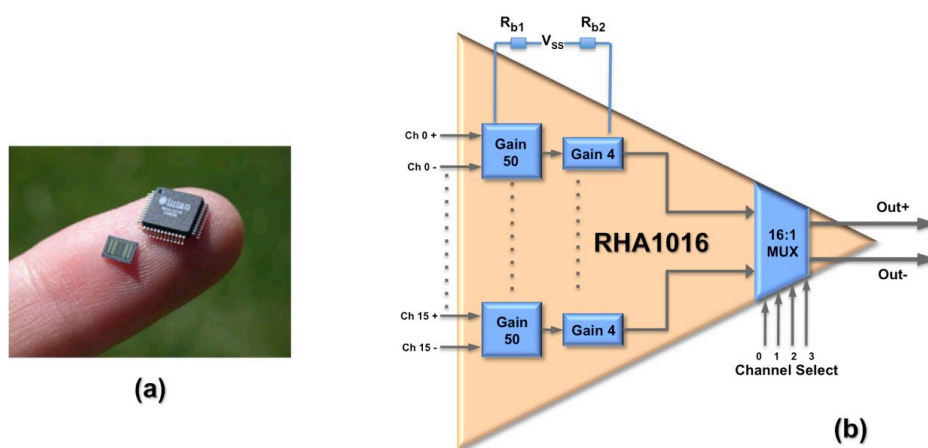


Fig. 5-14: An RHA1016 Biopotential Amplifier. (a) RHA1016 in packaged and bare die form [27] and (b) a simplified block diagram of RHA1016 internal circuit.

RHA1016 - A Biopotential Amplifier

The low-power, small RHA1016 (RHA) shown in comes in 48-lead LQFP surface-mount package (see Fig. 5-14a). Fig. 5-14b shows an internal block diagram of RHA. Some of the important features of the RHA1016 are as following [27]:

- The RHA contains 16 differential amplifiers (gain = 200) with programmable bandwidths suitable for many bioinstrumentation monitoring and recording applications.
- The internal micro-power circuit design allows for portable, battery-powered operation without sacrificing the low input-referred noise levels needed for detection of micro-volt level biopotentials.
- The bandwidth of the amplifiers can be programmed to any frequency between 10 Hz and 10 kHz by means of two external resistors, R_{b1} , and R_{b2} .
- Each amplifier had a 3rd-order Butterworth low-pass filter to reject signals and noise beyond the desired bandwidth and to minimizing aliasing.
- Internal capacitors reject large DC offset voltages at the input pins. This is important when it is necessary to eliminate the effect of built-in potential at electrode-tissue interfaces.
- The amplifiers are AC-coupled with a one-pole high pass filter below 0.05 Hz.
- Analog multiplexer (MUX) routes a selected amplifier signal of the chip and permits all channels to be sampled at max. 30 ksamples/sec/channel.

RHA1016 Circuit Design

Fig. 5-15 shows a circuit of RHA required for the Active Belt ECG system. A single channel ECG approach made the circuit very simple and required only few components. The two leads of textile electrode on the chest belt were required to connect to IN0+ and IN0- terminal of the RHA chip. Ground electrode needed to connect to analog supply ground. Although the RHA also supports dual power supply, +5V power supply is chosen in order to reduce the number of wires. Differential outputs OUT+ and OUT- bring the conditioned ECG signal for the analog to digital conversion.

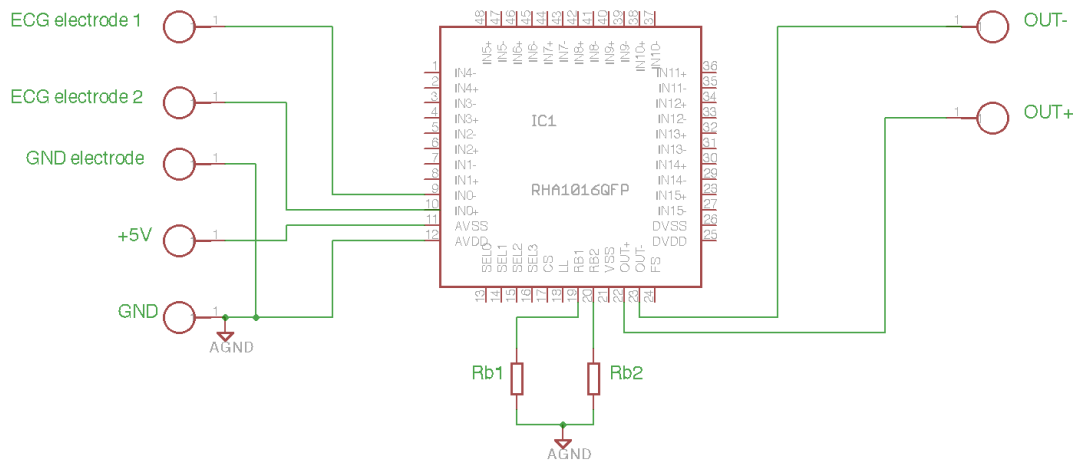


Fig. 5-15: An RHA circuit design for the Active Belt ECG system.

Setting a Cut-off Frequency:

As discussed earlier in filter circuits, the ECG signal contains max. 250 Hz frequency components. Hence, 250 Hz was selected for cut-off frequency of the built-in low-pass filter in the RHA chip. According to the list of combination for the resistor values shown in, the values of resistors R_{b1} and R_{b2} were selected as following.

Table 5-3: Selection of the resistors.

Cut-off Frequency	R_{b1}	R_{b2}
250 Hz	383 k Ω	1.15 M Ω

Moreover, the RHA chip has a built-in high-pass filter with cutoff frequency below 0.05 Hz which is sufficient in case of diagnostic ECG conditioning.

Amp PCB Deign

The goal was to place the RHA circuit as close as possible to the textile electrodes in order to minimize the antenna and capacitance effect. The other requirement was to enclose the PCB into a mountable device or a plug. Thus, the 1.6cm x 2cm cell-phone plug (AXR72161, Masushita Electric Works, Ltd) was selected to confine the RHA circuit (see Fig. 5-16). The phone plug has 22 pins that were used for commu-

nication between the RHA chip and an ADC and power supply. The open side of the plug is a passage for the textile electrode connections. The RHA circuit was designed in the Eagle software and constricted to the available space inside the plug. All components used in the double-sided PCB were surface mounted and manually soldered to comply with the temperature requirements of the RHA chip. A snap connector was stucked on the bottom surface of the plug in order to mount on the chest belt. The phone connector, which carries the RHA biopotential amplifier circuit, is called an Amp Plug.

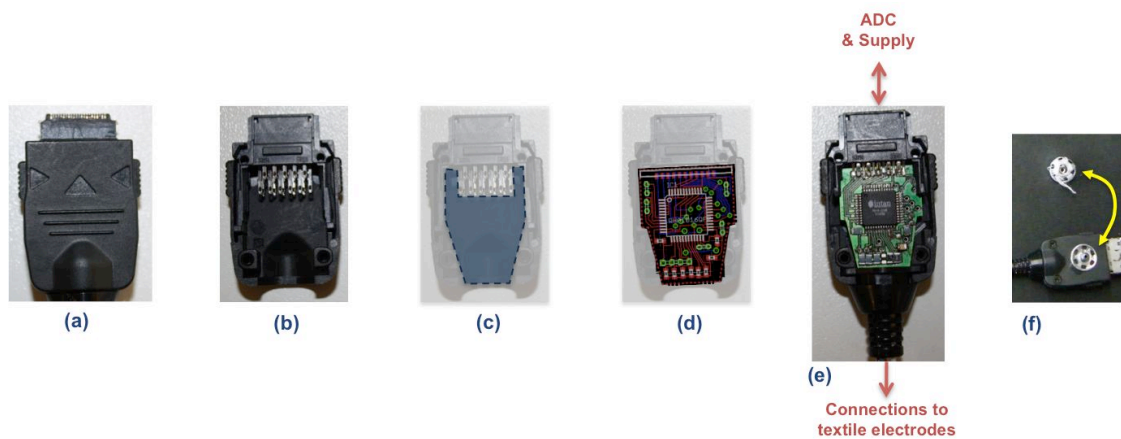


Fig. 5-16: A PCB design of the Amp Plug.

(a) A cell-phone plug selected for the Active Belt system, (b) an internal view of the plug, (c) a room for the RHA circuit, (d) an eagle board diagram of the RHA circuit, (e) the RHA amplifier PCB confined inside the plug and (f) the Amp Plug with a snap connector on the bottom to attach on the chest belt.

Digital Module

The digital module, which consists of the ADS1258EVM and the BeagleBord, has been discussed thoroughly in the section 4. As shown in Fig. 5-17, the digital module receives analog, differential ECG signal from the Amp Plug. The 24-bit ADC, ADS1258 digitizes the signal and makes it available on the SPI communication port. A dual-core smartphone processor, OMAP3530 on the BeagleBoard runs a SPI fetch program to control the ADS1258 and to collect the digital data. In the BeagleBoard, the digital data is processed, saved and displayed on the Ångström desktop environment.

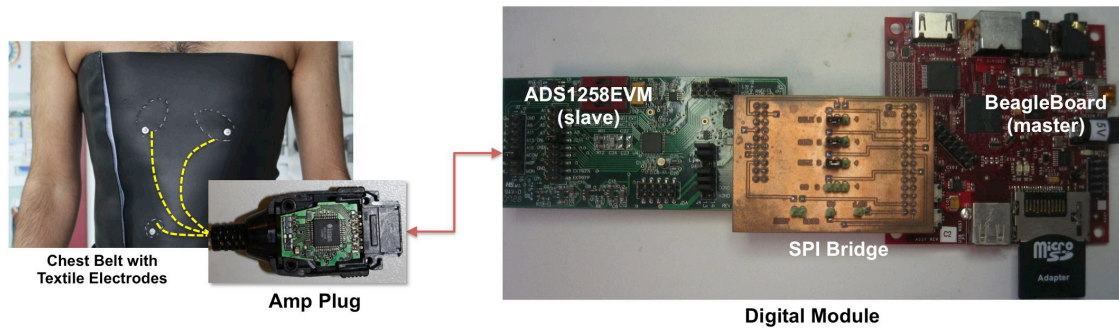


Fig. 5-17: The digital module for the Active Belt System.

5.4 ACTIVE BELT FIRMWARE

There are two algorithms associated with the Active Belt system: Active-ECG and Active-HR. The Active ECG algorithm is a plain, continuous ECG plotting on the desktop environment. While the Active-HR extracts the heart-rate from the received ECG signals.

Active-ECG

As shown in Fig. 5-18, the Active-ECG program is an extension of the spi-ads algorithm. The scaling is applied to the ECG decimal values in order to bring the signal into the plotting boundaries.

Active-HR

The Active-HR applies combination of low-pass and high-pass filters and extracts the heart rate values from the ECG decimal values. 17-tab low-pass filter restricts the signal to the frequency of 100 Hz. 17-tab high-pass filter detects the QRS complex. Time period of consecutive QRS complex is measured and plotted on the screen.

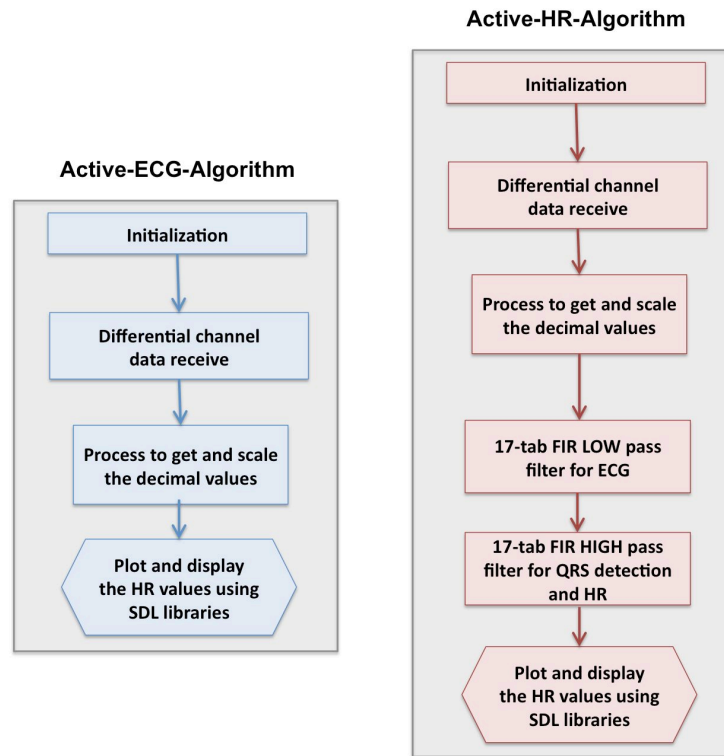


Fig. 5-18: Active-ECG and Active-HR algorithms for the Active Belt system.

5.5 EXPERIMENTS & RESULTS

Textile Electrodes under Test

Skin-Electrode Impedance Measurements

In long-term surface biopotential recordings, the skin-electrode impedance plays a major role in the quality of signals. Experiments were conducted to measure the skin-electrode impedance of the textile electrodes in comparison with commercial gelled disposable ECG electrodes with the help of an USB amplifier (g.USBamp, Guger Technologies, Austria).

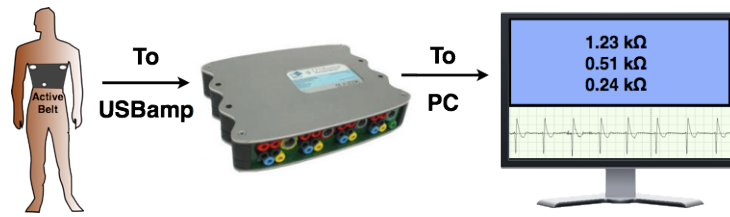


Fig. 5-19: An electrode performance measurement setup.

The experimental setup shown in Fig. 5-19 shows the worn chest belt with stitched textile electrodes. The conventional ECG electrodes were attached on the skin in proximity to the textile ones. All the electrodes were channeled to the USB amplifier, which is connected to a PC. A matlab code running on the PC measures the skin-electrode impedance of each electrode and displays the value on the screen. With such setup, a long-term (4 hours) impedance measurements were performed with interval of half an hour.

As shown in Fig. 5-20, the conventional electrode has a flat response over time. The impedance measured from the textile electrodes on the Active Belt shows exponential decrease during the beginning hours. The hypothesis behind such exponential decline in impedance is that secreted sweat under the textile electrode location improves the contact. To corroborate the hypothesized theory, a sweat phantom (saline-0.9% NaCl) was injected into one of the textile electrodes. At the same moment, the impedance of the injected textile plummeted far below the impedances of the conventional and dry textile electrodes.

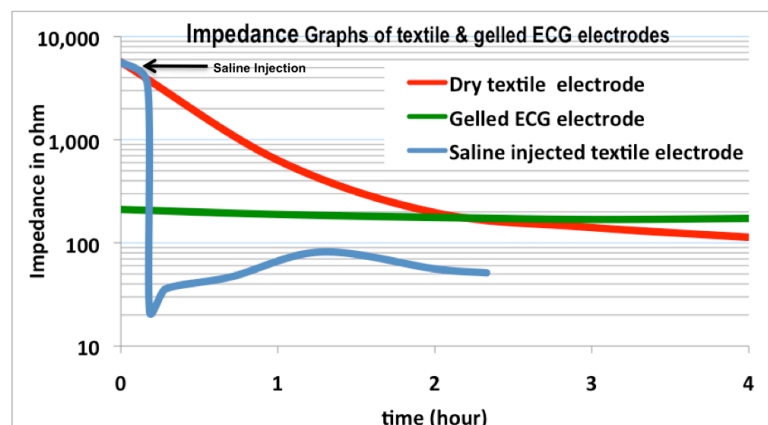


Fig. 5-20: The Impedance graph. In a long-term recording, the textile electrodes improve the contact impedance in comparison to the conventional electrodes.

Signal-to-Noise Ratio (SNR) Measurements

To evaluate the performance of the textile electrodes for long-term ECG recording, the signal-to-noise ratio (SNR) was calculated for ECG signals captured by the textile electrodes. For this, the same commercial USB amplifier was used to measure SNR at intervals of 1 hour. Fig. 5-21 depicts an increase in SNR after some hours as the textile electrodes improve their skin contact and hence enhance ECG signal quality.

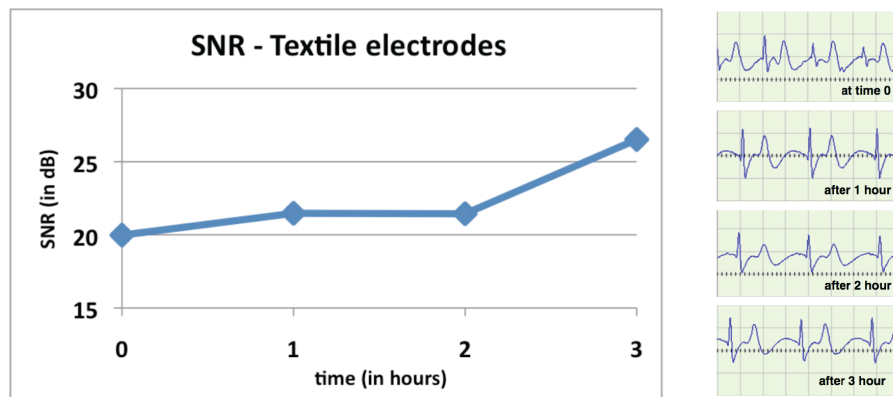


Fig. 5-21: SNR results of the textile electrodes. SNR over time (left) and long-term ECG recordings (right) from textile electrodes with USB amplifier.

Long-term ECG Recordings with Textile Electrodes

Two commercial systems, a patient bedside monitor and G.Tec USB amplifier were selected to obtain a single-channel ECG signals from the textile electrodes. Fig. 5-22 shows ECG signals captured by textile as well as by conventional Ag/AgCl electrodes in connection with a commercial monitor. The resulting signals on the screens infer that that the textile electrode possesses a sufficiently good quality for ECG recording.

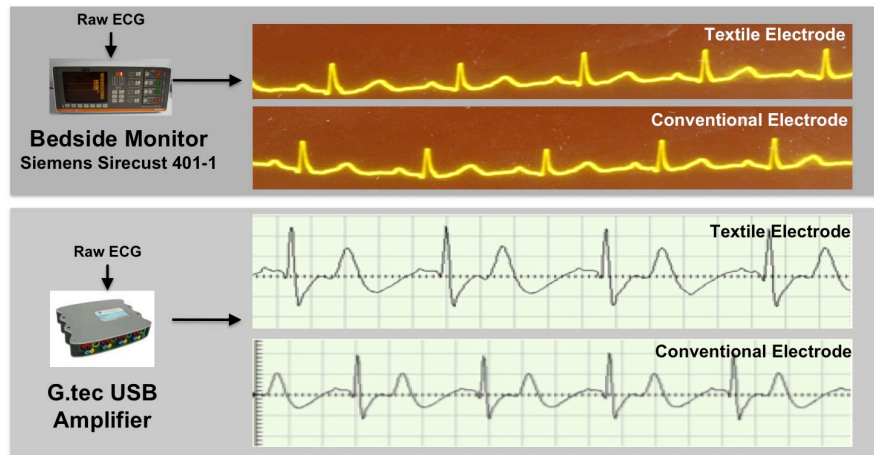


Fig. 5-22: The ECG recordings by commercial monitors.

Amp Plug under Test

Measurements on electrical properties of the Amp Plug

The Amp Plug confines the biopotential chip RHA1016 along with several components which performs the signal conditioning of the ECG signal collected by the textile electrodes. In this section, the Amp Plug’s evaluation procedure and results is discussed. The devices used in the performance test are shown in Fig. 5-23. The Amp Plug was powered by a battery based 5V supply.

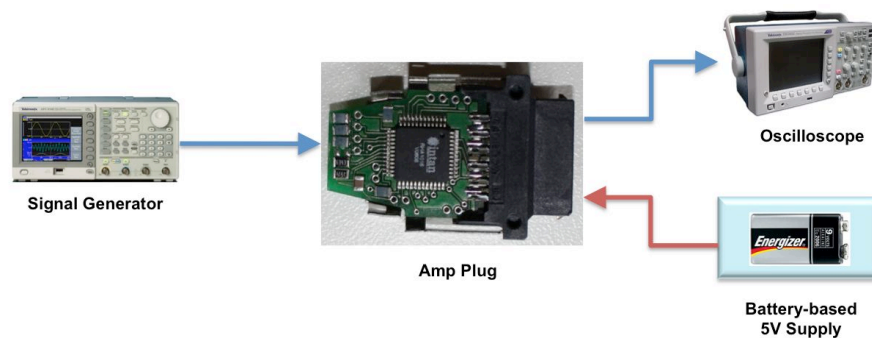


Fig. 5-23: An experimental setup for the Amp Plug tests.

Gain-Frequency Response

A sinusoidal of voltage signal was fed to the input channels of the Amp Plug. The gain was calculated for a wide frequency bandwidth. The graph shown in Fig. 5-24 shows that the gain began to fall down when the input signal frequency went beyond

the 200 Hz. The experiment met the expected gain value at 250 Hz considered during the circuit design process (section 4.3.3).

CMRR Measurement

The RHA1016 is a differential gain amplifier and hence should provide a high CMRR. The experiment was carried out in which the common voltage was applied at the input channels of the Amp Plug. In such case, the least voltage output was to observe. In order to know the CMRR value of the Amp Plug, the following calculations based on the available technical data of the RHA are necessary to note down [27]:

$$\text{Common Mode Voltage, } CMV(\text{gain}) = \frac{V_{out}}{V_{in}} = \frac{20mV}{2.5V} = 0.008 \quad \text{Eq. 5-5}$$

$$CMRR = 20 \log \left[\frac{\text{Gain}(RHA)}{CMV(\text{gain})} \right] (dB) = 20 \log \left[\frac{200}{0.008} \right] (dB) = 87.95 dB \quad \text{Eq. 5-6}$$

The graph in Fig. 5-24 reveals that the CMRR of the Amp Plug remains around 88dB, which is adequate to reject the noise in the wearable and battery-operated ECG monitoring.

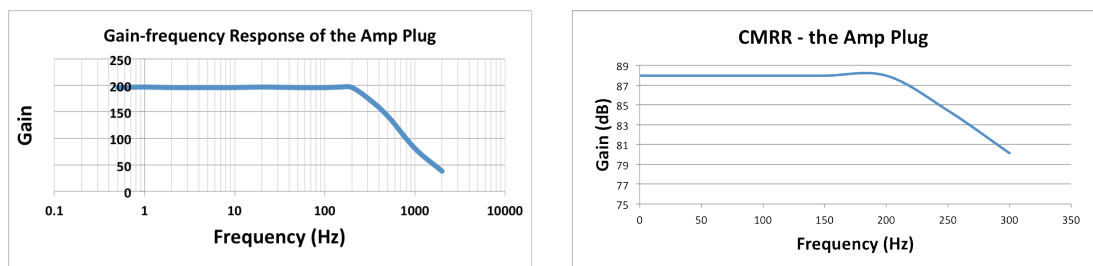


Fig. 5-24: The electrical properties of the Amp Plug.

ECG Recording with the Amp Plug

After the thorough electronic test procedure of the Amp Plug, it was examined for its ultimate usage of the ECG recording. Fig. 5-25 depicts ECG signals as output of the amplifier plug. These amplified signals (Fig. 5-25) are indistinguishable from the signals of the commercial amplifiers (Fig. 5-22) and hence validate the performance of the amplifier plug circuit. Moreover, the Amp Plug brings the amplitude of the ECG signals up to 500mV, which is significant for the digitization and processing. The Amp Plug showed a high SNR, which increased the ECG signal quality for diagnostic purpose.



Fig. 5-25: ECG recorded by the Amp Plug.

Active-ECG Recording with the Active Belt

The analog, differential ECG signal from the Amp Plug arrives at the digital module for digitization, further processing and display. The resulting processed signal in the BeagleBoard shown in Fig. 5-26 depicts that the ECG signals from convention electrodes are even more contaminated by power-line noise than the textile electrode signals. Quantization resolution of the ECG signals out of the ADS1258 is very high resolution with 24-bit at selectable sampling frequency (in this case, it was 23 ksp/s).

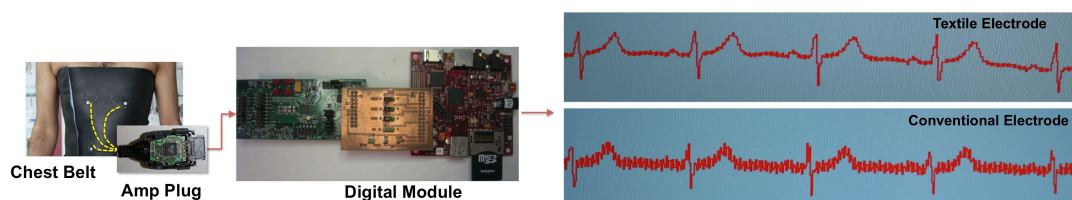


Fig. 5-26: The ECG monitoring with the Active Belt System.

Our C++ embedded application “Active-ECG” running on the ARM side of OMAP3 fetches digital ECG signals from the ADC and converts them into decimal values.

The application also plots the signals in real-time on the Ångström desktop environment utilizing the SDL library.

2-Lead ECG recording with the Active Belt

In order to explore different possible locations to detect ECG on the body, 2-lead electrode configuration was setup with the Active Belt system. In this configuration, the ground electrode is omitted and the floating ECG signals are detected. In this work, the textile electrodes detect the floating ECG on two index fingers of each hand and process the data in the same manner as mentioned earlier.

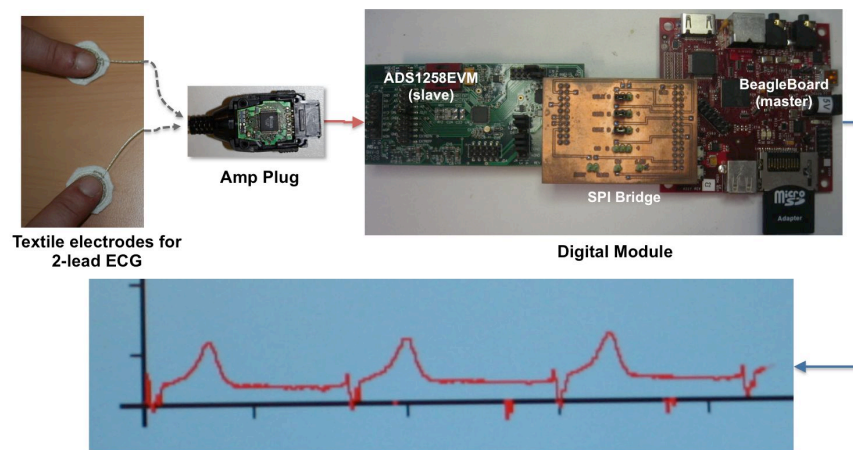


Fig. 5-27: Active-ECG plotting for 2-lead electrode configuration.

It can be seen from Fig. 5-27 that the ECG recorded using 2-lead configuration looks different than that of conventional 3-lead ECG setup. However, it still possess the QRS complex which can be detected for the heart rate monitoring.

Active-HR with Active-Belt Signal

Active-HR algorithm, which extracts the heart rate from the detected ECG signals, is shown in Fig. 5-27. HR was successfully monitored for both configurations; 3-lead and 2-lead. It can be seen from the plots that there have been data corruption during the SPI communication between ADS1258 and the BeagleBoard, which was not possible to avoid, since the McSPI on the BeagleBoard doesn't provide interrupt handling facility. This data corruption appears as an artifact in the HR plotting.

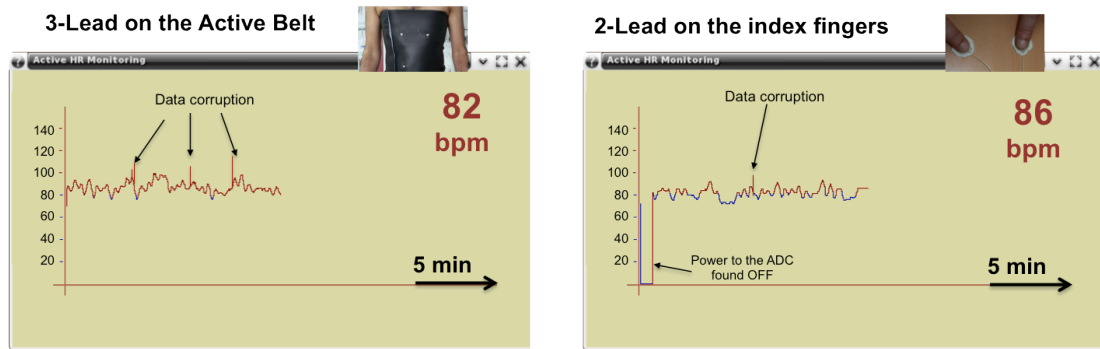


Fig. 5-28: Active-HR algorithm monitoring heart rate for 3-lead and 2-lead ECG configurations.

5.6 CONCLUSIONS & OUTLOOK

A successful implementation of a wearable single channel ECG Active Belt for a long-term ECG recording has been demonstrated. The Active Belt was designed to increase the diagnostic capabilities of the current ECG system. Therefore, the textile electrodes along with a tiny hardware circuits were developed to deliver a good quality of the ECG detection and conditioning. The dual-core smartphone processor was selected for the processing the ECG signal in real-time.

Initially, the textile electrode was compared with the conventional electrode in terms of their ability to perform long-term recording. The textile electrode has shown a promising outcome by exhibiting low skin-electrode impedance and a high SNR for long-term recording. The textile electrode showed a better performance in ECG detection when they were made in contact with the constant pressure.

Consecutively, analog-processing hardware – Amp Plug was designed to fit into tiny cell-phone connector, which is detachable and mounted in the vicinity to the ECG detection site. The Amp Plug passed different stages of the electronic verification and validation test. More, the Amp Plug was facilitated with the expandability for more physiological signals.

Finally, the amplified ECG signal entered into the digital module consisted of the ADS1258EVM and OMAP3-based embedded system, BeagleBoard. The BeagleBoard successfully collected, processed and displayed the ECG signals arriving from the Active Belt hardware by running the Active-ECG algorithm. The Active-HR al-

gorithm successfully extracted HR from the received ECG data and plotted them on the desktop environment. A successful implementation 2-lead ECG with the Active-Belt system enables to use the system for different setup, which will be explored in the section 8.

Thus, the Active Belt brings a long-term ECG recording in patient's daily life and helps in the future by on-site analysis and/or remote experts to diagnose cardiovascular problems earlier. The Active Belt system is also an integral part of the multimodal wearable health monitor and hence its usability will be discussed in the section 8.

5.7 REFERENCES

- [1] A. Gruetzmann, S. Hansen, and J. Mueller, "Novel dry electrodes for ECG monitoring.," *Physiological measurement*, vol. 28, 2007, pp. 1375-90.
- [2] N. Taccini, G. Loriga, A. Dittmar, and R. Paradiso, "Knitted Bioclothes for Health Monitoring," in Proceedings of the 26th Annual International Conference of the IEEE EMBS, San Francisco, CA, 2004, pp. 2165-2168.
- [3] R. Paradiso, G. Loriga, and N. Taccini, "Wearable System for Vital Signs Monitoring," in *Wearable eHealth Systems for Personalised Health Management: State of the Art and Future Challenges*, vol. 108, Studies in Health Technology and Informatics, A. Lymberis and D. de Rossi, Eds. Nieuwe Hemweg 6B, 1013 BG Amsterdam: IOS Press, 2004, pp. 253-259.
- [4] R. Paradiso, G. Loriga, and N. Taccini, "A wearable health care system based on knitted integrated sensors," *IEEE Transactions on Information Technology in Biomedicine*, vol. 9, pp. 337-344, Sept., 2005.
- [5] P. Grossman, "The LifeShirt: A Multi-Function Ambulatory System Monitoring Health, Disease, and Medical Intervention in the Real World," in *Wearable eHealth Systems for Personalised Health Management: State of the Art and Future Challenges*, vol. 108, Studies in Health Technology and Informatics, A. Lymberis and D. de Rossi, Eds. Nieuwe Hemweg 6B, 1013 BG Amsterdam: IOS Press, 2004, pp. 133-141.
- [6] <http://www.sensatex.com/>
- [7] P.S. Pandian, D. Bioengineering, C.V. Nagar, K.P. Safeer, P. Gupta, D.T. Shakunthala, B.S. Sundershesu, V.C. Padaki, D. Bioengineering, and C.V. Nagar, "Wireless Sensor Network for Wearable Physiological Monitoring," *Journal of networks*, vol. 3, 2008, pp. 21-29.
- [8] C. Park, P.H. Chou, Y. Bai, R. Matthews, and A. Hibbs, "An Ultra-Wearable , Wireless , Low Power ECG Monitoring System," Proceedings of the 29th Annual International Conference of the IEEE EMBS Cité Internationale, Lyon, France: 2007, pp. 1659-1662.
- [9] R.R. Singh, "Preventing Road Accidents with Wearable Biosensors and Innovative Architectural Design," 2nd ISSS
- [10] John Webster. *Medical Instrumentation : Application & Design*. John Wiley & Sons,

INC. 2010

- [11] Geselowitz DB. On the theory of the electrocardiogram. *Proc IEEE* 77:857, 1989.
- [12] A. Grimbergen, A. C. MettingVanRijn, A. P. Kuiper, A. C. Linnenbank and A. Peper, "Instrumentation For The Recording And Digital Processing Of Multichannel ECG Data," *Proceedings of the Annual International Conference of the IEEE Engineering in Medicine and Biology Society*, pp. 726-727.
- [13] J. Enderle, S. Blanchard and J. Bronzino, *Introduction to Biomedical Engineering*, Elsevier Academic Press, 2005.
- [14] Berbari, E. J. "Principles of Electrocardiography." *The Biomedical Engineering Handbook: Second Edition*. Ed. Joseph D. Bronzino Boca Raton: CRC Press LLC, 2000
- [15] E. McAdams, "Bioelectrodes," in *Encyclopedia of medical devices and instrumentation vol. 1*, J. G. Webster, Ed., 2 ed: Wiley, 2006, pp. 120-166.
- [16] L. Beckmann, C. Neuhaus, G. Medrano, N. Jungbecker, M. Walter, T. Gries, and S. Leonhardt, "Characterization of textile electrodes and conductors using standardized measurement setups.," *Physiological measurement*, vol. 31, 2010, pp. 233-47.
- [17] Geddes L A and Baker L E 1968 *Principles of Applied Biomedical Instrumentation* (New York: Wiley)
- [18] Schwan H P 1968 Electrode polarisation impedance and measurements in biological materials *Ann. New York Acad. Sci.* **128** 191–209
- [19] Muehlsteff J and Such O 2004 Dry electrodes for monitoring of vital signs in functional textiles *Proc. 26th Int. Conf. of the IEEE EMBS (San Francisco, USA)* pp 2212–5
- [20] Beckmann L, Kim S, Dueckers H, Luckhardt R, Zimmermann N, Gries T and Leonhardt S 2008a Characterization of textile electrodes for bioimpedance spectroscopy *Proc. Int. Scientific Conference Smart Textile—Technology and Design, Ambience 2008 (Boras)* pp 79–83
- [21] Medrano G, Ubl A, Zimmermann N, Gries T and Leonhardt S 2007 Skin electrode impedance of textile electrodes for bioimpedance spectroscopy *Proc. XIII Int. Conf. on Electrical Bioimpedance and VIII Conf. on Electrical Impedance Tomography (Graz)* pp 260–3.
- [22] B. Christe, *Introduction to Biomedical Instrumentation*, Cambridge University Press, 2009.

- [23] S. Hargittai, "Efficient and fast ECG baseline wander reduction without distortion of important clinical information," *2008 Computers in Cardiology*, 2008, pp. 841-844.
- [24] S. Chaudhuri, T. D. Pawar, and S. Duttagupta, *Ambulation Analysis in Wearable ECG Devices*, Springer, 2009.
- [25] H. A. Kestler, F. Schwenker, J. Wohrle, V. Hombach, G. Palm, and M. Hoher. Combined Assessment of Beat-to-Beat Micro-Variability and Signal-Averaged ECG parameters. In *IEEE CC 2001*, pages 28:73-28:76, 2001.
- [26] www.titv-greiz.de, "The Institute for Special Textiles and Flexible Materials."
- [27] RHA1016 Datasheet: Intan Technologies LLC, 2006, www.intantech.com/products.html
- [28] Recommendations for measurement standards in quantitative electrocardiography. *Eur. Heart J*, 6:815-825, 1985.
- [29] J.M.R. Delgado, "Electrodes for Extracellular Recording and Stimulation." in W. L. Nastuk(ed.). *Physical Techniques in Biological Research*. New York: Academic Press, 1964

6. A MINIATURIZED CEREBRAL OXIMETER

Alarming increase in the cardiovascular disorder especially in the greying society has made the cardiac operating procedure very common. Hence, cerebral injury due to hypoxia is currently one of the most dreadful outcomes in cardiac surgery and general anaesthesia. Electroencephalography, which is a predominant method in monitoring the cerebral damage during surgery, is being challenged due to its complexity of use and the data analysis. The cerebral injury is not limited to the surgical interventions, but also extended to the post-operative recovery period. Thus, it is highly required to monitor the cerebral parameters even out-of-the-hospital environment. In recent years, the application of the non-invasive cerebral oximetry is increased because of its ease of use and valuable information deliverance. However, the bulkiness of the standard cerebral oximeter limits its use in the hospital environment. This section presents the miniaturized design of a cerebral oximeter using the OMAP3530. The miniaturization in the design increases the portability and brings the monitor in the daily life use as well. The section also presents a design of the pulse oximeter, which shares similarity in principle and device architecture with the cerebral oximeter.

6.1 A DEMAND FOR THE MINIATURIZED OXIMETRY SYSTEM

Due to raise in the number of the cardiovascular patients globally, the open-heart surgery and cardiac procedures have become increasingly common. The brain injury results as a side effect to the cardiac procedure and is occurred to the fraction of the patients. The U.S. study [2] found a 6% incidence of major brain injury following myocardial revascularization, whereas the international study [3], performed on patients at least 60 years of age, noted an alarming 26% incidence of marked cognitive decline postoperatively. An occurrence of the postoperative neurocognitive deterioration has also been observed in long-term studies [4]. The deterioration is closely associated with a diminished quality of life and is age-related. Moreover, Brain injury

(including brain damage, stroke and awareness) represents the single largest fraction (17%) of anaesthesia malpractice claims [1].

Besides the unhealthy conditions, the "aging process" is known to cause specific cardiovascular changes that impair heart and blood vessel function. Although the human body is surprisingly robust in many ways, the physiological process of sustaining proper cell function via oxygen transport is a delicate and complex control system; one, which if altered too significantly could become unstable and insufficient for meeting oxygen tissue demands. Cardiac arrest is one of such condition, during which the heart fails to contract effectively and is unable to circulate the blood normally. The cardiac arrest causes a total decrease in the level of oxygen, known as anoxia. Table 6-1 lists the survival times for the different organ after the onset of anoxic cardiac arrest [16]. The cerebral cortex becomes the fastest victim of the condition. This data also estimates that the short-or long-term hypoxia (low oxygen level) may damage the cerebral functioning and diminish the life quality.

Table 6-1: Organ robustness to anoxic cardiac arrest. Adapted from [23].

Organ	Survival time after anoxic cardiac arrest
Cerebral cortex	Less than a min
Heart	5 min
Liver and kidney	10 min
Skeletal muscle	2 h

In order to take the measures against the brain damage in the graying society, the continuous cerebral monitoring is suggested during surgery as well as post-operative recovery period [6]. Sometimes, it is even required to monitor the cerebral parameters in out-of-hospital environment. A predominant method in cerebral monitoring, intraoperative electroencephalography (EEG) is associated with challenges in data collection and interpretation and requires trained personnel during surgery [7]. Moreover, the EEG is unable to provide the brain oxygenation information. In contrast, cerebral oximetry is an application of near infrared spectroscopy (NIRS) for non-invasive continuous monitoring of cerebral metabolism and oxygen consumption and very easy to implement [7]. NIRS is very flexible, biochemically specific and highly sensitive to detect small substance concentrations [8].

The cerebral oximeter furnishes the valuable brain information such as cerebral oxygenation and hemodynamics, which are important parameters to be monitored during anaesthesia conditions. The cerebral oximetry is also useful in evaluating the progress and recovery of patients with head injury or cerebrovascular accidents [7]. Even though the cerebral oximetry is a useful monitoring method during post-surgical condition, its use is currently limited to the hospital environment and commonly to the surgery room and ICUs due its bulky size and weight. The usefulness of the cerebral oximetry in out-of-hospital environment encourages to miniaturize the design of the cerebral oximeter and to bring it into daily life monitoring to increase the quality of the patient's life.

The following presents a novel design of a cerebral oximeter (CereOxi), in which the smartphone processor OMAP3530 miniaturizes the system design and also provides the high computing power to perform complex diagnostic signal processing. In the featured design (Fig. 6-1), the OMAP3530 generates the pulse signal to drive a light source and receives the digitized sensor signals after analog processing. The OMAP3530 analyzes and displays the detected signal. Moreover, due to the similar design principle, the system facilitates the pulse oximetry measurements as well.

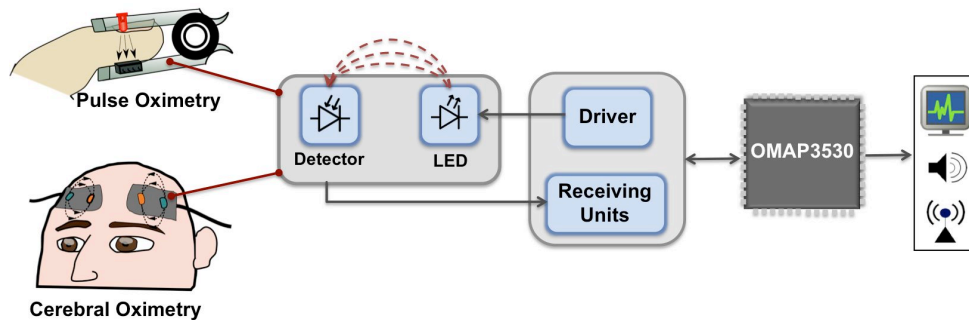


Fig. 6-1: The concept of the miniaturized oximetry system.

6.2 BACKGROUND THEORY

The oximetry is a very general term in medicine. Oximetry is a procedure for measuring the concentration of oxygen in the blood. This procedure is performed by photoelectrical device called oximeter, which uses the probe to irradiate the skin along with underlying tissue and detects the oxygen saturation from the blood vessels.

Some background theories and principles, which play major role in designing the oximeter, are discussed in the following paragraphs.

Tissue Optical Properties

Optical properties of tissue are used in biomedical applications for diagnosis, treatment and surgery. Tissue is in general an inhomogeneous medium with different and randomly distributed absorbers and scatters. Light incident on tissue can undergo different “events” which are shown in Fig. 6-2. The ballistic components are the light that passes through tissue unaffected by the absorbers and scatters within the tissue. The “snake” component consists of photons that propagate along a zigzag path only slightly off the straight path and arrive later than the ballistic component [13]. Photons that scatter many times will diffuse the light such that it is propagating in all directions and will therefore be responsible for both diffuse reflectance and transmittance. Scattering also increases the absorbance due to an increase of the light path.

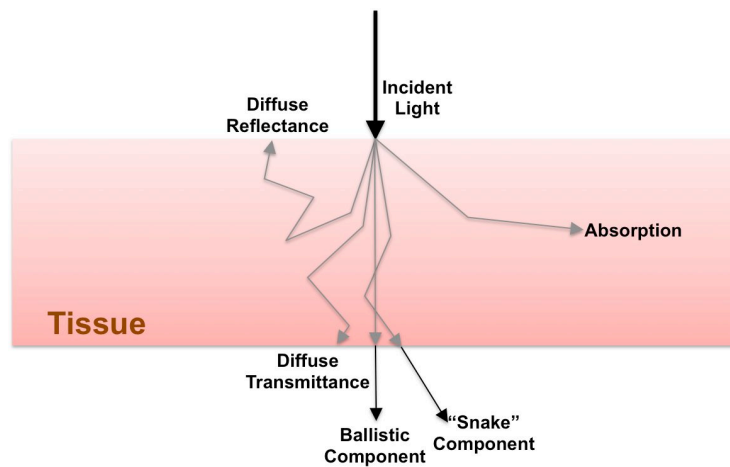


Fig. 6-2: An illustration of light-tissue interaction.

The Role of NIRS in Tissue Oximetry

In comparison to normal light, NIR light within the optical window (650nm-950nm) exhibits less scattering within biological tissue and therefore penetrates deeper inside than plain visible light [10]. When penetrating human tissue, NIR light undergoes two important phenomena, namely absorption and scattering, which can be derived by the modified Beer-Lambert law as following [11]:

$$A = \log_{10}(I_o / I) = a \cdot c \cdot d \cdot DPF + G \quad \text{Eq. 6-1}$$

Where,

A = the measured absorbance,

I_o = the incident light intensity,

I = the transmitted light intensity,

a = the wavelength dependent extinction coefficient of a medium,

c = concentration of a medium,

d = the light travel distance,

G = additive term, due to the scattering losses,

DPF = differential path length factor, to account for the increased optical path length due to the scattering.

Due to inhomogeneous nature of the tissue, photons scatter and lose their original directions after interacting with tissue compounds. This phenomenon furnishes the theory to detect hemodynamic changes in living tissue [11]. By knowing the intensity of the incident (I_o) and transmitted (I) lights, the absorbance (A) can easily be calculated from Eq. 6.2. The absorbance (A) is in proportion to the optical parameters of tissue components, which also contain the information regarding the blood oxygen saturation.

Pulse Oximetry in Principle

Pulse oximetry is the method for non-invasive measurements of two important quantities to describe the medical and physical condition of an individual:

- The oxygen saturation of blood
- The heart beat rate – pulse

The unique feature of pulse oximetry is to measure the oxygen saturation and thereby detect a lack of oxygen in the blood i.e. hypoxemia. The measuring principle of pulse oximetry relies on spectrophotometry i.e. measurement of the absorptivity or extinction coefficient of a given substance at particular wavelengths. In the case of pulse oximetry, the subject of interest is oxygen in the blood.

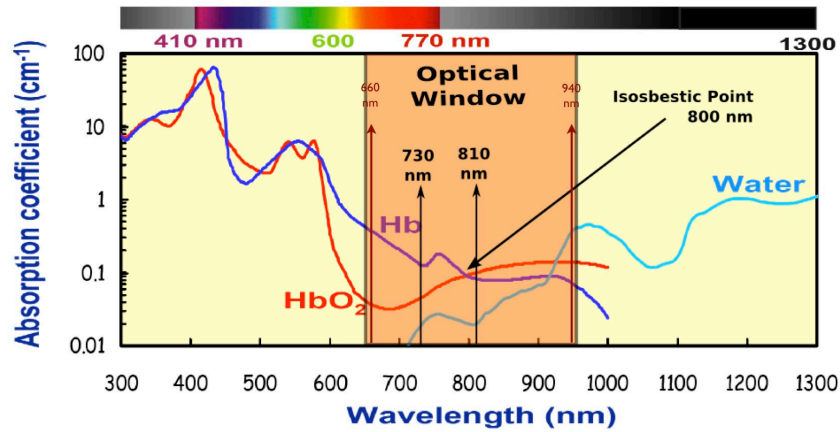


Fig. 6-3: Absorption spectra of deoxygenated Hb (Hb), oxygenated Hb (HbO₂) and water [7]. The wavelengths, 660nm and 940 are for pulse oximetry. The wavelengths, 730nm and 810 are for cerebral oximetry.

The transport of oxygen in the body is performed by the protein haemoglobin (Hb) in the red blood cells. Oxygen is bound to Hb in the lungs whereby Hb becomes oxygenated (HbO₂), and transported by the blood to the cells. The oxygen saturation is then defined as the fraction of the concentration of oxygenated Hb (HbO₂) to the total concentration of Hb. It has been observed that HbO₂ absorbs less red and more infrared than Hb (see Fig. 6-3) [11] [13]. The measurement of light absorption at two wavelengths (chosen such that $\lambda_1 < \lambda_{\text{iso}} < \lambda_2$, where λ_{iso} is the NIR isosbestic wavelength at 800nm) across the tissue gives the concentrations of HbO₂ and Hb. Generally, 660nm and 940nm wavelengths of the light is used in the pulse oximetry. Hence, the tissue oxygenation index (TOI) can be calculated by the following equation [12]:

$$TOI = (HbO_2 / [Hb + HbO_2]) \times 100 \quad \text{Eq. 6-2}$$

Pulse oximetry is typically performed at extremities of the body e.g. a finger. The reason for this is that these body parts are generally well perfused with blood vessels [15] and the volume fraction of blood is therefore high. Pulse oximetry measurement geometry is divided into two categories: transmittance and reflectance.

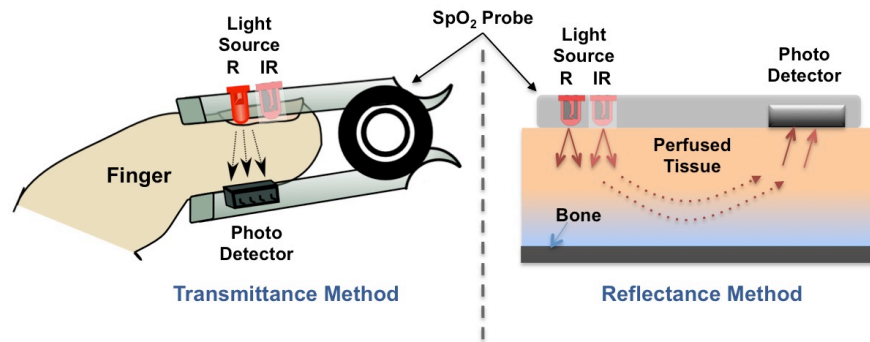


Fig. 6-4: The SpO_2 measurement methods; a transmittance method (in left) and a reflectance method (in right).

In transmission mode (Fig. 6-4a), the light sources and light detector are placed on the opposite side of the finger and light is shined through the finger. This configuration is used more frequently in monitoring systems today, because the sensor can be attached to the finger with a simple and reusable clip, as schematically illustrated in Fig. 6-4, and because it under normal and raised body temperatures gives a good signal quality [16, 17].

The concept of reflectance mode is shown in Fig. 6-4b, in this case the light sources and light detector are placed on the same surface which allow for a smaller solution where light sources and light detector are integrated and therefore can be placed within one patch. The reflectance mode has also less restriction for placement on the body and therefore has been chosen for the presented work.

Fig. 6-5 illustrates the pulse oximetry measurement signal, which is called a photoplethysmogram, where photo denotes that an optical method is used and plethysmogram that variations are caused by changes in volume (here blood vessels) due to blood pressure. There are several contributors to the absorbance of the light during the oximetry. Skin, tissue and bones make a constant absorbance together with the venous blood and the non-pulsating arterial blood. Thus the constant absorbance brings the DC level in the measured plethysmogram. The alternating signal, which is denoted as the AC part of the signal, is due to the pulsatile arterial blood flow. The pulsating signal represents a cardiac cycle, which consists of systole and diastole. A dicrotic notch in the plethysmogram represents a transient increase in aortic pressure.

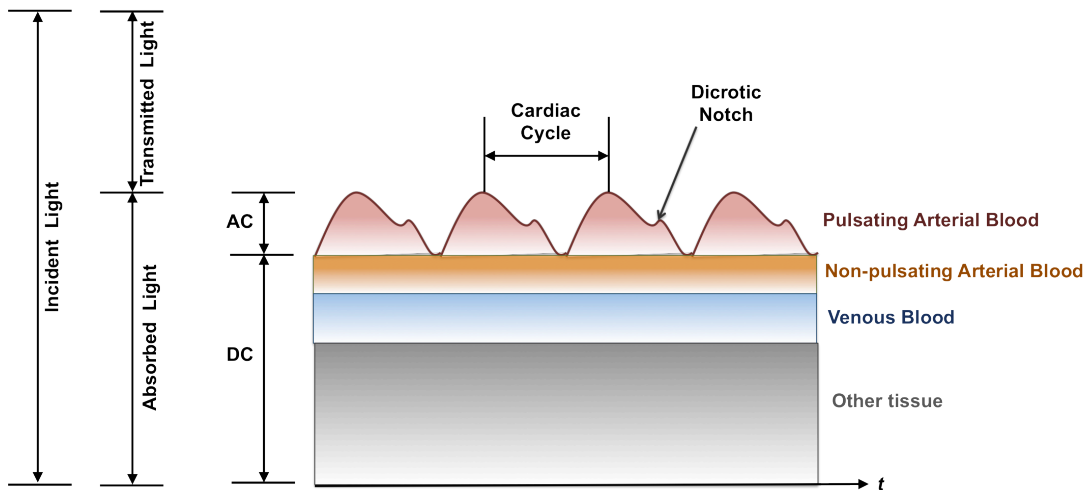


Fig. 6-5: A schematic of the photoplethysmogram [16]

Cerebral Oximetry

The cerebral oximeter relies on principles of near-infrared spectroscopy similar to those used for peripheral pulse oximetry with one important difference. Pulse oximeters measure a pulse-gated change in optical density and hence monitor arterial O_2 saturation [20]. Pulse oximetry becomes less reliable with non-pulsatile perfusion and peripheral vasoconstriction [19]. Cerebral oximeters measure total optical density and hence monitor oxygen saturation in the total tissue bed including capillaries, arterioles, and venules [20].

In cerebral oximetry measurement, a light source with NIR light at 730nm and 810nm wavelengths is used. Difference in the wavelengths for cerebral oximetry from the pulse oximetry is due to the change in the location of the sensor as well as the composition of the targeted tissue. As shown in Fig. 6-6a, the light source injects photons into the skin over the forehead. After passing through skin, scalp, skull, dura and brain, some small fraction of the injected photons are backscattered to the detectors on the skin surface (Fig. 6-6b). By measuring the quantity of the photons impinged on the detectors, one can accurately estimate the spectral absorption of the targeted tissue and hence determine the average regional oxygen saturation.

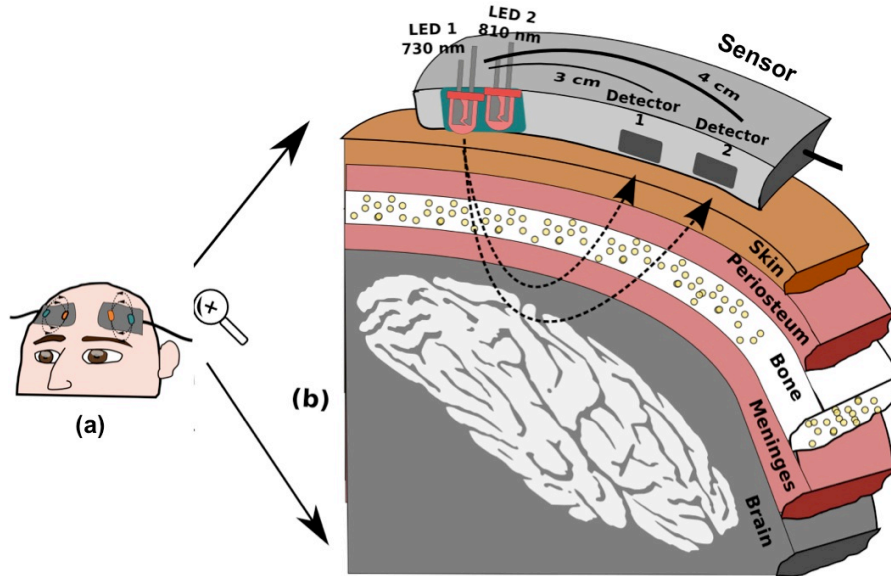


Fig. 6-6: (a) the locations of the cerebral oximetry sensors on the frontal bones (forehead) and (b) a descriptive sketch of the cerebral oximetry principle.

To minimize the impact of extracerebral oxygen, two detectors are differentially spaced at 3cm and 4cm to record photons reflected from extracranial (shallow) and intracranial (deep) tissue, respectively. Subtraction of the signals from the shallow to deep region thus results in the recording of dominant photon reflected from the cerebral cortex [18]. To calculate the regional oxygen saturation (rSO_2) of the brain, the Eq. 6-1 can be modified in the following manner [19]:

$$A_{deep} - A_{shallow} = a \cdot (c_{deep} - c_{shallow}) \cdot d \cdot DPF \quad \text{Eq. 6-3}$$

Where,

$(A_{deep} - A_{shallow})$ = The measured change in absorbance of light from deep to shallow region of the brain.

$(c_{deep} - c_{shallow})$ = The difference between the concentration of the mediums from deep to shallow region of the brain

DPF value of 6 was obtained for the human brain [9]. In other words, for an interop-tode spacing of 4 cm, a mean distance, which the light actually travels in the head, is approximately 24cm. Once d , a and DPF are known in Eq. 6-3, the change in the medium concentration can be computed from the measured absorbance. This ap-

proach is sufficient to detect hemodynamic changes in a cortical area under the probes. As mentioned previously, the concentration change of HbO₂ and Hb can be determined by measuring the change in attenuation at two wavelengths (730nm and 810nm) and using the known extinction coefficients of HbO₂ and Hb at these wavelengths.

In brain tissue, the vascular compartment is predominantly venous (70–80%) versus arterial (20–30%) [19]. The oxygen saturation of cerebral venous blood is about 60%, versus 98–100% in the arterial blood [19]. Based on these assumptions, the average regional oxygen saturation is 60–70% and yields non-pulsating signal [19].

Fig. 6-7 shows the recording of cerebral oximetry during the cardiopulmonary bypass procedure, which is an open-heart surgery [19]. The symmetrical decline rSO₂ can be observed during the operation period and also indicates the decline in the oxygen supply to the brain. This is caused by hemodilution reducing the oxygen-carrying capacity of the blood and decreased pulsatility [19]. This example of the rSO₂ recording indicates that the heart procedure decreased the oxygen supply to the brain and may cause the damage to the brain not only during the procedure but also in the recovery period.

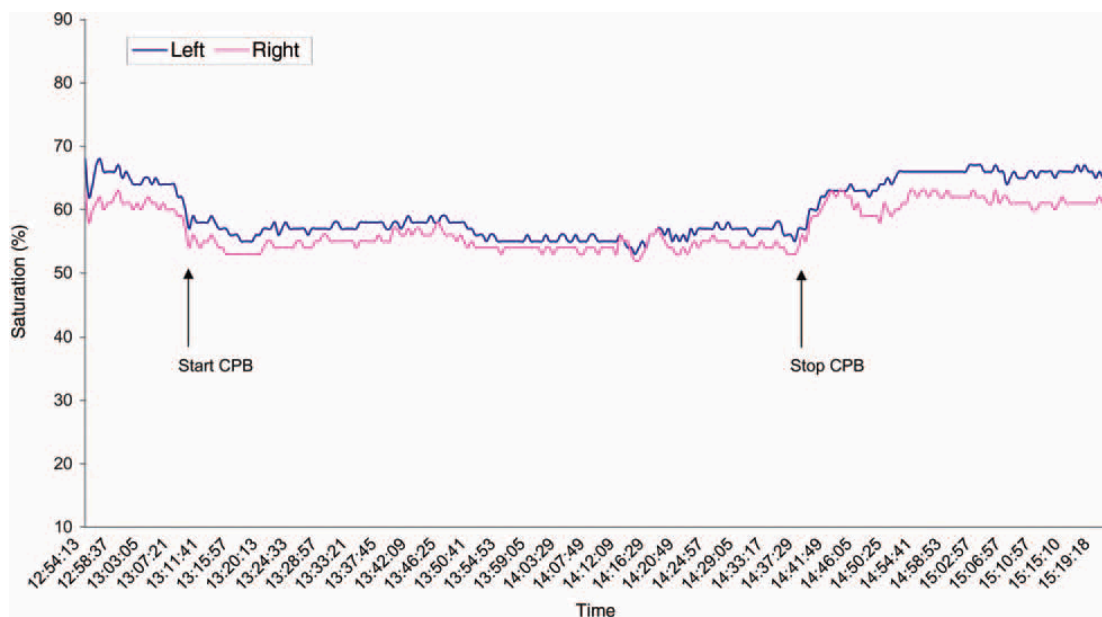


Fig. 6-7: Recording of near-infrared spectroscopy during coronary artery bypass grafting. CPB = cardiopulmonary bypass. Adapted from [19].

Frontal Bone Spectroscopy

The human brain is protected in the thick skull bone. It is always intriguing to know the optical property of the skull bone, since the NIR light penetrates this thick layer twice during its curved optical journey during cerebral oximetry. Therefore, in order to investigate the optical property of the human frontal bone in NIR spectrum, the skull of a 60+ aged male (Institute for Anatomy, University of Luebeck, Germany) was illuminated by the halogen lamp at foramen magnum (Fig. 6-8a). A portable spectrometry system (Avantes BV, The Netherlands) facilitated detection, display and analysis of the transmitted light through frontal bone.

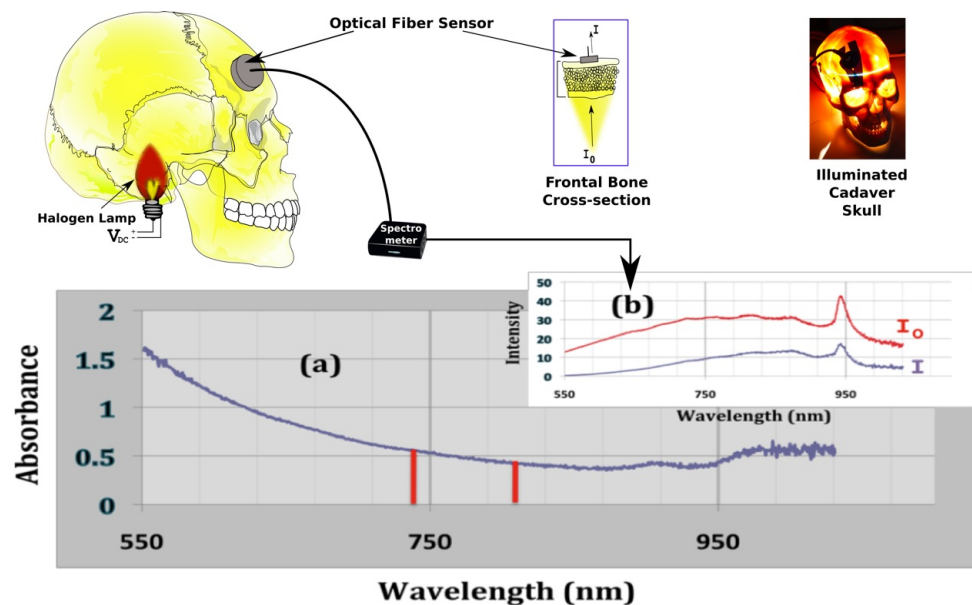


Fig. 6-8: (a) A setup for a human frontal bone spectroscopy and (b) a graph of absorbance vs. wavelength showing a decline in absorbance for NIR window used for cerebral oximetry.

From the graph in Fig. 6-8b, it is apparent that the human frontal bone absorbs more visible light than light in a near infrared. Moreover, at the wavelengths of 730nm and 810nm, the frontal bone has lower absorption and hence is a suitable location to carry out cerebral oximetry. Several other locations on the human skull were also taken during this experiment. A parietal bone (behind the ear) showed similar results for the NIR experiment. None of the locations show such a large decline in absorbance for NIR light. The different absorbance on the skull bones is due to the variation in the thickness of the bones. By observing the original picture of the illuminated skull

in Fig. 6-8a, it is obvious that the illumination at the frontal and parietal bones is much brighter than at other locations.

6.3 SYSTEM COMPONENTS

Fig. 6-9 shows the generalized oximetry hardware which can be implemented for both cerebral and pulse oximetry with some variations. The following presents the analog hardware design for the cerebral oximetry and pulse oximetry. For ease of understanding, the cerebral oximetry is referred to as CereOxi and pulse oximetry as PulseOxi.

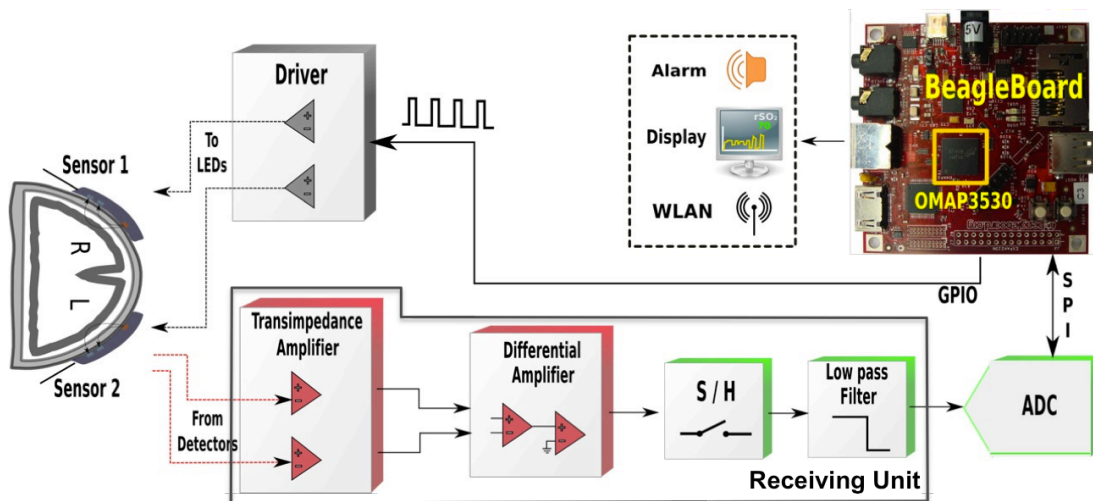


Fig. 6-9: A simplified block diagram of the Oximetry system

As shown in Fig. 6-9, the oximetry system consists of four different parts: sensor, driver circuit, receiving unit and digital module. In our case, the digital module is combination of the ADS1258EVM and the BeagleBoard, which has thoroughly been explained in section 4. OMAP3530 generates the pulse to trigger driving circuit and eventually light source on the sensor. The sensor illuminates the tissue from the skin surface. The detector on the sensor receives the photos from the tissue and converts them into electrical form. The receiving unit is made of many stages to process the received signal and send it to the digital module.

Oximetry Sensors

A commercial, disposable optical sensor (SomaSensor 4100-SAF, Somanetics Corp., USA) was used to illuminate the forehead in order to carry out the cerebral oximetry using the CereOxi system [24]. The sensor shown in Fig. 6-10 is made of light sources and photo-detectors. There are two LEDs (730nm and 810nm) embedded on a single site. One of the two photo-detectors is 3cm apart from the light source, while the other is 4cm.

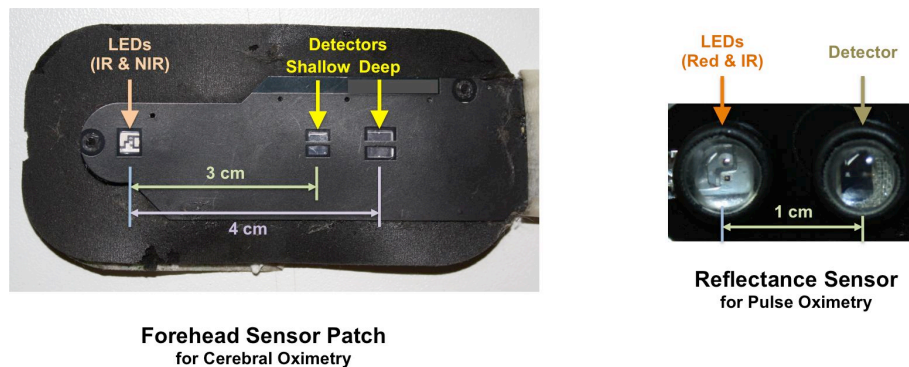


Fig. 6-10: Pictures of commercial sensors used for the cerebral oximetry [24] and the pulse oximetry [25].

For the pulse oximetry, a commercial sensor (MaxFast, Nellcor, USA), which is a reflectance sensor, was used [25]. The light source on the sensor consists of two LEDs (660nm and 940nm). As shown in Fig. 6-10, the distance between light source and detector is 1 cm which is lower than that of the cerebral oximeter patch, because the light doesn't need to penetrate deeper in the tissue to collect the SpO₂ signal.

LED Driver

Two technical approaches are very common for NIR spectroscopy: continuous wave (CW) and the time resolved spectroscopy (TMS) [8]. CW approach uses the continuous wave light source and hence is very simple and flexible [8]. Although, CW has a strong contribution to the signal changes by superficial, extracerebral structures, the separation of deep and superficial layers can be approximated by multiple source-detector separations [8]. Time resolved spectroscopy provides the high resolution in

quantifying concentration changes and hence requires the demanding technology. For our CereOxi and PulseOxi systems, there is a demand of miniaturization and low-power which suggest to implement the CW method.

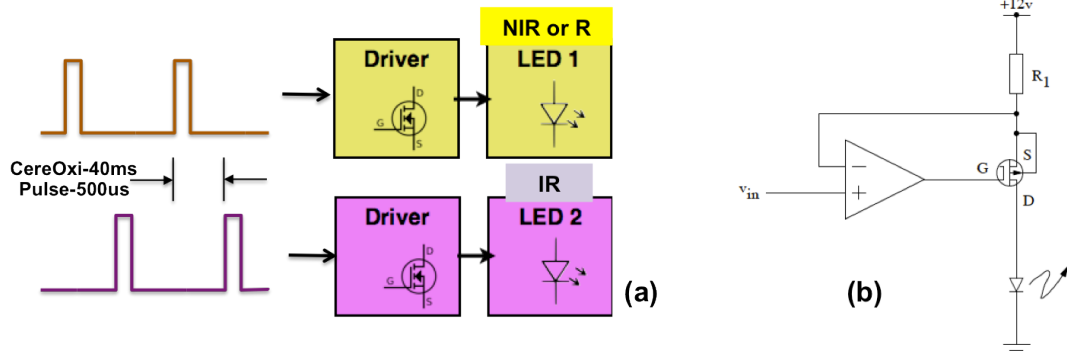


Fig. 6-11: (a) An illustration of pulse chain required to drive the LEDs and (b) a typical constant current source as an LED driving circuit for the oximetry.

In order to illuminate the forehead region during cerebral oximetry, the driver circuit supplies the controlled current to the two LEDs (IR and NIR) on the sensor patch in an interleaved manner (Fig. 6-11). There are several factors to be considered to choose the pulse repetition frequency. In order to investigate the suitable frequency for the cerebral oximetry, a thorough experiment was conducted and described later in this section. In case of PulseOxi system, the pulse repetition rate of 380 Hz, which is a standard rate for SpO_2 measurements [16], was chosen. MOSFET-based constant current source was implemented due its low base current error compare to the transistor-based circuit. A program on the OMAP3530 is designed to generate the pulses via general purpose I/O (GPIO) pins. The program will be discussed further in the firmware topic of this section.

Receiving Unit

As shown in Fig. 6-9, the receiving unit for the CereOxi system processes the raw signals from the two photodiodes and treats them at different stages. The function of the individual circuit is as following:

- A trans-impedance amplifier provides a gain of 97M to the deep detector and 27M to the shallow detector signals.

- Consecutively, the differential amplifier subtracts the shallow signal from the deep one and thus minimizes the impact of extracerebral blood oxygen.
- The sample/hold circuit holds the sample value till the next signal arrives.
- A low pass filter with a cut off frequency of 0.5Hz eliminates unwanted signals and smoothens the cerebral signals.

For the PulseOxi system, there is only a single detector, which eliminates the need of the differential stage. Furthermore, a band pass filter with cut-off frequencies of 0.3 and 10Hz are used.

Finally, a 16-channel, 24-bit ADS1258 (Texas Instruments Inc., USA) digitizes the analog oximetry data and channels it to the BeagleBoard via serial peripheral interface (SPI) port.

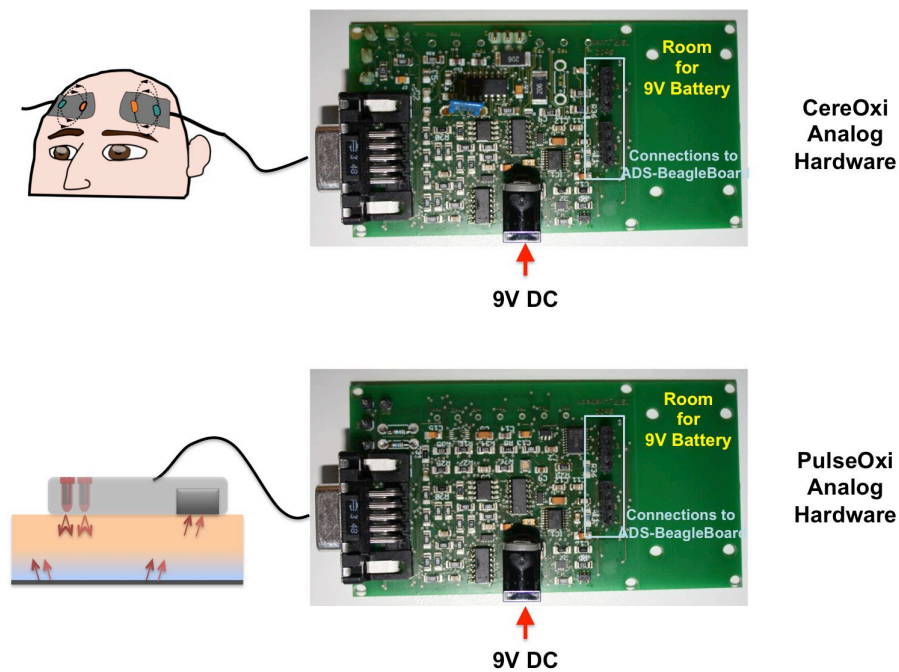


Fig. 6-12: Images of analog PCBs for the cerebral oximetry (top) and pulse oximetry (bottom).

Analog PCBs

Considering the requirements of miniaturization and low power, two miniaturized circuit board were designed: CereOxi and PulseOxi Analog PCBs. Fig. 6-12 shows the images of the PCBs. The circuit of these PCBs is too complicated to be explained

thoroughly in this report. However, the design layout of these PCBs is the same as the generalized block diagram shown in Fig. 6-9. The circuit schematics and board files can be found in the Appendix. Both PCBs measure 9.8cm x 5.2cm and contain only surface-mounted components. The surface mounting of the components on the PCB was achieved with an automatic laboratory soldering station. The PCBs facilitates three important connections; to sensor (via RS232 port), to 9V power adaptor and to digital module (ADS1258-BeagleBoard).

The power requirement for each block of the oximetry varies according to the function. As an example, the driver circuit demands the higher current to illuminate the LEDs and eventually the tissue. Therefore, the PCBs are facilitated with the regulated power supply circuits. The power to the PCBS can be provided by analog adaptor or by on-board battery.

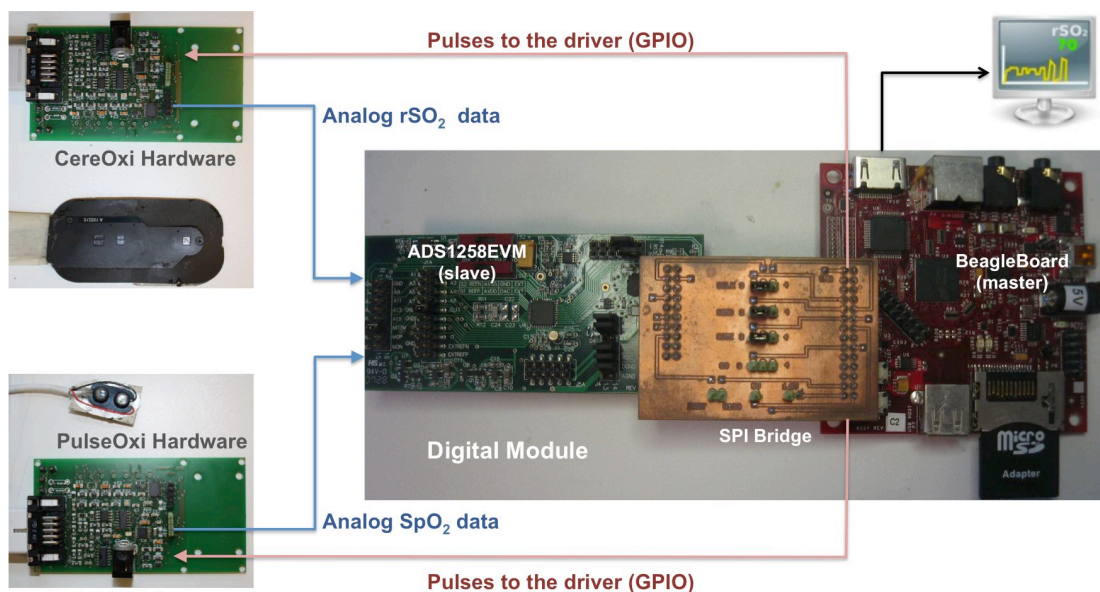


Fig. 6-13: A picture of the complete CereOxi and PulseOxi systems with the illustrations of the connections.

Digital Module

The digital module, which consists of the ADS1258EVM and the BeagleBord, has been discussed thoroughly in the section 4. As shown in Fig. 6-13, the digital module receives analog, differential oximetry signal from the receiving module. The 24-bit

ADC, ADS1258 digitizes the signal and makes it available on the SPI communication port. A dual-core smartphone processor, OMAP3530 on the BeagleBoard runs a SPI fetch program to control the ADS1258 and to collect the digital data. In the BeagleBoard, the digital data is processed, saved and displayed on the Ångström desktop environment. The algorithms to extract the rSO₂ and SpO₂ values from the analog signals are discussed in the following topic.

6.4 SYSTEM FIRMWARE

The system firmware for the CereOxi and PulseOxi systems were designed and are customized version of the spi-ads algorithm, which performs collecting, processing and displaying the data. The firmware requires to manipulate the differential signals arriving from the system hardware and scaling them to produce the oxygen saturation values.

CereOxi Algorithm

As shown in Fig. 6-14, the CereOxi algorithm has two parallel processes: generating the pulses and receiving the data. For pulse generation, the algorithm enables GPIO 168 and 169 as output pins on the expansion header. Consecutively, it generates the pulses to drive one of the two LEDs. Secondly, it adds delay in the pulses to drive another LED. The selection of the pulse rate is shown in the next topic. On the other hand, it continuously receives the data via SPI protocol as mentioned in the section 4. Since, the signal is already differential, it doesn't require subtraction and hence can be plotted after converted into decimal values.

PulseOxi Algorithm

Similar to the CereOxi algorithm, the PulseOxi algorithm is also divided into two parallel processes: generating the pulses and receiving the data. The pulse generation is the same as in the CereOxi algorithm except the pulse rate of 380 Hz.

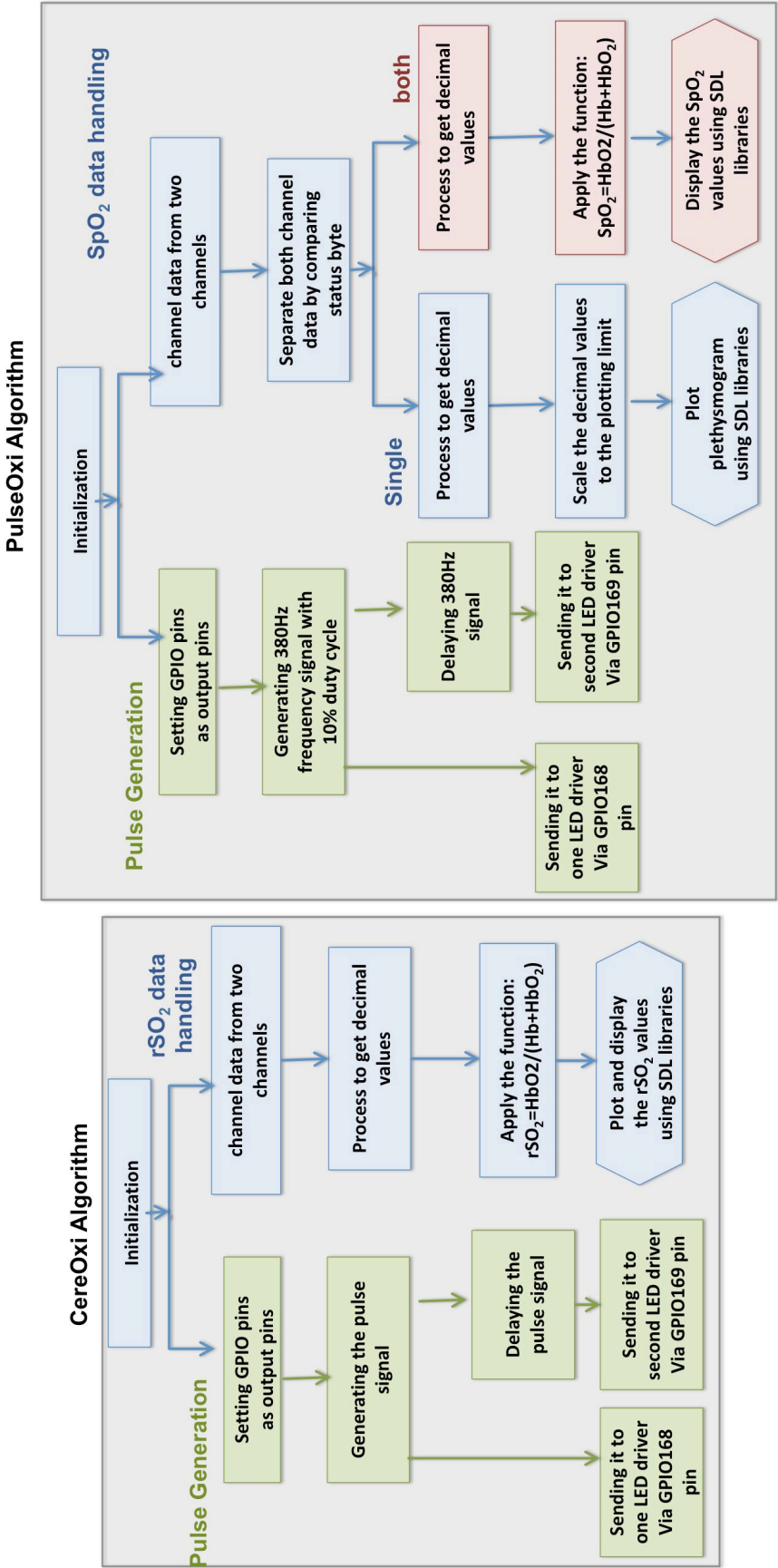


Fig. 6-14: Flowcharts of the CereOxi and PulseOxi algorithms.

On the other hand, it also continuously receives the data via SPI protocol. Since, the photoplethysmogram is pulsating signal, it requires to be handled differently. The differential and single channel data are separated. The differential signal conveys the value of oxygen saturation and the single channel signal is pulsating and can be plotted using the SDL library.

6.5 EXPERIMENTS & RESULTS

Pulse Rate Selection for CereOxi

Our application uses the continuous-wave (CW) approach due to its simplicity and flexibility [5]. The frequency of pulse repetition for the light source is very important factor and needs to be chosen very carefully, because it decides the timing of the pulse arrival at detector. Pulse arrival at the detector needs to be synchronized with the analog hardware circuits. The temperature of the light source follows the pulse repetition rate. Extremely higher pulse rate may cause the damage to the forehead skin.

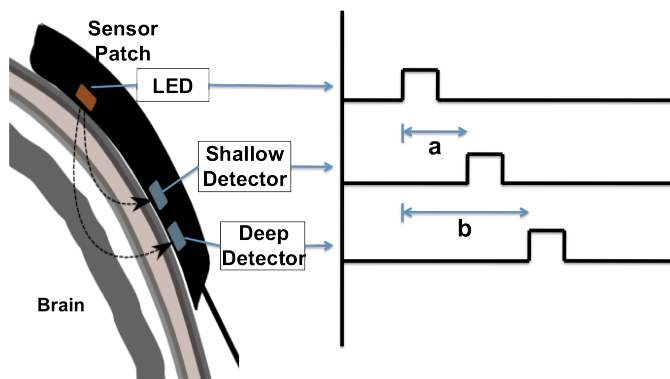


Fig. 6-15: A sensor patch on the forehead and the timing diagram of the pulse signal.

Table 6-2: The pulse frequency vs. measured delay of the detected signals.

Pulse Rate (Hz)	a (ms)	b (ms)
5	1	6
10	1	3
12	1	3
25	1	3
80	0.5	1.96
400	0.5	1.28
1k	0.536	0.636
4k	0.174	0.183

In order to decide the pulse repetition frequency for the CereOxi system, an experiment was conducted. In this experiment, the train of pulse signal is fed to the LEDs

of the cerebral oximeter sensor. Consecutively, the backscattered pulsed signal is detected on both detectors with some time delay based on the optical path length (Fig. 6-15). In order to assess the delay time of the arriving pulses, we tested different pulse frequencies. Table 6-2 shows the inverse proportionality of the pulse frequency and the time delay. For the lower pulse repetition rate, the difference of the delays remains constant. Above 12 Hz pulse rate, the temperature increase of the light source location was observed by finger touch. Thus, the pulse rate of 12 Hz with 10% duty cycle, which is also found in commercial cerebral oximeters, was chosen for this application.

Driver Circuit under Test

As discussed in the CereOxi firmware, the GPIO pins of the BeagleBoard produces the pulses to drive the LEDs on the sensor and to illuminate the forehead with IR and NIR lights. Fig. 6-16 shows the practical implementation of the pulse signal generation. The oscilloscope screenshot displays two signals with 12 Hz frequency and 10% duty cycle. Both signal also show a time lag which important to distinguish the signals from each LEDs.

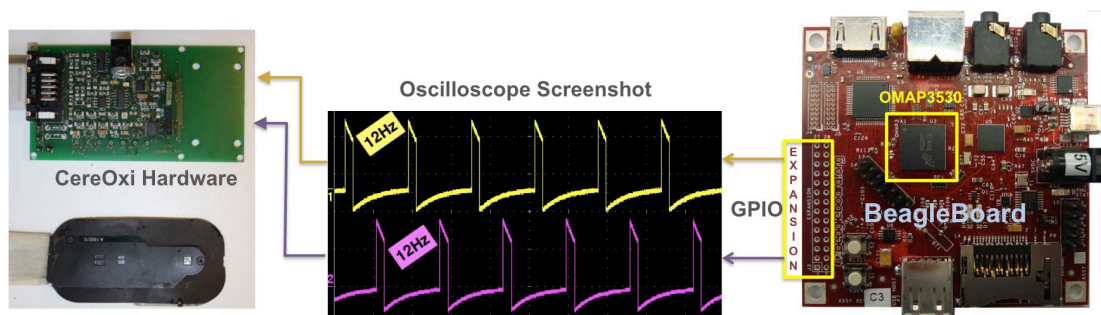


Fig. 6-16: An implementation of the driver pulses produced from the BeagleBoard GPIO pins.

PulseOxi System Measurements

Our Pulse hardware was tested in comparison with a commercial pulse oximeter (Masimo Radical Masimo Corp., USA) on a finger as well as the ECG signals. As shown in the Fig. 6-17, the finger sensors simultaneously perform the pulse oximetry on a subject in sitting position. The signal detected by the commercial sensor on the

middle finger is shown on the pulse oximeter LCD screen (Fig. 6-17a). The sensor on the index finger is connected to the PulseOxi analog hardware. The oscilloscope screenshot reveals that the plethysmogram and the pulse rate from the PulseOxi hardware are almost identical to those of the commercial system. Additionally, the pulse width of the plethysmogram is equal to RR interval of ECG with the delay of 320 msec.

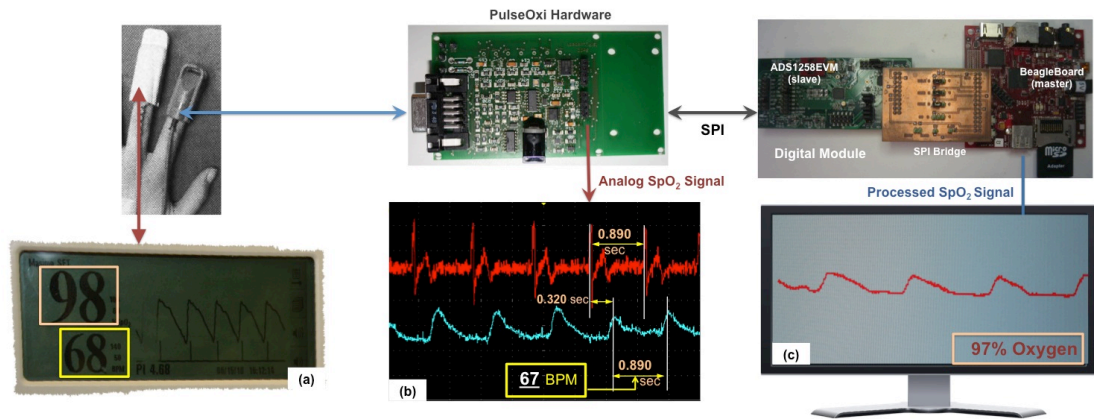


Fig. 6-17: The measurements with the PulseOxi system.

(a) the SpO₂ measurement with the commercial pulse oximeter, (b) the oscilloscope screenshot showing analog plethysmogram processed by PulseOxi hardware and the ECG measured with the ActiveBelt system and (c) the plotting display of the PulseOxi algorithm showing a processed plethysmogram and the oxygen saturation value.

Fig. 6-17c shows the screenshot of the PulseOxi application running on the Beagle-Board desktop environment. It plots the plethysmogram of the data arriving from the PulseOxi hardware. It can be also observed that the measured SpO₂ value by the PulseOxi system is 97%, which is approximately equal to the commercial pulse oximeter with error of 1%. Thus, the PulseOxi system demonstrated successful measurement of the SpO₂ data along with the plethysmogram and the SpO₂ value in real-time.

PulseOxi on Different Locations of the Head

PulseOxi system was also investigated to perform the photoplethysmography on the different locations of the face, because there are number of commercial reflectance oximeters offering the pulse oximeter on the forehead and hence motivating us to seek for more locations. Fig. 6-18 reveals that the PulseOxi system is capable of de-

etecting the plethysmographic signals on the face skin. The amplitude of the receiving signal varies according to the location of the sensor on the skin. The sensor attached on the nose and on the backside of the ear is in good shape and show a minor dicrotic notch. On the side of the forehead, the signal is noisier.

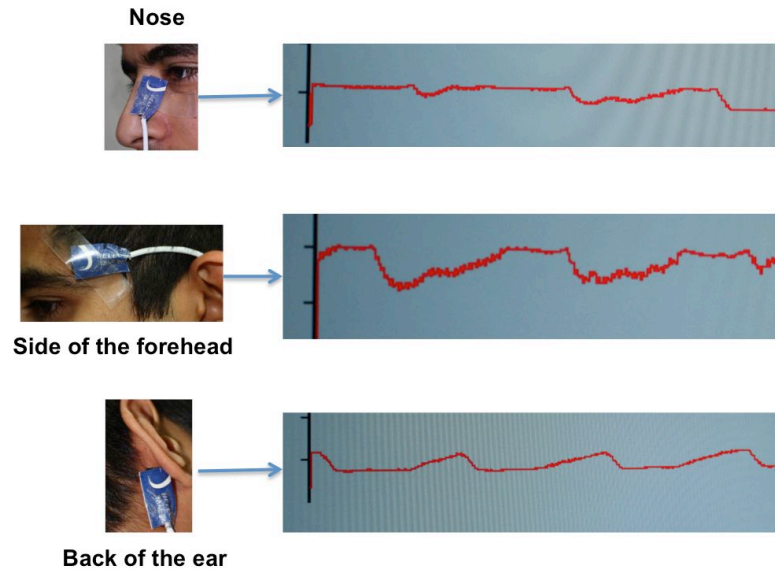


Fig. 6-18: The performance of photoplethysmography with the PulseOxi system on different locations of the head.

CereOxi System Measurements

The final experiment was conducted to test the CereOxi hardware in connection to the digital module. One of the objectives was to measure Hb and HbO₂ concentrations with the CereOxi hardware. Fig. 6-19 shows a 3min plot of the detected signals at two different wavelengths from the SomaSensor placed on the forehead. The measurement at 810nm represents the total (Hb + HbO₂) concentration, while at 730nm the Hb concentration is measured. The same signals were fed to the digital module for digitization, processing and data display.

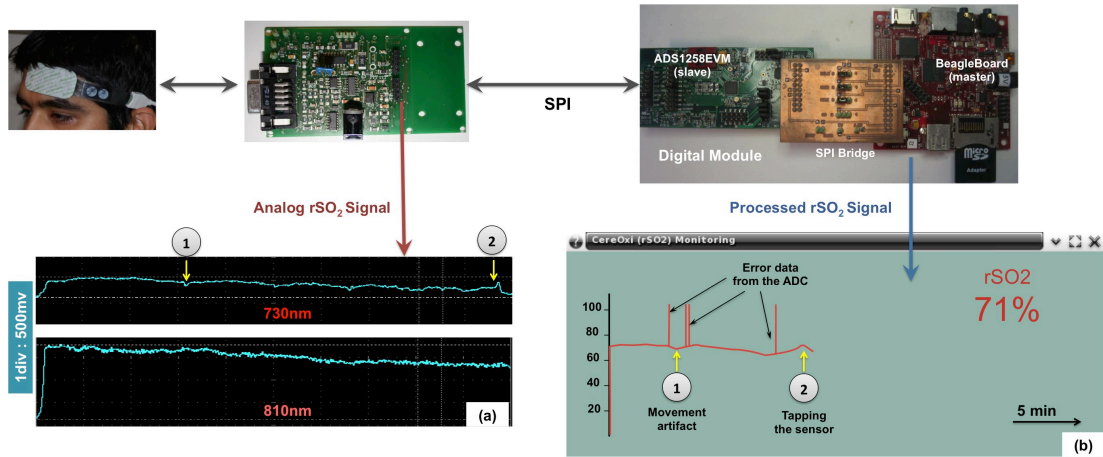


Fig. 6-19: rSO₂ measurements with CereOxi system

(a) the oscilloscope screenshot of the analog rSO₂ signals detected at two different wave-lengths and (b) a screenshot of the CereOxi application running on the BeagleBoard showing the 3min plot of the measured rSO₂ signal and the real-time value of rSO₂.

The CereOxi application running on the BeagleBoard desktop environment collected the digital data and processed it to extract the rSO₂ value. Finally, the computed rSO₂ value is plotted on the desktop screen window along with the real-time data. In order to widen the window timing with the rSO₂ plotting for longer period, the decimal values were further averaged for 1000 samples. Hence, the rSO₂ plots approx. every 0.5sec of data with sampling rate of 1.8ksps. Certain errors, which can be observed in the plots, are produced by the ADC, ADS1258 during data transmission. The error is occurred when the SPI communication is chosen without implementation of interrupt function [26]. The plotting window updates every 5min. The CereOxi algorithm also saves the decimal values in an excel file sheet in the same directory for the future analysis of the patient data.

Due to restriction of the commercial forehead sensors for the cerebral oximetry, we were unable to validate the CereOxi system with the commercial cerebral oximeter. However, The concept of measuring rSO₂ values with miniaturized design has successfully been implemented with the possibility of future expansion.

6.6 CONCLUSIONS

This research work presents a successful implementation of a miniaturized cerebral oximeter as well as pulse oximeter using the OMAP3530 as a processing unit. The objective behind building a miniaturized design of the oximeter is to bring it into the daily lives of the people who are suffering from the cardiovascular diseases or brain injuries. Current methods of cerebral oximetry, EEG and commercial cerebral oximeters are too bulky to be implemented in day-to-day life monitoring. Hence, this encouraged us to design a miniaturized oximeter.

First of all, to verify a suitable location for cerebral oximetry measurements the optical properties of a human frontal bone were performed on a cadaver skull. The experiment suggested the frontal and parietal bones as the most suitable locations for the cerebral oximetry. Due to ease of implementation and access to the bare skin, the frontal bone (forehead) was selected for the cerebral oximetry.

Similarity in cerebral and pulse oximetry device architectures motivated us to proceed for the developments of both CereOxi and PulseOxi devices simultaneously. The smartphone processor OMAP3530 is used as processing unit, which generates the pulses to drive the light source of oximetry sensors. It also receives the digital oximetry signals from the receiving circuits. Tiny oximetry hardware for CereOxi and PulseOxi system were designed and provide the connections to sensor and digital module.

First experiment was conducted to select the pulse rate for cerebral oximetry in order to avoid the heating of the light source. Secondly, the BeagleBoard algorithm was tested for driving the LEDs. At last, the PulseOxi and CereOxi hardware were put under test. The PulseOxi system performed as equal to the commercial quality and successfully plotted the plethysmogram and displayed real-time SpO₂ value on the BeagleBoard desktop environment. Additionally, the PulseOxi system achieved successful photoplethysmography on the different location of the face, which will further be explored later in the section 8. In the same way, the CereOxi succeeded in performing cerebral oximetry with real-time rSO₂ data display and plotting. The corrupted data communication temporarily disturbed the rSO₂ graph.

Thus, the goal of miniaturizing the cerebral oximetry was achieved by designing tiny analog circuit linking to the digital module. As shown in Fig. 6-20, the touchscreen module will enable the completeness of the miniaturization. Further developments towards a fully assembled CereOxi system will realize the goal of miniaturization and portability of a cerebral oximeter and will bring the rSO₂ monitoring in the daily lives of the people. The PulseOxi and CereOxi are integral parts of the multimodal wearable health monitor. Hence, their usability will be explored in the section 8.



Fig. 6-20: A physical comparison between commercial cerebral oximeter and our CereOxi system.

6.7 REFERENCES

- [1] Caplan RA. The ASA closed claims project: Lessons learned. ASA Annual Refresher Course 1998: 221
- [2] Roach GW, Kanchuger M, Mora-Mangano C, Newman M, Nussmeier N, Wolman R, Aggarwal A, Marschall K, Graham SH, Ley C. Adverse cerebral outcomes after coronary bypass surgery. *N Engl J Med* 1996; 335: 1857-1863
- [3] Möller JT, P Cluitmans, Rasmussen LS, Houx P, Rasmussen H, Canet J, Rabbit P, Jolles J, Larsen K, Hanning CD, Langeron O, Johnson T, Lauven PM, Kristensen PA, Biedler A, van Beem H, Fraidakis O, Silverstein JH, Beneken JE, Gravenstein JS. Long-term postoperative cognitive dysfunction in the elderly: ISPOCD1 study. *Lancet* 1998; 351: 857-861
- [4] Newman MF, Kirchner J, Phillips-Bute B, Phillips E, Han D, Braudet B, Grigore AM, Reves JG, Blumenthal JA. Perioperative neurocognitive decline predicts long-term (5-year) neurocognitive deterioration after CABG. *Anesth Analg* 1999; 88: SCA93
- [5] Newman MF, Croughwell ND, Blumenthal JA, White WD, Lewis JB, Smith LR, Frasco PF, Towner EA, Schell RM, Hurwitz BJ, Reves JG. The effect of aging on cerebral autoregulation during cardiopulmonary bypass: Association with postoperative cognitive dysfunction. *Circulation* 1994; 90: II243-II249.
- [6] H.L. Edmonds, "DETECTION AND TREATMENT OF CEREBRAL HYPOXIA KEY TO AVOIDING INTRAOPERATIVE BRAIN INJURIES," *Journal of Clinical Monitoring and Computing*, vol. 16, 2000, pp. 69-74.
- [7] S.K. Samra, "Cerebral Oximetry," *seminars in anesthesia perioperative medicine and pain*, vol. 16, 1997, pp. 69-77.
- [8] Villringer and H. Obrig, "Near-Infrared Spectroscopy and Imaging," *Brain Mapping The Methods*, A.W. Toga and J. Mazziotta, Academic press, 2002, pp 141-158.
- [9] Duncan A, Meek JH, Clemence M et al. Measurement of cranial optical path length as a function of age using phase resolved near infrared spectroscopy. *Pediatr Res* 1996; **39**: 889-894.
- [10] Jöbsis FF. Noninvasive infrared monitoring of cerebral and myocardial sufficiency and circulatory parameters. *Science* 1977; **198**: 1264-1267.
- [11] Smythe PR, Samra SK. Monitors of cerebral oxygenation. *Anesthesiol Clin North America* 2002;20:293-313.
- [12] S. Fantini and B. Engineering, "Near-infrared spectroscopy for the study of biological tissue," pp. 1-3.

- [13] Mannheim PD. The light-tissue interaction of pulse oximetry. *Anesth Analg* 2007;105(6 Suppl):10S-17S.
- [14] J. Welch and M. J. C. van Gemert. *Optical-Thermal Response of Laser-Irradiated Tissue*. Plenum Press, 1995.
- [15] John TB Moyle. *Pulse Oximetry*. BMJ Books, 2 edition, 2002.
- [16] J. G. Webster. *Design of Pulse Oximeters*. Institute of Physics Publishing, 1997.
- [17] Whitepaper on pulse oximetry, <http://www.nellcor.com>.
- [18] Edmonds HL Jr. Advances in neuromonitoring for cardiothoracic and vascular surgery. *J Cardiothorac Vasc Anesth* 2001;15:241-50.
- [19] M.A. Schepens and F.G. Waanders, "Monitoring the brain: near-infrared spectroscopy," *Aortic Arch Surgery: Principles, Strategies and Outcomes.*, J.S. Coselli and S.A. LeMaire, Wiley-Blackwell, 2008.
- [20] Samra S. K., Dorje P., Zelenock G. B., Stanley J. C., Cerebral oximetry in patients undergoing carotid
- [21] endarterectomy under regional anesthesia, *STROKE*, **27**, 49- 55, 1996.
- [22] Grolimund P. Transmission of ultrasound through the temporal bone. In: R Aaslid (ed), *Transcranial Doppler Sonography*. Springer-Verlag, New York, 1986: 10–21.
- [23] Nunn J F 1987 *Applied Respiratory Physiology*.
- [24] SomaSensor 4100-SAF user manual, www.somanetics.com
- [25] MaxFast user manual, www.nellcor.com
- [26] ADS1258 Datasheet, Texas Instruments Inc. www.ti.com

7. MULTIMODAL, WEARABLE HEALTH MONITORING THROUGH DAILY-LIFE OBJECTS

As in the beginning, the objective was established to design and develop a multimodal wearable health monitor utilizing the high-performance capability of the current smartphone processors. Later explained the design and development of the individual monitoring modules using the OMAP3530-dual core smartphone processor. This section presents the integration of these modules in order to bring a multimodality as well as the application of a monitor into daily life health monitoring. There are a number of potential field of applications such as health monitoring of aged people at home, monitoring recovery conditions of cardiovascular- or neuro-patients, monitoring the health and body environment of individuals with for asthma or COPD, etc., where there is a need of multi-parametric as well as wearable health monitoring. This wearable monitor system is aiming at multi-parametric personalized health monitoring with minimally obtrusive sensor array incorporated in the daily life objects. This section also unfolds the results of multi-modal wearable monitor facilitating onsite individual's health parameter display in real-time as well as continuous data recoding for future analysis.

7.1 DEMAND OF A MULTI-PARAMETRIC WEARABLE MONITOR

Worldwide population growth has also increased a number of individuals with chronic diseases such as diabetes, cardiovascular problems, sleeping disorder (apnea), vestibular (balance) disorder, etc. [1]. Therefore, a number of personalized health monitoring devices for disease management are also growing in consumer market [10].

Table 7-1 enumerates a few of personal devices previously mentioned in section 1. All of these devices are aiming at monitoring of an individual for a specific health problems. Some of the listed devices focus on the cardiovascular health monitoring. Increasing number of individuals with sleeping problems has recently encouraged a growth in sleep-monitoring devices. Falling detection has been integrated in the sole of the shoes to prevent the vestibular patient from falling. Most of the listed devices are either wearable or handheld health monitors.

Table 7-1: A list of personalized health monitoring devices.

<p>Heart rate monitor</p> <p>WearLink, Polar, Finland consists of a chest belt and monitors beat-to-beat interval of wearer's heart during sports and daily activity [9].</p>	
<p>Glucose monitor</p> <p>Mendor, Finland developed a cellphone-sized all-in-one blood glucometer [10] for diabetic patients.</p>	
<p>Zio™ Patch</p> <p>iRhythm Technologies, USA designed a long-term cardiac rhythm monitor Zio Patch, which is a sticky patch for the chest and facilitates cardiovascular patient a continuous ECG monitoring for up to 7-14 days [3].</p>	
<p>PiiX™</p> <p>PiiX (Corventis, USA) adheres to the chest-skin and detects, records and transmits physiological information [4].</p>	
<p>SMHEART LINK™</p> <p>The Link (iTMP Technologies, Inc., USA) communicates with a variety of fitness sensors to enable integration with iPhone apps [5].</p>	
<p>Fitbit</p> <p>The Fitbit, USA tracks with accelerometers person's calories burned, steps taken, distance traveled and sleep quality [6].</p>	

<p>Zeo</p> <p>Zeo, Zeo Inc., USA produces a device designed to detect different stages of person's sleep and to analyse and improve its pattern [7].</p>	
<p>iShoe™</p> <p>iShoe, USA detects the individual's balance and also prevents from falling [8].</p>	

Wearable health monitoring systems have increasingly become popular in medical monitoring in recent years as well [10], because they allow continuous monitoring of an individual in an out-of-the-hospital environment. The implications and potential of the wearable health monitoring technologies in medical monitoring are paramount. Since they could [15]:

- enable the detection of early signs of health deterioration,
- notify health care providers in critical situations,
- find correlations between lifestyle and health,
- maintain privacy and individual's freedom [11],
- bring health monitoring to remote locations, and
- ultimately transform health monitoring by providing doctors with multi-sourced, real-time physiological data.

In order to make these wearable devices practical, a series of technical, legal and sociological obstacles need to be overcome. For example, these devices need to be non-intrusive, comfortable to wear, efficient in power consumption, preserve privacy, multi-modal/multi-parametric in function and have a user-friendly interface. They would also need to have very low failure rate and highly accurate alarm triggers, especially if used for diagnostic purposes.

State-of-the-Art Wearable Health Monitors in Research

Beyond the life-style wearable technologies, there are a number of wearable health monitors in research and development in the medical fields for assisting individuals

at high health risks. One of them is Microsoft Research, which has developed and tested the wearable real-time health monitoring system “HealthGear” [10]. They have demonstrated an exemplary application of the HealthGear for detecting sleep apnea by implementing wearable continuous pulse oximetry [10]. Another project, AMON (Advanced care and alert portable telemedical MONitor), which was financed by EU, was targeted for high-risk cardiac/ respiratory patients [13]. The system includes continuous collection and evaluation of multiple vital signs, intelligent multiparameter medical emergency detection, and a cellular connection to a medical centre. Now that, the people become better informed, organized and educated regarding their health, health monitoring is increasingly shifting into daily life activity [14].

In last decade, smartphones have become ubiquitous and brought tremendous possibilities in health monitoring because they remain in proximity to the user. One of such multi-parametric health monitoring approaches using smartphone is shown in “opportunistic sensing” [15], which provides platform to collect the data from on-body sensors modules and transmit wirelessly to the smartphone for again long-distant transmission. In this approach, a smartphone, which is actually capable of performing very complex functions, is merely used as a transceiver or communication gateway. Previously, this research work has demonstrated the capability of the smartphone processors to process and analyse the data. Now, this section further explores the application of smartphone processor in multi-modal health monitoring. This section also demonstrates deployment of the sensors on some of wearable daily-life objects to enable minimally-obtrusive on-body sensing.

Multimodal Wearable Health Monitor (MHM)

In our approach, we present a multi-modal, wearable health monitor (MHM), which can monitor body physiological parameters as well as body-environment with the real-time visual feedback. Since the MHM is aimed for personalized health monitoring, the following requirements were taken into account:

- It is necessary to embed health sensors as unobtrusively as possible into daily life devices such that a user doesn't need to care about the handling and the sensor array can efficiently perform the detection.
- Visual real-time feedback to a user is required to easy understanding effortlessly.
- The MHM should also perform continuous health data records in a way that an user or expert can analyse the data in later period.

Selection of the parameters to be monitored is also an essential task. And it is necessary to know the diseases, which are very common in the society. A study conducted by NIEHS, USA suggests that cardiovascular and respiratory diseases prevail over other disorders globally [17]. Furthermore, it has been observed that the cardiovascular problem may result into the neurological malfunction or deterioration [18]. Therefore, early during defining the objectives of this research work, the cardiovascular, respiratory and neurological system were given the highest priority in choosing the health monitoring parameters. And individual wearable modules for ECG, SpO₂ and rSO₂ (section 5 and 6) are built and integrated with the OMAP3530-based Beagle-Board to form the MHM. The surrounding environment sensors for humidity and temperature (section 4) have also been be integrated into the MHM. Therefore, the following presents the MHM aiming at self-health monitoring and also recording the data continuously for future analysis. The MHM also offers expandability to telemonitor individual's data at a remote location if required.

7.2 SYSTEM COMPONENTS

Overview of the Multimodal Wearable Health Monitor

Fig. 7-1 illustrates an overview of our multimodal wearable health monitor. It is apparent that the MHM is an integration of the previously discussed individual monitoring devices; Active Belt, miniaturized oximeter and body environment monitoring module, in which the smartphone processor OMAP3530 is in the heart of their system design.

The MHM consists of mainly two parts: Sensors with corresponding front-end analog circuits and digital module containing the ADC and the dual-core smartphone processor OMAP3530. Further, sensors are divided into two categories:

- On-body sensors collecting physiological data
- Peripheral sensors detecting body-environment

The primary objective of the MHM is to embed the sensors on daily-life objects in the way that they become minimally obtrusive. Secondly, the corresponding hard modules are required to be mounted in vicinity to the sensor locations. Finally, the data and information need to be visually displayed after being processed and analysed by the OMAP3530. The biofeedback should be user friendly and possess ease in interpretation.

In the previous sections, the following things have been thoroughly shown:

- Detection of the physiological parameters from body mounted sensors.
- On-site analog conditioning of the detected signals
- Processing, saving and displaying of the parameter by the OMAP3530-based BeagleBoard.

Hence, the following topic will begin with the display of the measured data onsite as a user-biofeedback.

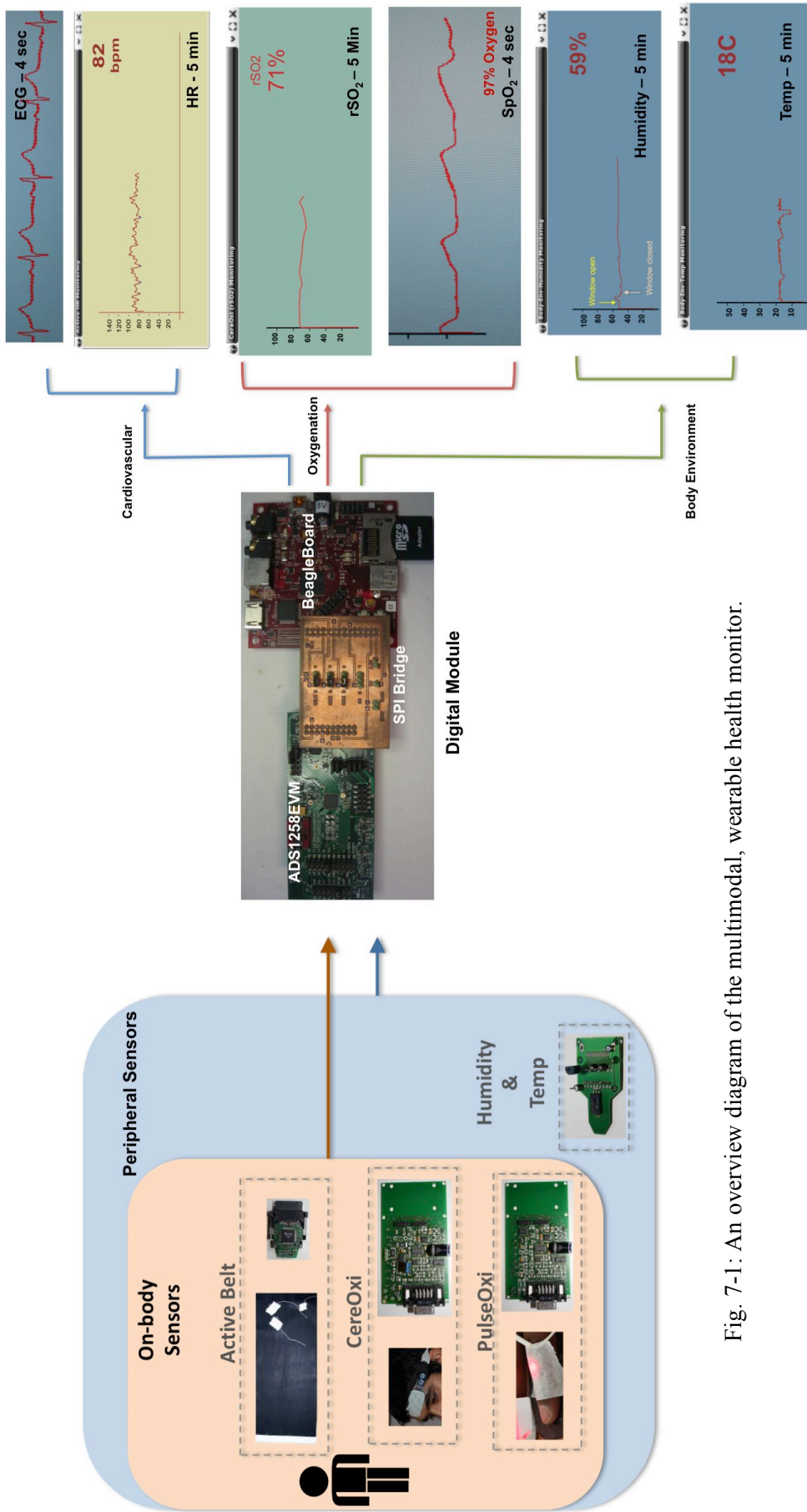


Fig. 7-1: An overview diagram of the multimodal, wearable health monitor.

Onsite-Display Modules

As discussed earlier, health and body environment parameters, which are conditioned by their corresponding modules and processed by the OMAP3530 on the Beagle-Board, are required to be displayed on-site for the user. There are several requirements to be fulfilled by the display module:

- The display module needs to be portable.
- It is required to be handheld, wearable or mountable on daily-life objects
- It is highly required that the user is able to read their health parameters comfortably.

Based on the above requirements, a tiny and mountable projector was selected as a display module.

Pico DLP Projector Development Kit

In recent years, the projectors are not only found in meeting or conference rooms but also integrated in handheld devices such as Samsung W7900 smartphone, NTT DOCOMO, etc. These smartphones contain in-built tiny projector based on the DLP Pico technology [29]. The DLP Pico chipset is a miniaturized version of the popular DLP chip found in today's projectors on the market [6]. The DLP Pico technology from Texas Instruments upgrades the technology from small hand-held LCD screen to a wider screen display and eases the user interaction. The use of DLP Pico projectors is recently widened among the youth [29]. However, DLP Pico projectors are so new concept that its application has not been imported to wearable devices. In this research work, the feasibility of DLP Pico in health monitoring is presented. Thankfully, the BeagleBoard extensively supports the DLP Pico projectors.

Fig. 7-2 shows the DLP Pico projector kit along with the BeagleBoard and provides information about its physical dimensions in comparison with the BeagleBoard. The self-powered kit provides connection to the BeagleBoard via VGA to mini-VGA adaptor cable. Using microscopic mirrors, the DLP Pico Chip reflects light to project an image on any surface e.g., wall. The Pico DLP project has a resolution of 0.17-inch HVGA and contrast ratio of 1000:1. It is 4.48cm x 6.74cm x 1.42 cm in size

with VGA interface. The OMAP3530 doesn't require a special driver to display on the Pico projector. The following will present how the Pico projector is used as an integral part of the MHM.

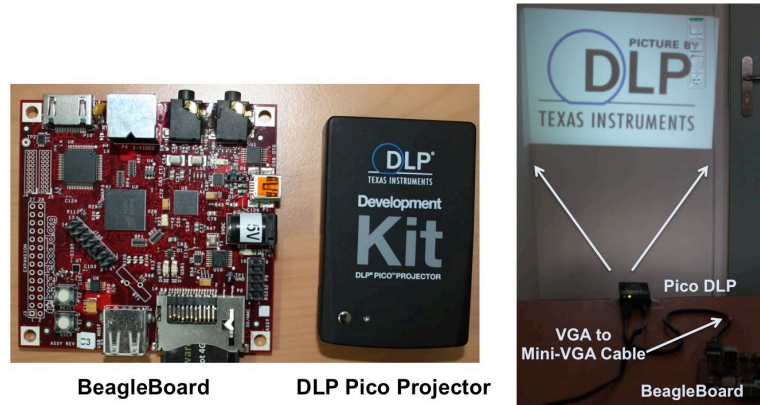


Fig. 7-2: An image of the Pico DLP Projector kit along with the BeagleBoard (in left). A pico DLP projector connected to the BeagleBoard with the projection on the wall (in right).

Daily-life objects with Minimally Obtrusive Sensor Array

As mentioned earlier, the sensors for this research work are required to be mounted on daily-life objects in such a way that the people can easily monitor their health and body environment information. Certain parameters need to be considered in selection of the potential daily-life objects:

- The object should be wearable and provide the firm contact to the suitable body locations.
- The object needs to be a part of their daily use, rather than compulsion to use it especially for health monitoring.
- The daily-worn object should not become hindrance or annoyance during daily life activity.
- The object should also furnish the space to mount the hardware modules.
- The daily object is required to be used in the outdoor environment as well.

Following the above prerequisites, several daily-worn or daily-used objects commonly found among the people of all ages are short-listed and shown in Appendix with their pros and cons. Among them, a cap (or hat) and glasses are found to be the most suitable devices due to availability of locations for sensor contacts. However, few

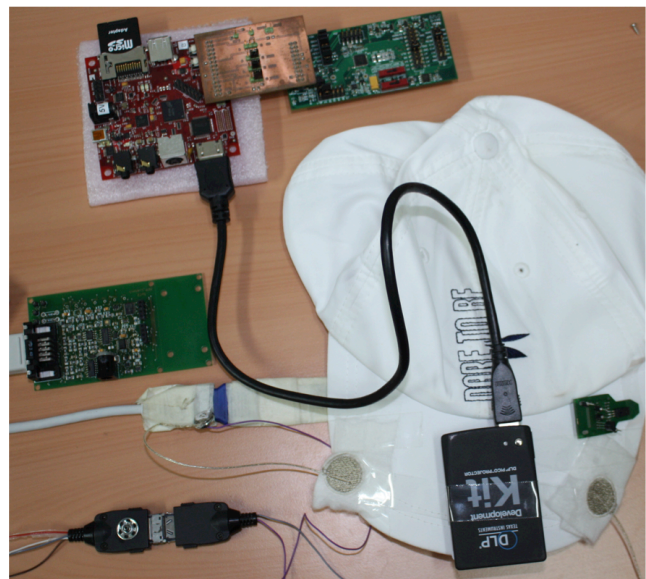
other devices such as, computer mouse, switchboard, wheelchair, office chair are also taken into the feasibility check for the MHM system (see Appendix).

Vital-cap

A cap was designed to integrate a sensor array containing cerebral oximetry sensor, 2-lead ECG textile electrodes, humidity and temperature sensors. Placement of the sensors shown in Fig. 7-3 clearly offers minimally-obtrusive connection to the body. A cerebral oximetry sensor can be fixed on the bottom side of the cap, where the ring makes firm contact with the forehead. Two textile electrodes for ECG are mounted on the side of the visor, easily touched by fingers. The humidity and temperature sensors are placed also on the corner of the visor. The DLP pico connected to the BeagleBoard lies on the middle surface of the visor and projects front-side (wall) of the body. The SpO2 sensor has been omitted in the vital cap to reduce hardware during measurements, although be fixed along with the cerebral oximeter sensor.



(a)



(b)

Fig. 7-3: Images of the Vital-cap carrying minimally obtrusive sensor array (a and b) and corresponding hardware module. The Vital-cap also holds the pico DLP projector.

Thus, the wearer could monitor and visualize his health parameters by wearing the Vital-cap. For clearer understanding of the setup, the wire connections among the

sensors and hardware modules are not shown. The experiment and result section will provide the details on the function of the vital-cap in health monitoring.

Vital-glasses

Since a majority of senior citizens suffers from some type of wrong sightedness, many of them are bound to wear corrective glasses. Consequently an example for unobtrusive monitoring by using existing infrastructure, frames from a standard spectacle will be equipped with an array of miniature sensors to collect physiological data and body environment information during every day activity. As shown in Fig. 7-4, an SpO₂ sensor takes place in the nose pad, ECG electrodes are integrated on the temples, and a humidity and a temperature sensor found their place in the temple arms. This way health monitoring becomes more friendly, and as easy as the proverbial “putting on glasses in the morning”.

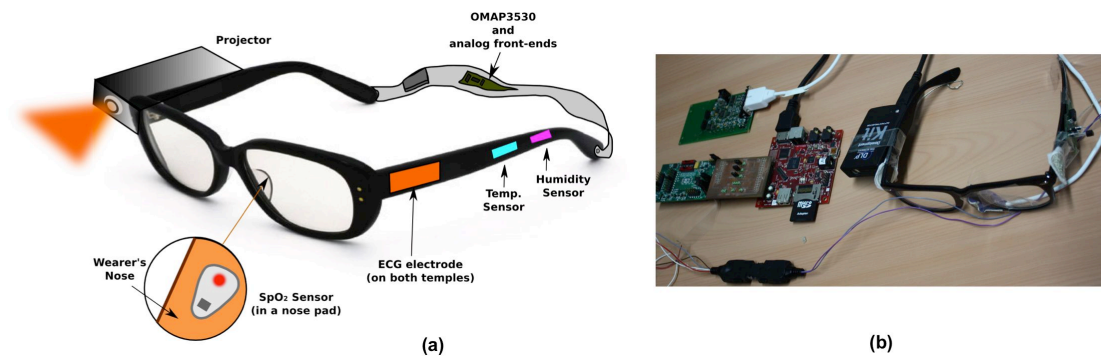


Fig. 7-4: Images of the Vital-glasses carrying minimally obtrusive sensor array (a and b) and corresponding hardware module. The Vital-glasses also holds the pico DLP projector.

7.3 SYSTEM FIRMWARE

In order to simultaneously monitor the parameters collected by the sensor array, two algorithms were designed. Each algorithm fulfills the requirement of different methods of monitoring.

10sec-&-Display Algorithm

The algorithm “10sec-&-display” on the OMAP3530 facilitates a patient-centric approach, in which the user can touch the ECG electrodes mounted on the Vital-cap or the Vital-glasses for 10 sec and can visualize the detected parameters on the projected beam by the Pico DLP. In this approach, the sensors other than ECG electrodes also automatically detect the parameters during 10 sec measurement cycle. The flow chart in Fig. 7-5 shows the step-by-step procedure of the multi-channel data receive and handling. The data’s are separated by continuously monitoring the status byte. Finally, decimal values of individual parameters are retrieved from the digital data. All the algorithms explained previously in section 4, 5, 6 and 7 are integrated to generate the parameter values. The parameters are finally displayed on the desktop environment of the BeagleBoard via the DLP Pico.

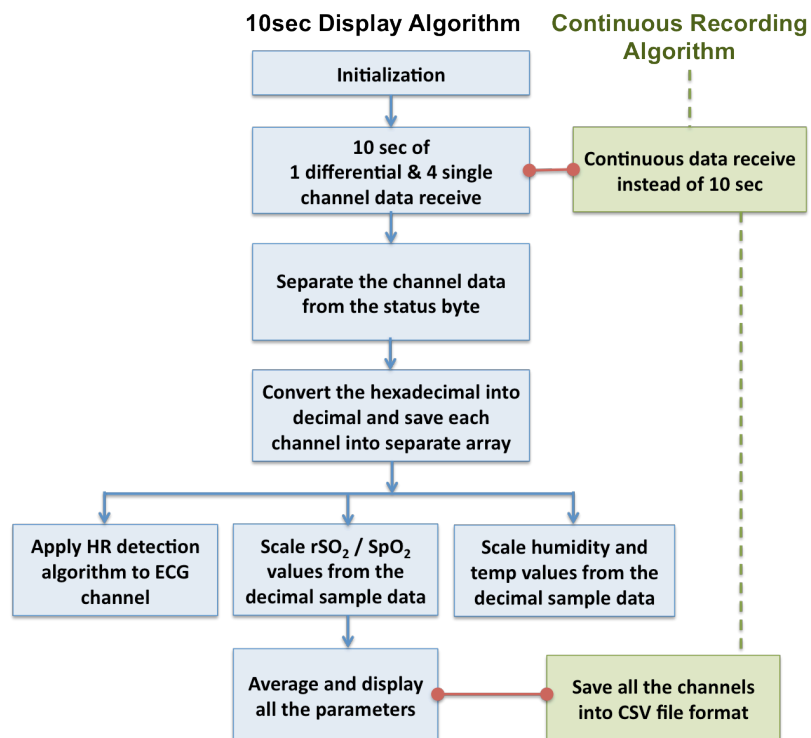


Fig. 7-5: Algorithms for the MHM. 10sec-&-Display algorithm aims at the person-centred application. The continuous monitoring algorithm is for saving multichannel data and for further analysis.

Continuous Recording Algorithm

The “Continuous Recording Algorithm” running on the OMAP3530 is the solution for continuous data recording for future analysis. Since it is obvious that the ECG electrodes on the Vital-cap or the Vital-glasses can't be used in this case, the Active Belt, which has been discussed in section 5, is used in combination with the Vital-cap or the Vital-glasses. The algorithm only differs from the 10sec-&-Display algorithm at the time window of data receive. Here, the data are continuously received without restriction of time (such as 10 sec). The decimal values of the parameters are saved in a comma separated format (.csv) file for the future analysis.

7.4 EXPERIMENTS & RESULTS

The sensors mounted on the Vital-cap and the Vital-glasses are linked to their corresponding hardware (explain in section 4, 5, and 6). The BeagleBoard receives and displays multi-channel data from the sensor array hardware by running the algorithm “10sec-&-Display”. For continuous monitoring, the Vital-cap and the Vital-glasses are used in combination with the Active electrode and eliminate the need of touching the ECG textile electrodes by hands. The following presents the results on the conducted experiments with Vital-cap and Vital-glasses.

Vital-cap under test

Fig. 7-6 shows a subject wearing the Vital-cap and touching the ECG textile electrodes with his both hands. The Pico DLP projects the screen on the wall surface and shows the measured parameters after execution of the 10sec-&-Display algorithm. The displaying of the parameters was kept as simple as possible in order to convey interpretable information for the elderly. The biofeedback also comments on their health status as well as surrounding environment based on the measured parameters.

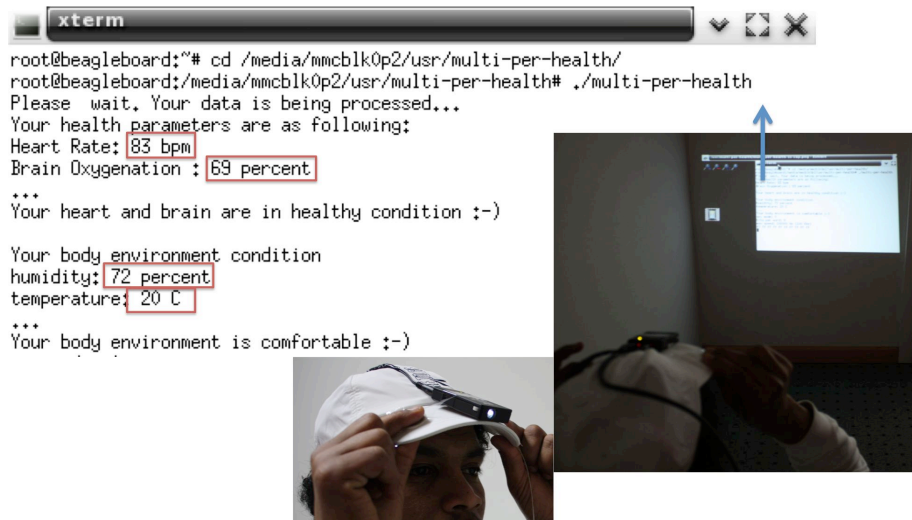


Fig. 7-6: A Vital-cap monitors and displays the multimodal body parameters along with its environment on the wall.

Sometimes, ECG signals are difficult to detect with the textile electrodes, since they are built for long-term ECG recording and have high input impedance during 10-sec measurements. An alternative to this problem is to imbed an active electrode on the textile electrode to improve the contact impedance [16]. Thus, the Vital-cap demonstrates an exemplary multi-modal health monitoring using a minimally-obtrusive sensor array, the corresponding hardware connected to the BeagleBoard.

Vital-Cap with the Active Belt for Continuous Recording

Continuous recording of the multimodal parameters using the Vital-cap was also performed by using the Active Belt. Fig. 7-7 shows the plots of the individual parameter saved during a multimodal experiment of 5 min. The graphs of HR, rSO₂, humidity and temperature of 5 min are plotted from saved data during the execution of the continuous recording algorithm. The graphs also show transients in the data values at several occasions. This occurs due to the data corruption during the ADS1258- BeagleBoard communication, which can be in the future be avoided by using McBSP and DMA controller. The measurement taken here was in seating position and therefore no movement artifacts were found. The laboratory prototype proved the concept of the continuous recording of the physiological and body-environment data.

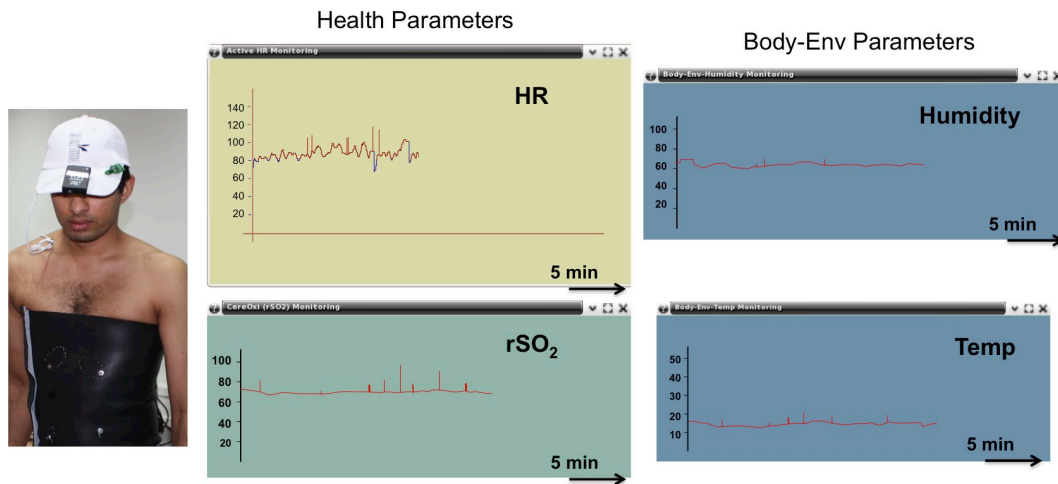


Fig. 7-7: Multimodal continuous recording of 5min using the combination of the vital-cap and the Active-Belt

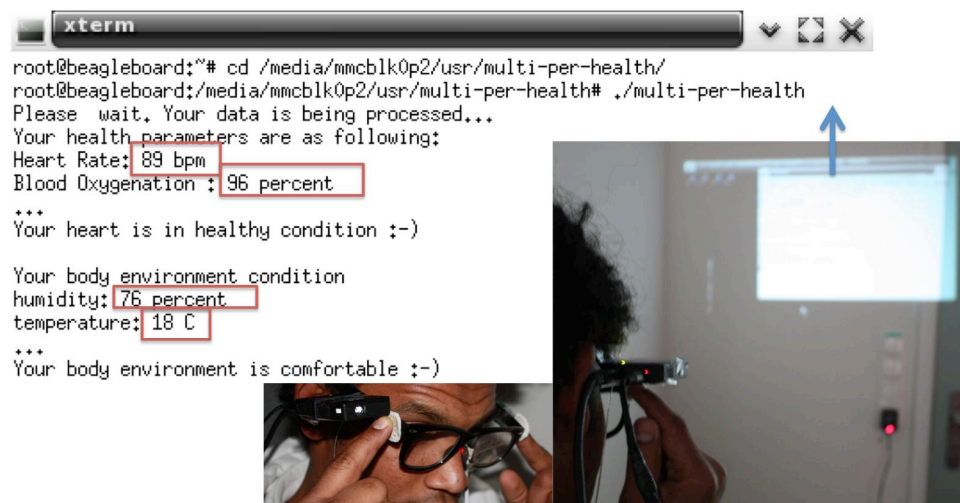


Fig. 7-8: Vital-glasses monitoring and displaying multimodal body and its environment on the wall. The DLP projected window displays measured parameters.

Vital-glasses under test

Similarly, the Vital-glasses were also taken for an experimental parameter display. Vital-glasses also perform equivalent to the Vital-cap as shown in Fig. 7-8. The Vital-glasses feature the SpO₂ instead of rSO₂ and hence do not give data regarding brain oxygenation. However, rSO₂ can also be integrated on the top of the Vital-

glasses if required. Thus, Vital-glasses provide a platform to perform daily health-check.

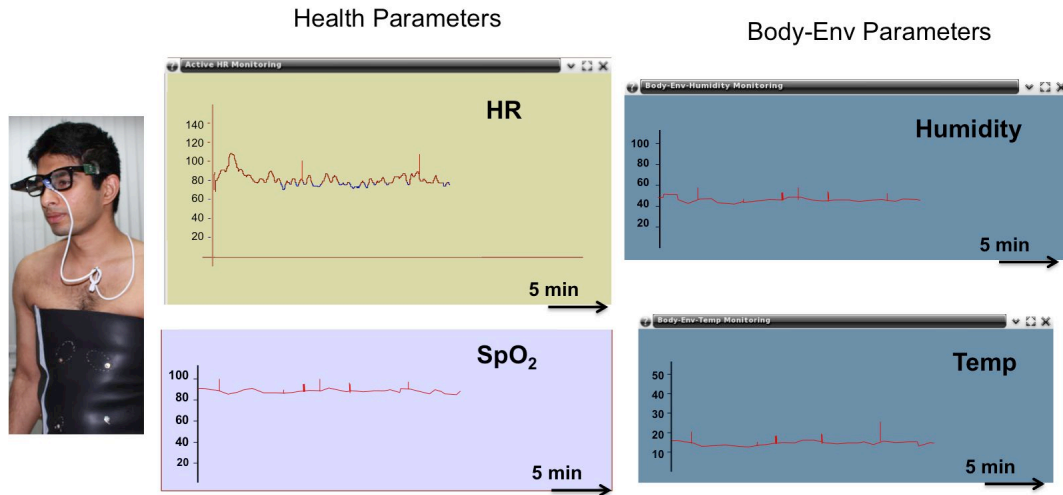


Fig. 7-9: Multimodal recording of 5 min using a combination of Vital-glasses and Active-Belt.

Vital-glasses with the Active Belt for Continuous Recording

The Vital-glasses with the Active Belt were tested with the continuous recording algorithm. The graphs in Fig. 7-9 also show contamination of the data plots by the data corruption at several spots. Moreover, the SpO₂ signal follows the bumps in the plot, which was the effect of the subject speaking during measurements. Such artifacts can be removed by implementing a sophisticated algorithm on the OMAP3530.

7.5 CONCLUSIONS

The presented work showed an implementation of a laboratory prototype design of the multimodal wearable health monitor (MHM). The MHM is aimed at fulfilling the need of user-friendly health monitoring device during daily-life activity.

Wearable health monitor was chosen as a targeted application, since it provides a platform for minimally obtrusive medical monitoring in out-of-the-hospital environment. The primary objective of the MPH was to monitor body as well as body-environment parameters, which is a completely new approach in the health monitoring. On top of that, integration of the biofeedback with the MHM system made its way different from the conventional telemonitoring, which is hindered by an immense amount of data collection.

Health data were selected based on the most common disease found among people with all age groups. The sensors were mounted on a cap and glasses to provide minimally-obtrusive health monitoring. A DLP-Pico tiny projector in connection with a BeagleBoard was chosen to facilitate the onsite display.

10sec-&-Display algorithm on the BeagleBoard enabled health monitoring of the subject by using the Vital-cap and the Vital-glasses. The Pico projector provides a huge projection on the wall displaying measured parameters. On the other hand, a continuous recording algorithm enabled the recording of the data during daily life activity and facilitated further analysis. The ECG textile electrodes on the Vital-cap and the Vital-glasses sometimes faced the problem on high input impedance, which can be eliminated by embedding the active electrode circuit [16]. Subject's speaking appeared as an artefact in long-term recording of the SpO₂ during the Vital-glass experiment and hence, sophisticated DSP algorithm on the OMAP3530 have to remove the artefacts in a second step.

Thus, the laboratory prototype of our MHM opened the door of the new era in health monitoring by providing the onsite data display in a seamless manner.

7.6 REFERENCES

- [1] “Insuring American’s Health: Principles and Recommendations.” Committee on insuring health, Institute of Medicine, Washington, DC, 2004.
- [2] iRhythm Technologies, Inc. <http://www.irhythmtech.com/zio-solution/zio-patch/>. Web. 22 Apr. 2010.
- [3] Corventis. <http://www.corventis.com/EU/medprof.asp>. Web. 22 Apr. 2010.
- [4] iTMP Technologies, Inc. <http://store.smheartlink.com/> Web. 22 Apr. 2010.
- [5] Fitbit, <http://www.fitbit.com/product>. Web. 22 Apr. 2010
- [6] Zeo Inc. <http://whatiszeo3.myzeo.com/hp/3/whatiszeo.php>. Web. 22 Apr.
- [7] iShoe. <http://www.i-shoe.net/products.html>. Web. 22 Apr. 2010.
- [8] WearLink. <http://http://www.polar.fi/>. Web 22 Apr. 2010.
- [9] All-in-one glucose meter. <http://www.mendor.com> Web 15 Sept. 2010.
- [10] Flores-Mangas, Nuria Oliver Fernando. HealthGear: A Real-time Wearable System for Monitoring and Analyzing Physiological Signals. Redmond, USA, 2005. Redmond, USA.
- [11] Mann, S. (1996) Smart Clothing Wearable Multimedia Computing and Personal Imaging to Restore The Technological Balance Between People and Their Environments ACM Multimedia Boston, Copyright ACM.
- [12] <http://www.realitydisfunction.org/heartdonor/>
- [13] Anliker, U, J A Ward, P Lukowicz, G Troster, F Dolveck, M Baer, F Keita, et al., A. “wearable multiparameter medical monitoring and alert system.” IEEE Trans. Information Technology in Biomedicine 8 (2004): 4415-427.
- [14] http://wwwhome.cs.utwente.nl/~broens/dloadcontent/Broens_TMSI_internship_report_v1.pdf
- [15] Edmund Seto, Eladio Martin, Allen Yang, Posu Yan, Raffaele Gravina, Irving Lin, Curtis Wang, Michael Roy, Victor Shia, Ruzena Bajcsy. Opportunistic Strategies for Lightweight Signal Processing for Body Sensor Networks, PETRA2010, June 23–25, 2010, Samos, Greece.
- [16] Mankodiya, K., Ayoub, et al. (2007). A design study on a Multisensory Cerebral Monitor. In Biomedizinische Technik 2007 (Vol. 43, pp. 1-2). Aachen, Germany.

- [17] <http://www.sciencedaily.com/releases/2006/03/060309081531.htm>
- [18] Möller JT, P Cluitmans, Rasmussen LS, Houx P, Rasmussen H, Canet J, Rabbit P, Jolles J, Larsen K, Hanning CD, Langeron O, Johnson T, Lauven PM, Kristensen PA, Biedler A, van Beem H, Fraidakis O, Silverstein JH, Beneken JEW, Gravenstein JS. Long-term postoperative cognitive dysfunction in the elderly: ISPOCD1 study. *Lancet* 1998; 351: 857-861

8. CONCLUSIONS & OUTLOOK

A growing demand of multi-parametric health monitoring in the current global societal situation with a growing number of individuals with chronic diseases, elderly people motivated us to design and develop a multi-modal health monitor providing the health as well as body environment parameters in a pervasive manner. Our solution to cope up with the high volume of the data in this regard was found in the current high performance smartphone processors. The complete market survey was conducted to select the best suitable embedded smartphone processor. TI's OMAP3530 won the battle among many candidates for providing the core of multimodal health monitoring.

OMAP3530's one of the cores, a superscalar ARM Cortex-A8 promises upto 2000MIPS which ensured its performance for handling the huge number of health parameters for our research work. On top of that, another core, which is a c64x+ DSP core, boosts the performance for real-time medical signal processing. In order to begin the development in the OMAP3530, the BeagleBoard was chosen as a hardware development platform due to its affordable price and especially open-source community support.

A virtual appliance containing the BeagleBoard development environment was created in order to design and cross-compile the OMAP3530 executable algorithms. The development environment eased the process of embedded software development for the OMAP3530. The development environment allowed us to run two tests on the BeagleBoard for checking its feasibility for the medical monitoring applications.

The feasibility test successfully monitored the heart rate of the polar belt wearer with real-time plotting window on the desktop environment on the BeagleBoard. The second feasibility test was also successful in collecting the data from the commercial patient monitors and producing a distinctive alarm output for both of them with the real-time plotting.

24-bit ADS1258 was chosen for the task of digitization of the analog data due to its high bit-resolution, 16-channel analog inputs and fast SPI data transfer protocol. The BeagleBoard, has an SPI-compatible protocol McSPI on its multi-functional expansion header. Applying changes into the bootloader and linux kernel of the BeagleBoard, the McSPI port was made available on the expansion connector and thus the communication between ADS1258 and the BeagleBoard was realized. The embedded program spi-ads on the BeagleBoard was developed to collect, convert and display data from the ADS1258.

Three health sensor modules; Active Belt, miniaturized oximeter and personal environment module were designed to facilitate ECG, oximetry and body environment monitoring in pervasive manner.

- Textile electrodes stitched on the chest belt detected a single channel ECG signal and pass it to the Amp Plug which is a tiny ECG analog amplifier circuit confined in a cellphone plug. The conditioned ECG data were successfully transferred to the BeagleBoard via the ADS1258. The embedded programs Active ECG and Active HR on the BeagleBoard finally visualized ECG and HR respectively of the Active Belt wearer.
- A miniaturized oximeter served two purposes: regional cerebral oximetry (rSO_2) and pulse oximetry (SpO_2). After a thorough literature review and laboratory experiment proving the theory of the cerebral oximetry, miniaturized oximetry hardware were designed and tested along with the BeagleBoard. The final system based on the OMAP3530 not only successfully monitored rSO_2 and SpO_2 in real-time, but also highly miniaturized oximeter design in comparison to the commercial cerebral oximeter.
- Personal environment monitoring module was made of the most common environment parameters humidity and temperature to prove the concept. Both sensors successfully detected the environment parameters and passed them to the BeagleBoard via the ADS1258. The module facilitated real-time monitoring of the body's environment.

At the end, the above mentioned modules were integrated with the ADS1258-BeagleBoard module to form a multimodal wearable health monitoring (MWM) system. At the moment, the MWM system is aimed at personalized monitoring for

home environments. The minimally-obtrusive sensor array from the above mentioned sensors was formed to embed it into daily-life devices and to enable wearable health monitoring of the user in a friendly manner. The patient-centric approach was taken into consideration and hence the real time visual biofeedback was facilitated along with health monitoring.

Although the MHM is currently a lab-prototype, it successfully furnished the advanced platform for the multi-modal health monitoring. The greatest challenges of programming a smartphone processor like OMAP3530 have been resolved during this development. The MHM offers the most state-of-the art hardware and technology by monitoring individual's health as well as body's environment, which has scarcely been found in any other academic research project. It also allowed the system to be ported into daily-life and home-based health monitoring, which has been a focus of the European Commission's ICT Work Programme 2011. Moreover, the MHM furnishes an innovative method of monitoring the health parameters in a more unobtrusive manner, where the general people remain free from the complicated procedures of medical device handling.

The MHM has indeed opened a gate of a new era where the health monitoring becomes truly multimodal, more pervasive and easier to handle.

8.1 PROBLEM ENCOUNTERED & RELATED SOLUTIONS

During design of the MPHIM system, many challenges appeared, with some of the challenges are still unsolved. The challenges, which were resolved, have previously been discussed in the corresponding sections. The following presents the current challenges and suggested solutions to them:

Integration of Hardware

In the presented work, to ease the process of prototyping and hardware interfacing, the complete hardware was subdivided into different modules fulfilling the need of individual health parameter monitoring. After the system has been fully developed, it

is time to integrate the modules into a single platform. The integration needs to be customized according to its field of application. As an example, consider an elderly individual comes back home from the respiratory surgery and requires to be monitored for his/her recovery. This individual doesn't require the cerebral oximetry but rather SpO₂, ECG and body environment monitoring. Thus, the function of the multimodality should be flexible and hence customized.

Besides, some of the modules are development boards such as ADS1258EVM and the BeagleBoard which should be redesigned and carry only necessary components in a final system design. For instance, many components on the BeagleBoard such as Svideo, JTEG, USB on-the-go, audio plug-in, etc. are not utilized in this application and should be omitted. Such customized module integration shown in Figure below has already started in our group at Institute for Signal Processing (ISIP), University of Luebeck, Germany.

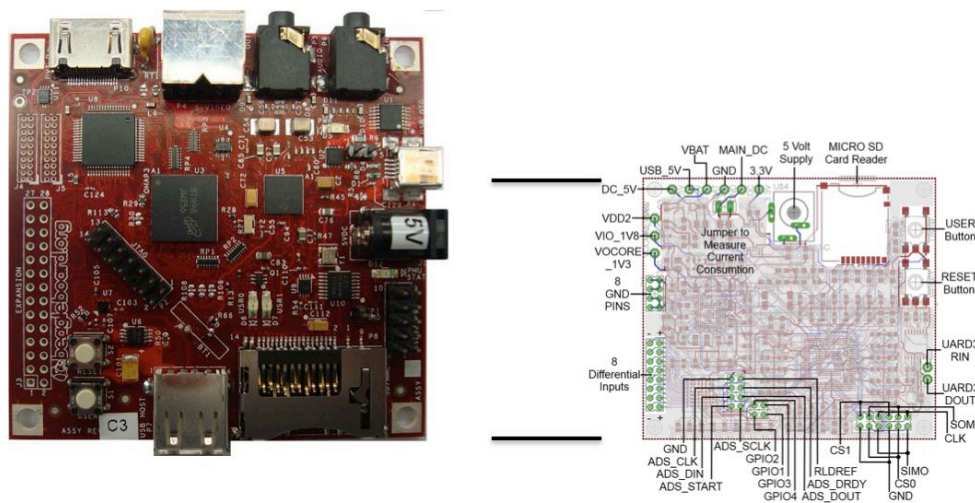


Fig. 8-1: The customized version of the OMAP3530 board, which is smaller than the BeagleBoard and contains only necessary components for the MHM

Sophisticated Algorithms

The algorithms used in this research work are based on C/C++ with some additional libraries such as SDL. The algorithms can be improved for GUI with more user friendly interactions. In the case of timely critical and low-power applications, the DSP core c64x+ can be utilized for the parallel processing. So the data handling task

for the OMAP3530 will be divided into two separate algorithms: 1) an algorithm running on the ARM core for collecting the data and displaying the resulting data and 2) an algorithm running on the DSP core for computing the data for applications of automatic diagnosis and analysis. The DSP/BIOS Link will facilitate the communication between the two cores of the OMAP3530.

Power-Supply Module

In this research work, the hardware modules were supplied by a laboratory power supply. Although, the CereOxi and PulseOxi PCBs contain on-board power supply units, the other modules such as Amp Plug, the personal environment module, the ADS1258 and the BeagleBoard require a regulated power supply. Below table enumerates the power dissipation of the each module and total power consumed by the MHM.

Table 8-1: Power consumptions of the MHM modules

Modules	Power requirements
BeagleBoard	1.75 W
ADS1258	42 mW
Amp Plug	2.6 mW
CereOxi Hardware	0.3 W
PulseOxi Hardware	0.3 W
Personal environment monitoring module	0.5 mW
TOTAL	Approx. 4.8 W

4.8W power dissipation of the MHM is indeed high and needs to be reduced by module integration. It is suggested that after the system is integrated in a single module, the regulated power supply unit fulfilling needs of each component power requirement should be designed. Since, the system is intended for the wearable and pervasive monitoring, the battery based power supply is necessary.

Connectivity

The MHM system does not yet provides any wireless data transmission facility, which is one of the aspects of the pervasive health monitoring. The OMAP3530 is designed for wireless portable application and hence found in smartphones. Therefore, its capability of the wireless transmission needs to be utilized by enabling the wireless connectivity module on the mentioned customized module.

Clinical Trials

After the system is integrated and powered by battery, it becomes a secure candidate to go into clinical trials. The system needs to be checked in clinical settings first to see its feasibility for medical applications. Consecutively, it should be supplied to the individual's home to run final clinical trial and to check its feasibility for its main purpose of home –based health monitoring.

Medical Device Certification

Most of the medical devices confront with the greatest challenges in receiving an approval for introducing it in the market. After the clinical trials are successful, the system should be placed into the medical device certification process, where the certification team will check its safety for the home environment use.

PUBLICATIONS ASSOCIATED WITH THE RESEARCH WORK

- 1) Mankodiya, K., Klostermann, M., et al. (2009). Teaching Signal Processing with a Dual-core Embedded Platform. 4th European DSP Education & Research Conference, EDERC2010, Nov. 2010, Nice, France.
- 2) Mankodiya, K., Opp, A., et al. (2010). Incorporating a Pulse Oximeter Sensor into Daily Life Devices. 4th German AAL-Congress, AAL 2011, Jan. 2011, Berlin, Germany.
- 3) Mankodiya, K., Ali Hassan, Y., et al. (2010). A Wearable ECG Module for Long-term Recordings using a Smartphone Processor. 5th International Workshop on Ubiquitous Health and Wellness, UbiComp'10, Sept. 2010, Copenhagen, Denmark.
- 4) Mankodiya, K., Vogt, S., et al. (2010). Near Patient Sensor Integration with Smart Phone Processors. In Biomedizinische Technik 2010, Rostock, Germany.
- 5) Mankodiya, K., Ali Hassan, Y., et al. (2010). Textile-based ECG Collection with Portable Dual-core Embedded System. 7th International Conference on Wearable Micro and Nano Technologies for Personalized Health, Berlin, Germany.
- 6) Mankodiya, K., Mohammedani, A. G., et al. (2010). A Miniaturized Regional Cerebral Oximeter based on Smartphone Processor. Proceedings of the International Biosignal Processing Conference. Berlin, Germany, 2010: 109:1-3
- 7) Mankodiya, K., Klostermann, M., et al. (2010). An Audible Display Integrating Patient Monitors. In Biomedizinische Technik 2010, Rostock, Germany.
- 8) Mankodiya, K., Vogt, S., et al. (2009). Portable electrophysiologic monitoring based on the omap-family processor from a beginners' perspective. In 16th International Conference on Digital Signal Processing, Santorini, Greece.
- 9) Mankodiya, K., Krapohl, et al. (2009). A Simplified Production Method for Multimode Multisite Neuroprobes. 4th International IEEE EMBS Neural Engineering Conference (pp. 5-8), Antalya, Turkey.

- 10) Klostermann, M., Christ, O., Mankodiya, K., et al. (2009). Omap 3 based signal processing for biomedical engineering teaching. In 17th European Signal Processing Conference (pp. 495-499), Glasgow, Scotland.
- 11) Mankodiya, K., Ayoub, et al. (2007). A design study on a Multisensory Cerebral Monitor. In Biomedizinische Technik 2007 (Vol. 43, pp. 1-2). Aachen, Germany.

LIST OF FIGURES

Section 1

Fig. 1-1: A multi-modal health monitoring scenario showing on-body and peripheral sensors.	4
Fig. 1-2: A system block diagram of the multi-modal wearable health monitor (MHM).	6

Section 2

Fig. 2-1: A generalized block diagram of an embedded system.	11
Fig. 2-2: Different packaging techniques of the embedded systems.	12
Fig. 2-3: The embedded processors and their role in the market	13
Fig. 2-4: An overview of a range of the ARM processors	15
Fig. 2-5: A system-level diagram of ARM Cortex-A8.	17
Fig. 2-6: The advancements in the OMAP dual-core application processors.	20
Fig. 2-7: (a) A generalized performance analysis of DSP and ARM processors.	21
Fig. 2-8: An overview of OMAP3530 subsystems.	24
Fig. 2-9: The BeagleBoard rev. C3 and its peripheral connections.	28

Section 3

Fig. 3-1: Out-of-box testing of the BeagleBoard.	33
Fig. 3-2: An image of the BeagleBoard with peripheral devices.	35
Fig. 3-3: The concept of BeagleBoard development environment.	36
Fig. 3-4: An illustration of a virtual appliance.	37
Fig. 3-5: A setup of the “Hello World!” program running on the ARM-core of the OMAP3530.	39
Fig. 3-6: An illustration of the heart rate monitoring using polar chest belt	41
Fig. 3-7: An illustration of the HRMI-BeagleBoard interface.	42
Fig. 3-8: A general scenario in patient monitoring.	44
Fig. 3-9 : A conceptual diagram of patient monitor integration.	44
Fig. 3-10: An illustration of the patient monitor integration	46
Fig. 3-11: An original practical setup of the patient monitor integration.	46
Fig. 3-12: The performance of the CapnoPlot.	47
Fig. 3-13: The performance of the CerePlot.	48

Section 4

Fig. 4-1: A generalized biosignal acquisition system.	52
Fig. 4-2: A block diagram a Delta-Sigma converter	54
Fig. 4-3: A system block diagram of the ADS1258.	55
Fig. 4-4: An image of the ADS1258EVM.	56

Fig. 4-5: An SPI master-slave communication protocol	57
Fig. 4-6: The timing diagram of the channel data read direct	59
Fig. 4-7: The timing diagram for the channel data read register	59
Fig. 4-8: The command byte and its three parts	60
Fig. 4-9: A layout of the expansion connector of the BeagleBoard with SPI ports highlighted	61
Fig. 4-10: A screenshot of the BeagleBoard's terminal program.....	63
Fig. 4-11: (a) A flowchart of the spidev-test program and (b) a loop-back test.....	64
Fig. 4-12: The connection between the ADS1258EVM and the BeagleBoard.....	65
Fig. 4-13: (a) A flowchart of the spi-ads program and (b) the screenshot of the spi-data.....	66
Fig. 4-14: (a) A flowchart of the D-to-A data conversion and plotting.....	67
Fig. 4-15: A screenshot of the terminal application	68
Fig. 4-16: A concept of the body environment monitoring	70
Fig. 4-17: Output voltage proportionality graphs of the humidity and temperature sensors.....	70
Fig. 4-18: A complete system of a personal environment monitoring module.	71
Fig. 4-19: A flowchart of a simple Body-Env Algorithm	72
Fig. 4-20: A screenshot of the Body-Env-Humidity monitoring.....	72
Fig. 4-21: A screenshot of the Body-Env-Temp monitoring.....	73

Section 5

Fig. 5-1: The state-of-the-art technologies in wearable physiological monitoring	76
Fig. 5-2: A conceptual diagram of textile-based ECG detection.....	78
Fig. 5-3: The electrical activity of a heart.	78
Fig. 5-4: Graphical illustration of standard 12-lead connection.....	79
Fig. 5-5: A commercial Ag/AgCl ECG Electrode.....	80
Fig. 5-6: Different types of the dry electrodes.....	81
Fig. 5-7: Skin-electrode models.....	83
Fig. 5-8: A generalized block diagram of the wearable ECG system.	85
Fig. 5-9: A concept of the power-line interference in the ECG signal	85
Fig. 5-10: Electrical properties of the electrophysiology signals	87
Fig. 5-11: The response of HPF, NF and LPF cascaded in ECG instrumentation.	88
Fig. 5-12: The textile electrodes used for the Active Belt system.....	90
Fig. 5-13: The chest belt of the Active Belt System.....	90
Fig. 5-14: An RHA1016 Biopotential Amplifier.....	91
Fig. 5-15: An RHA circuit design for the Active Belt ECG system.	93
Fig. 5-16: A PCB design of the Amp Plug.....	94
Fig. 5-17: The digital module for the Active Belt System.	95
Fig. 5-18: Active-ECG and Active-HR algorithms for the Active Belt system.....	96
Fig. 5-19: An electrode performance measurement setup	97
Fig. 5-20: The Impedance graph.....	97
Fig. 5-21: SNR results of the textile electrodes.....	98

Fig. 5-22: The ECG recordings by commercial monitors	99
Fig. 5-23: An experimental setup for the Amp Plug tests	99
Fig. 5-24: The electrical properties of the Amp Plug	100
Fig. 5-25: ECG recorded by the Amp Plug	101
Fig. 5-26: The ECG monitoring with the Active Belt System	101
Fig. 5-27: Active-ECG plotting for 2-lead electrode configuration	102
Fig. 5-28: Active-HR algorithm monitoring heart rate for 3-lead and 2-lead ECG configurations ..	103

Section 6

Fig. 6-1: The concept of the miniaturized oximetry system	110
Fig. 6-2: An illustration of light-tissue interaction	111
Fig. 6-3: Absorption spectra of deoxygenated Hb (HHb), oxygenated Hb (HbO ₂) and water	113
Fig. 6-4: The SpO ₂ measurement methods	114
Fig. 6-5: A schematic of the photoplethysmogram	115
Fig. 6-6: (a) the locations of the cerebral oximetry sensors on the frontal bones (forehead)	116
Fig. 6-7: Recording of near-infrared spectroscopy during coronary artery bypass	117
Fig. 6-8: (a) A setup for a human frontal bone spectroscopy	118
Fig. 6-9: A simplified block diagram of the Oximetry system	119
Fig. 6-10: Pictures of commercial sensors used for the cerebral oximetry	120
Fig. 6-11: (a) An illustration of pulse chain required to drive the LEDs	121
Fig. 6-12: Images of analog PCBs for the cerebral oximetry (top) and pulse oximetry (bottom).	122
Fig. 6-13: A picture of the complete CereOxi and PulseOxi systems	123
Fig. 6-14: Flowcharts of the CereOxi and PulseOxi algorithms	125
Fig. 6-15: A sensor patch on the forehead and the timing diagram of the pulse signal	126
Fig. 6-16: An implementation of the driver pulses produced from the BeagleBoard GPIO pins	127
Fig. 6-17: The measurements with the PulseOxi system	128
Fig. 6-18: The performance of photoplethysmography with the PulseOxi system	129
Fig. 6-19: rSO ₂ measurements with CereOxi system	130
Fig. 6-20: A physical comparison	132

Section 7

Fig. 7-1: An overview of the MHM	141
Fig. 7-2: An image of the Pico DLP Projector kit	143
Fig. 7-3: Images of the Vital-cap carrying minimally obtrusive sensor array	144
Fig. 7-4: Images of the Vital-glasses carrying minimally obtrusive sensor array	145
Fig. 7-5: Algorithms for the MHM. 10sec-&-Display algorithm aims at the user	146
Fig. 7-6: A Vital-cap monitors and displays the multimodal body parameters along	148
Fig. 7-7: Multimodal continuous recording of 5min	149
Fig. 7-8: Vital-glasses monitoring and displaying multimodal body and its environment	149
Fig. 7-9: Multimodal recording of 5 min using a combination of Vital-glasses and Active-Belt	150

Section 8

Fig. 8-1: The customized version of the OMAP3530 board 157

LIST OF TABLES

Table 1-1: A list of major diseases with the monitoring requirements (US-based study).....	3
Table 1-2: Potential sensors for continuous health monitoring and their data throughputs.....	5
Table 2-1: An comparative overview of major smartphone processors.....	16
Table 2-2: A list of OMAP3530 development boards available	26
Table 4-1: Typical system characterisitcs of the biosignals	52
Table 4-2: The BeagleBoard’s expansion connector signals.....	62
Table 5-1: The origins of various ECG segments	79
Table 5-2: Standard 12-lead ECG configuration.....	79
Table 5-3: Selection of the resistors.	93
Table 6-1: Organ robustness to anoxic cardiac arrest.....	109
Table 6-2: The pulse frequency vs. measured delay of the detected signals.....	126
Table 7-1: A list of personalized health monitoring devices.....	136
Table 8-1: Power consumptions of the MHM modules	158

LIST OF EQUATIONS

Eq. 3-1	47
Eq. 5-1	82
Eq. 5-2	84
Eq. 5-3	84
Eq. 5-4	86
Eq. 5-5	100
Eq. 5-6	100
Eq. 6-1	112
Eq. 6-2	113
Eq. 6-3	116

ABBREVIATIONS

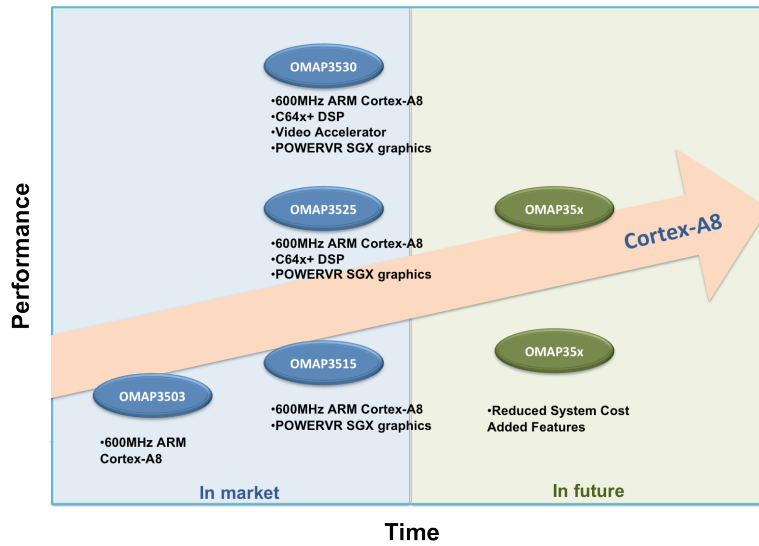
ICT	Information and Communications Technologies
mHealth	Mobile eHealth
FEV1	Forced Expiratory Volume in 1sec
ECG	Electrocardiogram
HR	Heart rate
BP	Blood pressure
COPD	Compulsive Obstructive Pulmonary Disease
EMG	Electromyogram
SpO₂	Saturation of peripheral Oxygen
rSO₂	Regional Oxygen Saturation
EtCO₂	End Tidal Volume
Hb	Hemoglobin
MIPS	Million Instructions per sec
OMAP	Open Media Application Platform
ADC	Analog-to-Digital Converter
LED	Light Emitting Diode
LCD	Liquid Crystal Display
ROM	Read Only Memory
EPROM	Erasable Programmable Read Only Memory
CPU	Central Processing Unit
DAC	Digital-to-Analog Converter
SoC	System-on-a-Chip
SiP	System-in-package
PoP	Package-on-package

ARM	Advanced RISC Machine
RISC	Reduced Instruction Set Computing
ISA	Instruction Set Architecture
OS	Operating System
MMU	Memory Management Unit
DMIPS	Dhrystone Million Instructions per sec
ETM	Embedded Trace Marcocell
GPP	General Purpose Procesor
DSP	Digital Signal Processor
PCB	Printed Circuit Board
DVI	Digital Visual Interface
HDMI	High Definition Multimedia Interface
USB	Universal Serial Bus
WLAN	Wireless Local Area Network
CCS	Code Composar Studio
IDE	Integrated Development Environment
API	Application Programming Interface
OpenGL	Open Graphic Library
SDL	Simple DirectMedia Layer
HRMI	Heart Rate Monitoring Interface
SAR	Successive Approximation Register
FIR	Finite Impulse Response
IIR	Infinite Impulse Response
SPI	Serial Peripheral Interface
McSPI	Multi-channel Serial Port Interface
McBSP	Multi-channel Buffered Serial Port
UART	Universal Asynchronous Receiver/Transmitter
MMC	Multi-Memory Controller

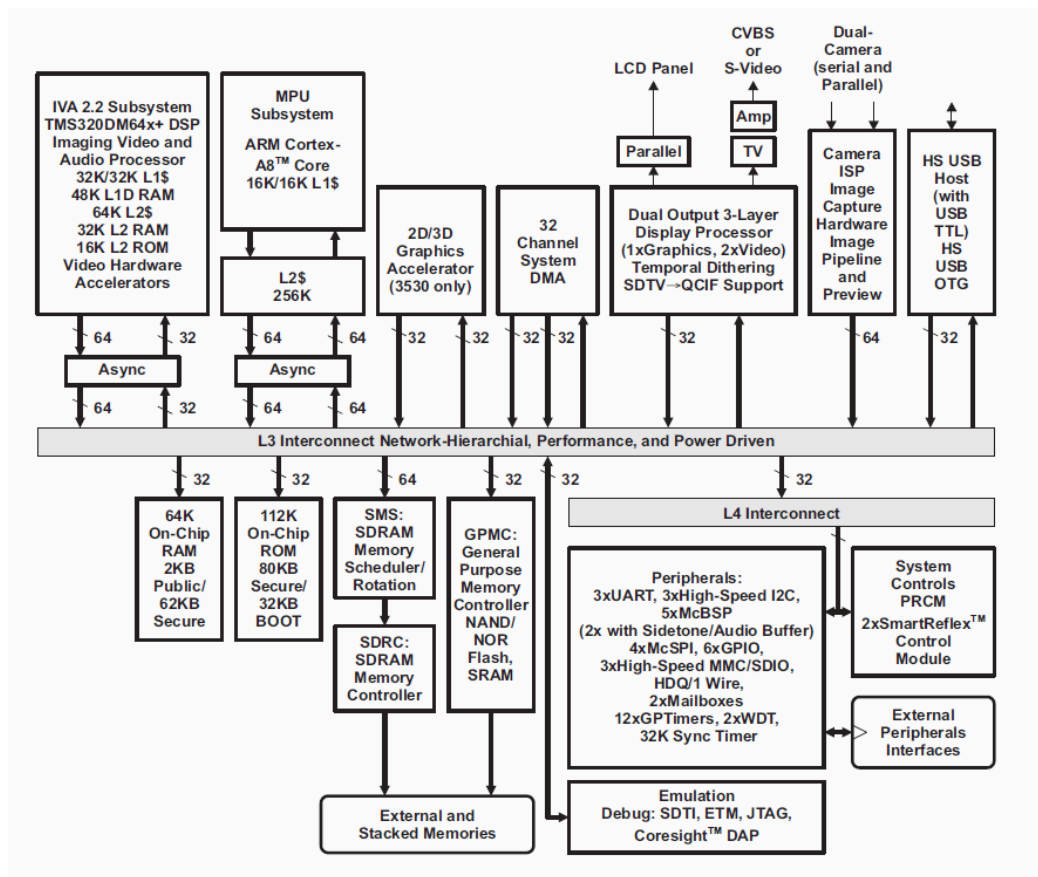
SCLK	Serail Clock
MOSI	Master-Out Serial-In
MISO	Master-In Serial-Out
CS	Chip Select
DIN	Data-In
DOUT	Data-Out
DRDY	Data Ready
GPIO	General Purpose Input/Output
OE	Open Embedded
CMR	Common Mode Rejection
CMRR	Common Mode Rejection Ratio
SNR	Signal-to-Noise Ratio
IA	Instrumentation Amplifier
ICU	Intensive Care Unit
NIRS	Near Infrared Spectroscopy
DPF	Differential Path Length Factor
HbO₂	Deoxygenated Hemoglobin
AAL	Ambient Assisted Living
MHM	Multimodal Wearable Health Monitoring

APPENDIX

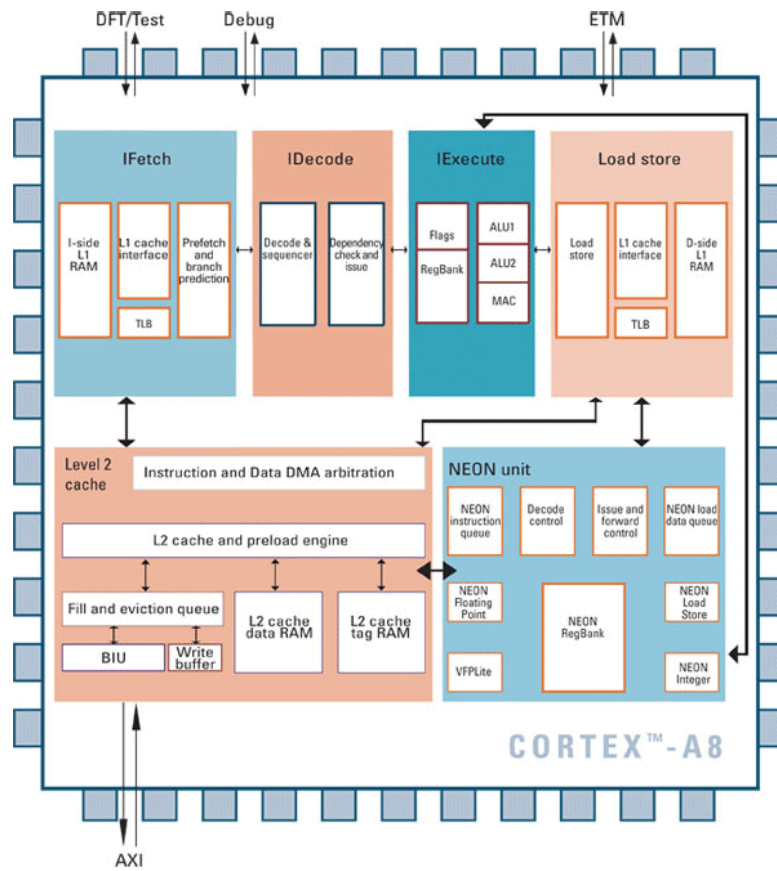
OMAP35xx Roadmap



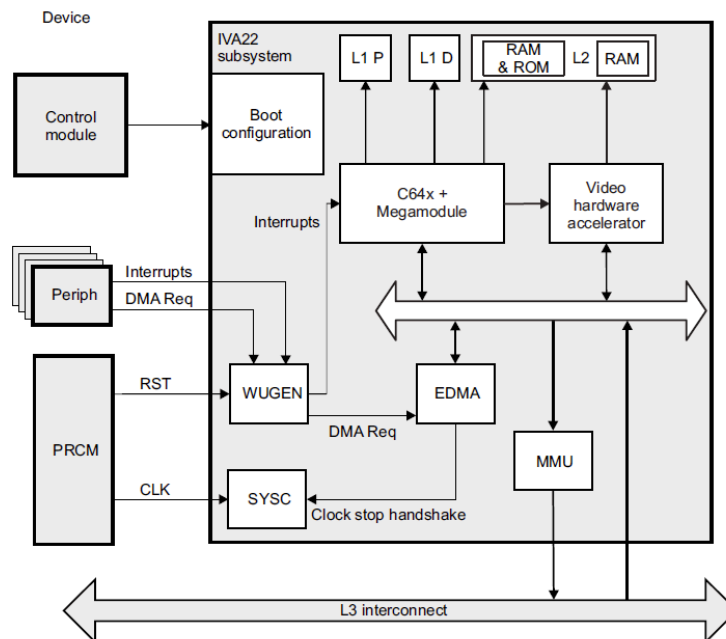
OMAP3530 Detailed Architecture



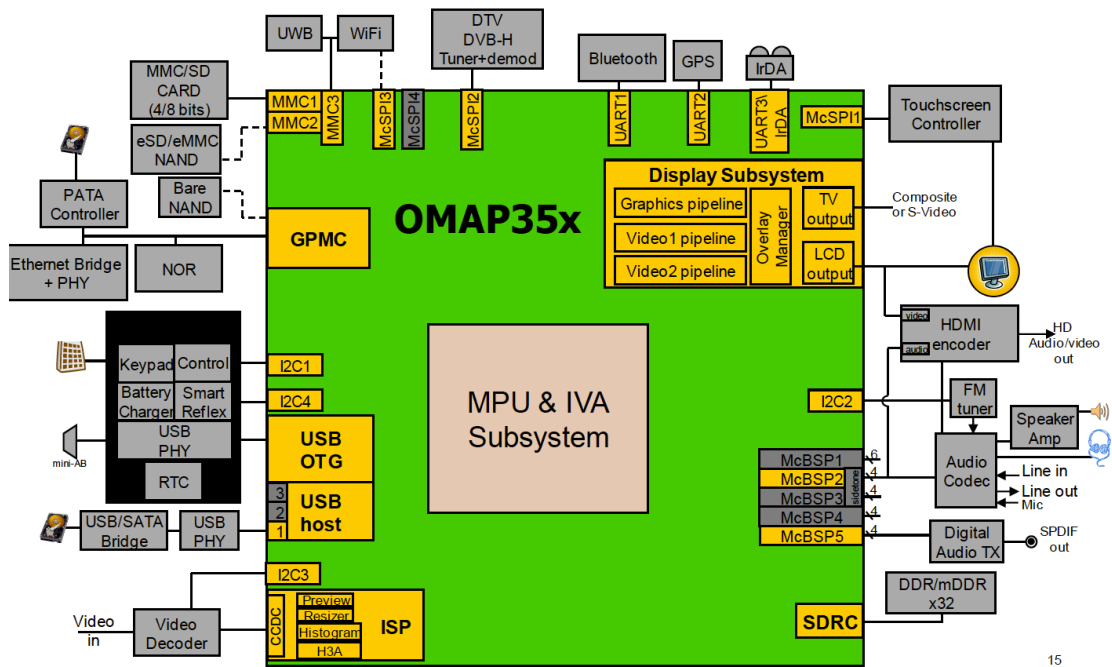
ARM Cortex-A8 Detailed Architecture



C64x+ Architecture



OMAP35x Connectivity Examples



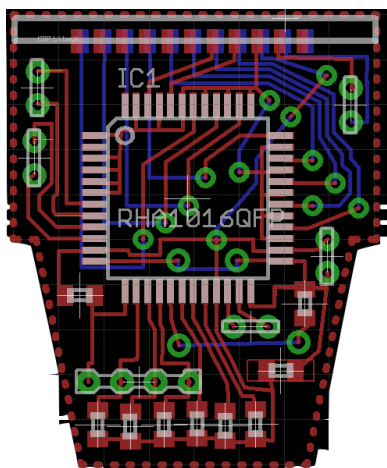
Complete List of OMAP3530 Development Boards

Board	Company	Peripherals	Support / Community	Price (\$)
OMAP35x EVM	TI with Mistral Solution	Nearly all	Commercial & open source TI developers community	1495.00
Cobra3530	Analogue & Micro Ltd.	Customized	Commercial -	995.00
CM-T3530	Anders electronics	Only for mobile devices	Commercial -	-
BeagleBoard	Beagleboard.org	Nearly all	Commercial & open source groups.google	149.00
Kit OMAP3530	Broadcon	Nearly all	Commercial & open source -	169.00
CSB740	Cogent Computer Systems	Nearly all	Commercial -	-
CM-T3530	Comouter Lab	Only for mobile devices	Commercial -	>55.00
EBVBeagle board	EBV Elektronik	Nearly all	Open source -	
Embest Dev-kit8000	Embest	Nearly all	Commercial & open source -	259.00
EMP3530	Empower	For video processing	Commercial & open source -	900.00
Overo	Gumtrix	Expansion board	Commercial & open source Gumtrix mailing list	219.00
KBOC System on Module	KwikByte	Customized	Commercial & open source -	>119.00
OMAP35x SOM-LV System on Module	Logic	For embedded networking field	Commercial & open source -	-
Zoom Dev. Kit	Logic	For medical dev.	Commercial & open source -	995.00
ICETEK-OMAP3530-MINI	RealTimeDSP	Nearly all	Commercial & open source -	135.00
SEED-OMAP3530	Seed	For video processing	Commercial	-
TAO-3530 System Modules	TechNexion	Baseboard	Commercial	>130.00
SOM3530	Techor	For handheld applications	Commercial	-
MAGiK-MX OMAP	TES Electronic Solutions	For audio/video processing	Commercial	-

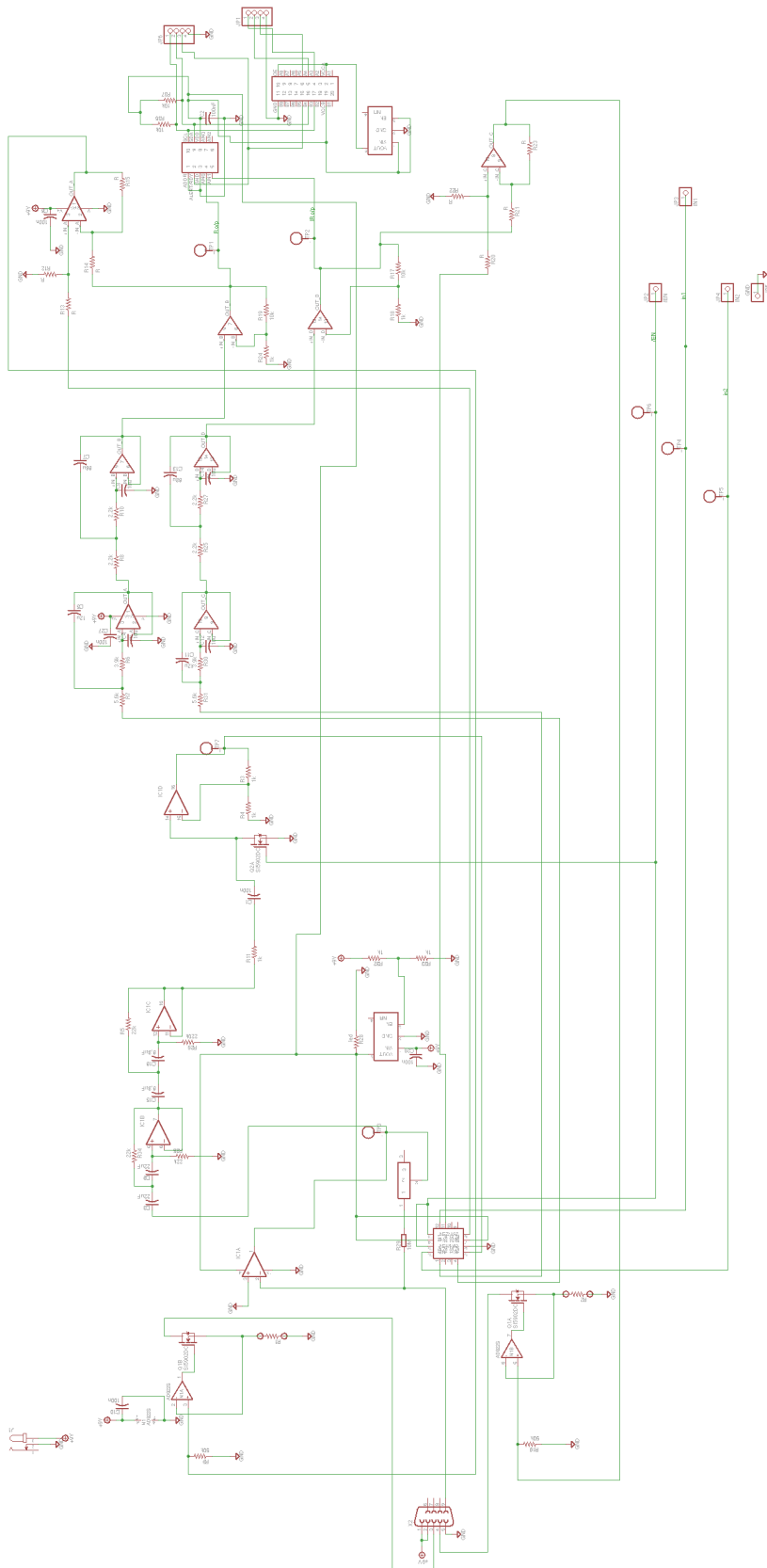
The technical details of the textile electrodes and the ELITEX® thread

Material	Layer - Polyamide Coating - 99% Silver
Yarn count	Basic yarn count - 235 dtex/f34 Final yarn count - 450 dtex Thickness of silver layer - 1-2 μm
Electrical resistance	20 Ω/m
Running length	22 m/kg
Tensile strength	750 cN
Melting point	259 °c
Light fastness	note 2-3 (DIN ISO 105 B02 up to note 8)
Washing temperature	30 ° c with light duty detergents
Solderability	Solderable with low-melting solders (less than 185° c)

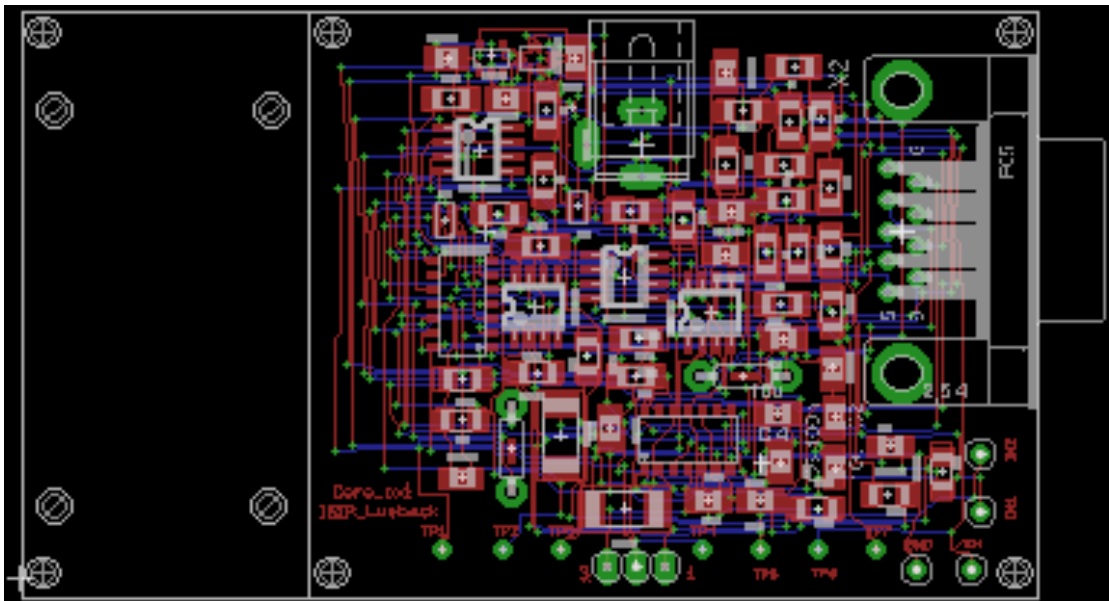
Amp Plug Board Desi



PulseOxi Circuit



CereOxi PCB



PulseOxi PCB

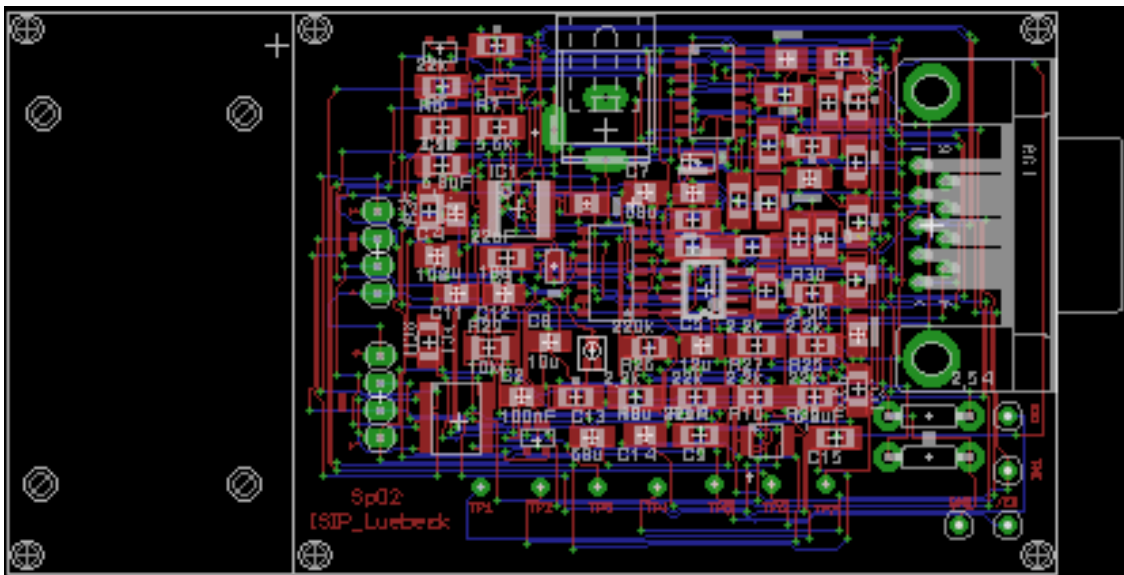
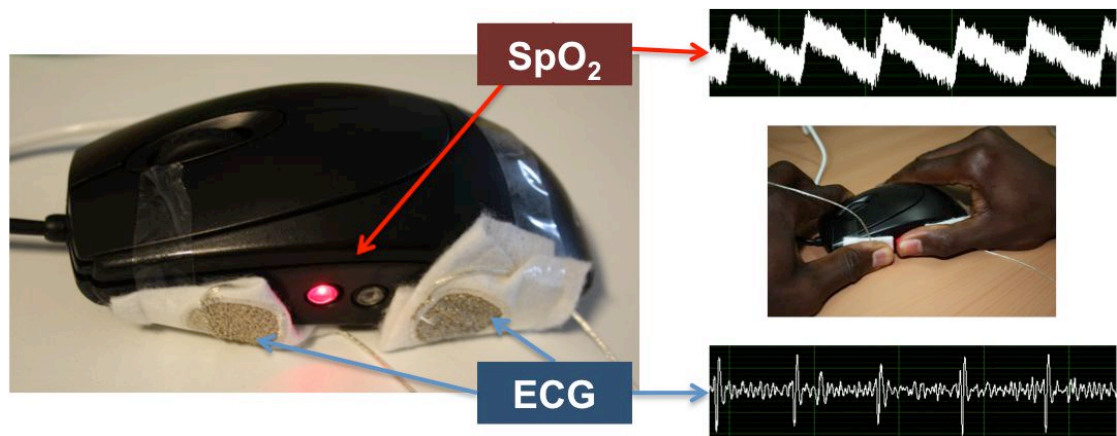


Table of checking feasibility of the daily-life objects for unobtrusive health monitoring

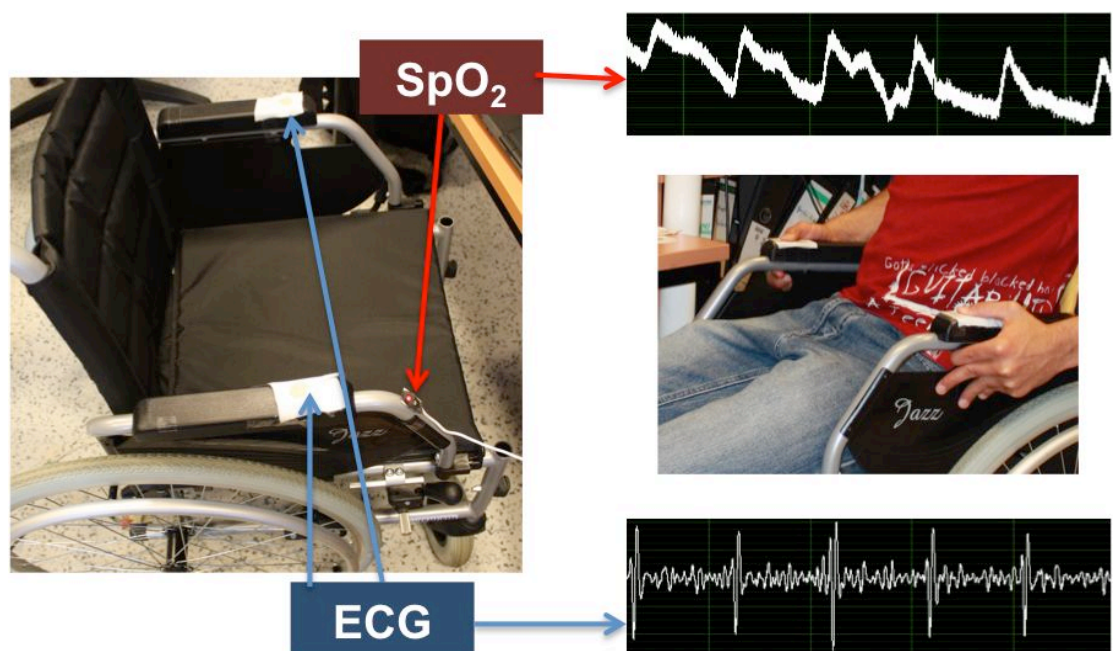
Daily-devices	Suitability check for the MPH M system	Remarks
Rollator	Not suitable for continuous monitoring	It has contacts at the handles which are susceptible to the movement artifacts
Wheelchair	Can be suitable for health monitoring	It requires the movement artifacts removal.
Resting/office chair	Suitable, but not for continuous monitoring	It provides the contacts at the armrests.
Bed	Not suitable	Highly susceptible to the movement artifacts. And worn objects may increase discomfort during sleep.
Toilet seats	Suitable for one time health check	This can be a very good option for monitoring health especially at the morning time.
Electric Switchboards	Suitable for one time health check	This can be a good option for monitoring the health parameters before going and after coming back to home from outside
Cap or hat	Very suitable	It provides firm contact to the head which is a location for cerebral and pulse oximetry sensors.
Glasses	Very suitable	It provides firm contact on the face, which is good location for pulse oximetry.
Daily garments	Partially suitable	It is susceptible to the movement artifacts. In order to avoid that, it requires being tight on the body and hence is less comfortable.
Computer mouse	Partially suitable	It is useful for those who use computer.

The following measurements were performed using our analog front-end hardware modules of ECG and SpO₂ linking to the Labview application on a PC via digital acquisition board.

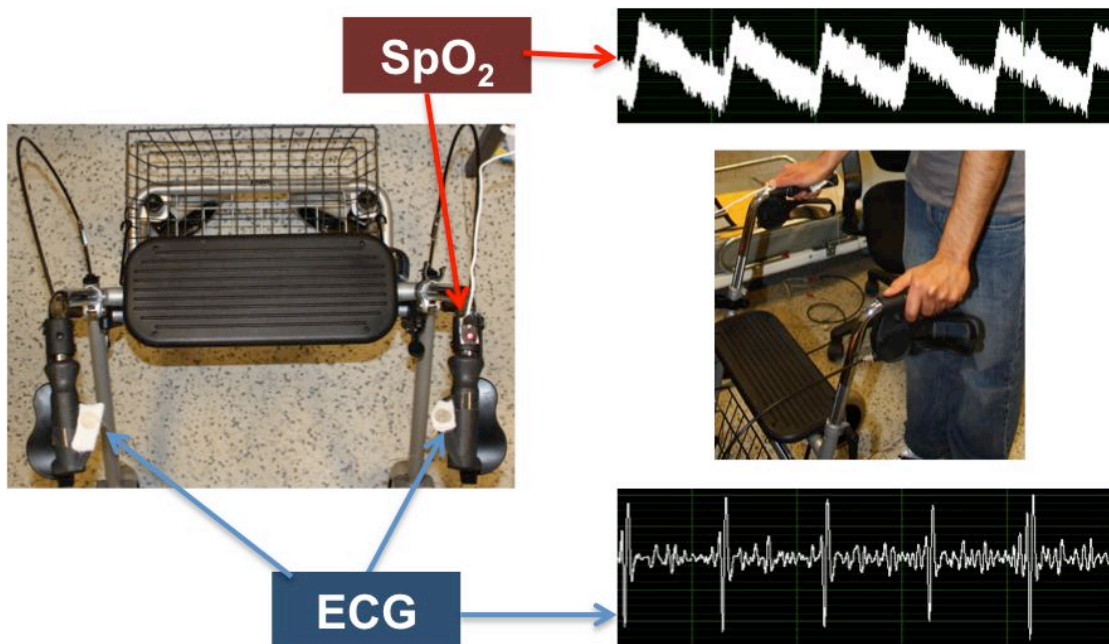
Vital-mouse measurements



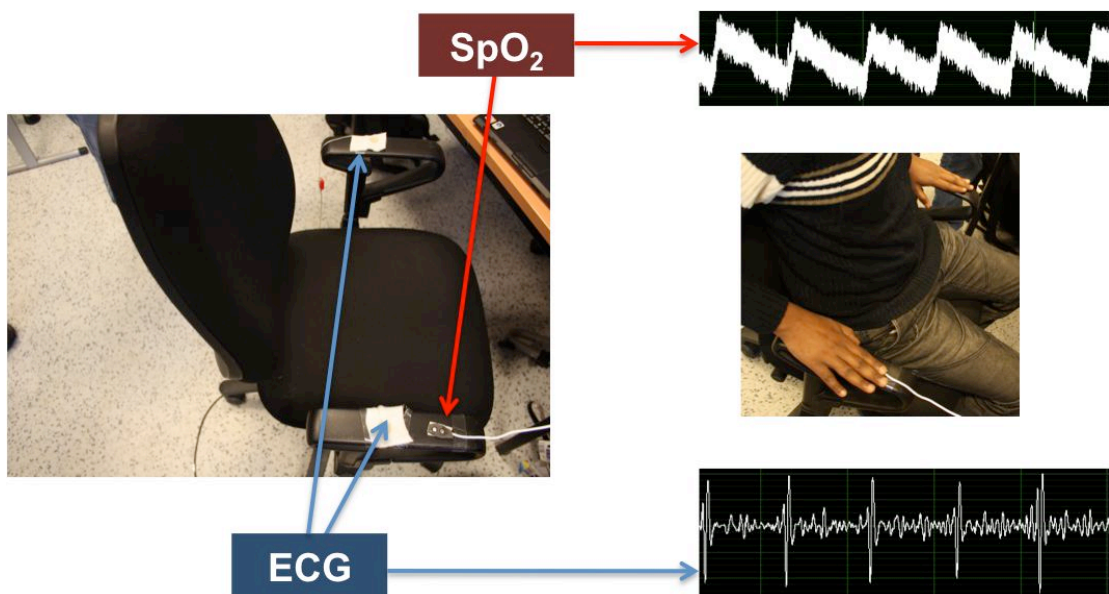
Vital-wheelchair Measurements



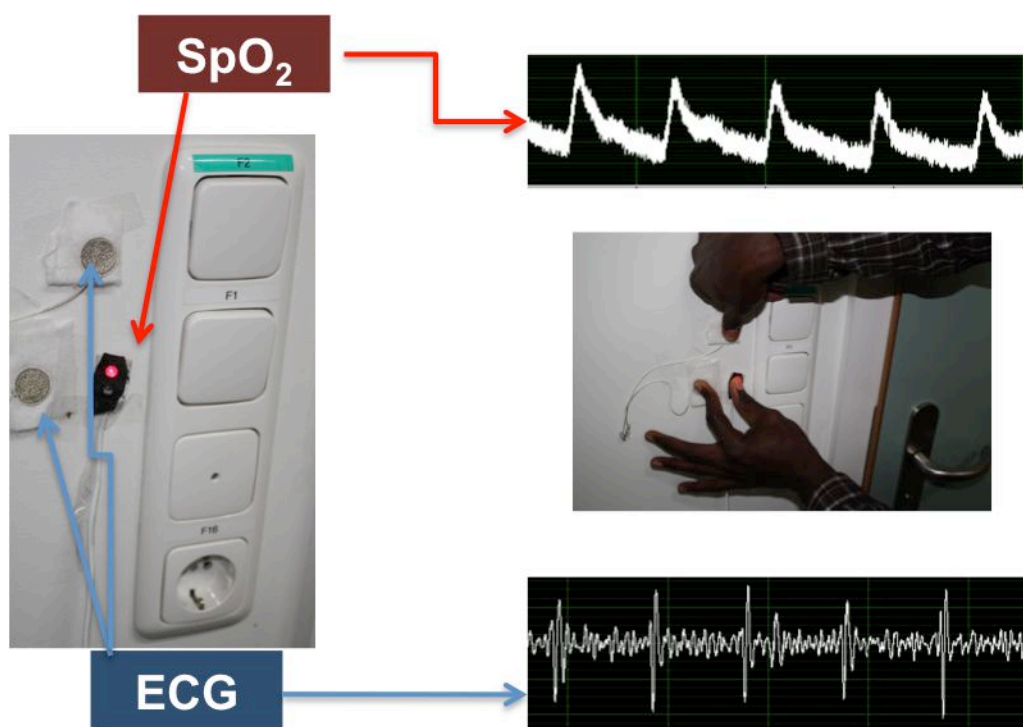
Vital-rollator



Vital-office chair



Vital-switchboard

**LCD Screen - BeagleTouch with BeagleBoard**

The BeagleTouch (Liquidware, USA) is an enhanced touchscreen display module that is designed to interface with the BeagleBoard to bring the single board computer functionality. It provides 480x272 resolution and 262k color touchscreen. It can be mounted on the LCD header for the display connection with the BeagleBoard. Moreover, BeagleJuice (Liquidware, USA), which is a power supply module for the BeagleBoard, completes the handheld smartphone like device if used with the BeagleTouch. BeagleTouch and BeagleJuice were chosen to fulfill the requirement of handheld display module with the BeagleBoard for the multimodal system.

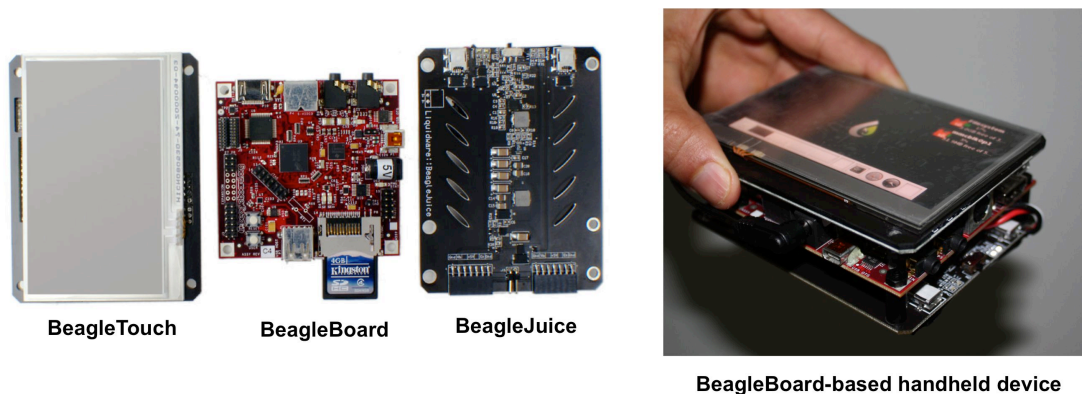
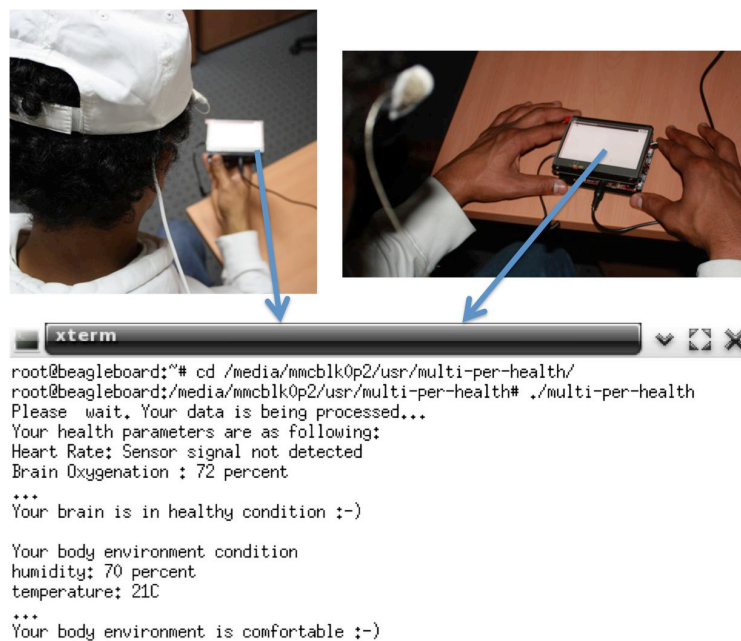


Fig: The BeagleTouch and BeagleJuice connecting to the BeagleBoard and forming a handheld device.

BeagleBoard Handheld Device for Multimodal Health Monitoring

The BeagleBoard handheld device which is a combination of the BeagleBoard, the Beagle-Touch and –Juice, is here demonstrated for its feasibility in the multimodal wearable health monitoring. The handheld system is not yet ready to communicate with the ADS1258 due to unavailability of the McSPI pin on the expansion header. The McSPI pins are already used for providing the UART functionality on the BeagleTouch. So, in the future, the McBSP can be utilized to communicate with the ADS1258 and to enable the multimodal health monitoring.



Definitions of the Emerging Fields in the Health Monitoring

This research work is associated with the state-of-the art technologies in medical technology, especially in health and patient monitoring. In recent years, several emerging fields in this area come into existence. This new fields and terms used extensively in this report. Although, the terms are defined and elaborated based on their context in the sections, the following presents their definition for quick reference.

mHealth

The mHealth field has emerged as a sub-segment of eHealth, the use of information and communication technology (ICT), such as computers, mobile phones,communications satellite, patient monitors, etc., for health services and information [1]. mHealth applications include the use of mobile devices in collecting community and clinical health data, delivery of healthcare information to practitioners, researchers, and patients, real-time monitoring of patient vital signs, and direct provision of care (via mobile telemedicine)[2].

Ambient Assisted Living (AAL)

Ambient Assisted Living (AAL), which is an initiative from the European Union (EU) to emphasize the importance of addressing the needs of the ageing European population by reducing innovation barriers on ICT with the goal to lower future social security costs [3]. AAL aims at extending the time older people can live in their home environment by increasing their autonomy and assisting them in carrying out activities of daily living by the use of intelligent products and the provision of remote services including care services [4]. Most efforts towards building ambient assisted living systems for the elderly people are based on developing pervasive devices and use Ambient Intelligence to integrate these devices together to construct a safety environment [4]. Ambient intelligence refers to electronic systems that provide services in a sensitive and responsive way to the presences of people, and unobtrusively integrated into our daily environment [8, 9].

Pervasive Health

The notion of pervasive health monitoring presents us with a paradigm shift from the traditional event-driven model (i.e. go to doctor when sick) to one where we are continuously monitoring a person's "well-being" through the use of bio-sensors, smart-environments, smart-homes and information networks. This allows more proactive health maintenance, as well as allowing the health care provider to make more informed decisions with a greater wealth of accurate data [5].

Wearable Computing / Technology

Wearable computers are computers that are worn on the body. This type of wearable technology has been used in behavioral modeling, health monitoring systems, information technologies and media development. Wearable computing" is an active topic of research, with areas of study including user interface design, augmented reality, pattern recognition, use of wearables for specific applications or disabilities, electronic textiles and fashion design [6].

Biofeedback

Biofeedback is a process that enables an individual to learn how to change physiological activity for the purposes of improving health and performance. Precise instruments measure physiological activity such as brainwaves, heart function, breathing, muscle activity, and skin temperature. These instruments rapidly and accurately 'feed back' information to the user. The presentation of this information — often in conjunction with changes in thinking, emotions, and behavior — supports desired physiological changes. Over time, these changes can endure without continued use of an instrument. [7]

References

- [1] Vital Wave Consulting (February 2009). *mHealth for Development: The Opportunity of Mobile Technology for Healthcare in the Developing World*. United Nations Foundation, Vodafone Foundation. p. 9.

- [2] Germanakos P., Mourlas C., & Samaras G. "A Mobile Agent Approach for Ubiquitous and Personalized eHealth Information Systems." Proceedings of the Workshop on 'Personalization for e-Health' of the 10th International Conference on User Modeling (UM'05). Edinburgh, July 29, 2005, pp. 67-70.
- [3] International newsletter on micro-nano integration.: Ambient Assisted Living, <http://mstnews.de>, no 6/07, (2007)
- [4] E. Aarts, R. Harwig and M. Schuurmans, chapter Ambient Intelligence in *The Invisible Future: The Seamless Integration Of Technology Into Everyday Life*, McGraw-Hil, 2001. E. Aarts, R. Harwig and M. Schuurmans, chapter Ambient Intelligence in *The Invisible Future: The Seamless Integration Of Technology Into Everyday Life*, McGraw-Hil, 2001.
- [5] Braecklein, M., J. Dehm, et al. (2007). *VDE Anwendungsempfehlungen für TeleMonitoring* H. Korb. Frankfurt, VDE.
- [6] http://en.wikipedia.org/wiki/Wearable_computer
- [7] "What is biofeedback?". Association for Applied Psychophysiology and Biofeedback. 2008-05-18. Retrieved 2010-02-22.
- [8] E. Aarts and J. Encarnação, *True Visions: The Emergence of Ambient Intelligence*, Springer, 2006.
- [9] Flores-Mangas, Nuria Oliver Fernando. *HealthGear: A Real-time Wearable System for Monitoring and Analyzing Physiological Signals*. Redmond, USA, 2005. Redmond, USA.